

©Copyright 2024
Natchanon Suaysom

Interest Rate Problems: Implied Volatility of Options on Bonds and Forward Rates, and Optimal Times to Buy and Sell a Home

Natchanon Suaysom

A dissertation
submitted in partial fulfillment of the
requirements for the degree of

Doctor of Philosophy

University of Washington

2024

Reading Committee:

Matthew Lorig, Chair

Jose Nathan Kutz

Hong Qian

Program Authorized to Offer Degree:

Applied Mathematics

University of Washington

Abstract

Interest Rate Problems: Implied Volatility of Options on Bonds and Forward Rates, and Optimal Times to Buy and Sell a Home

Natchanon Suaysom

Chair of the Supervisory Committee:
Matthew Lorig
Applied Mathematics

In this Thesis, we examine problems in financial mathematics whose characteristics are significantly influenced by the dynamics of the interest rate.

In the first part of the Thesis, we derive an explicit asymptotic approximation for the implied volatilities of Call options written on bonds and forward rates assuming the instantaneous short-rates of interest are described by Affine Term-Structure (ATS) models and Quadratic Term-Structure (QTS) models, respectively. For specific short-rate models, we perform numerical experiments in order to gauge the accuracy of our approximation.

In the second part of the Thesis, we derive the optimal stopping times to buy and sell a home. We begin by assuming that home prices are set by a representative home-buyer, who can afford to pay only a fixed cash-flow per unit time for housing. The cash-flow is a fraction of their salary, which grows at a rate that is proportional to the risk-free rate of interest. The mortgage rate paid by the home-buyer is fixed at the time of purchase and equal to the risk-free rate of interest plus a positive constant. In this setting, we consider an investor who wishes to buy and then sell a home in order to maximize his discounted expected profit. This leads to a nested optimal stopping problem, which can be solved using nonnegative concave majorant approach. Additionally, we provide a detailed analytic and numerical study of the case in which the risk-free rate of interest is modeled by a Cox-Ingersoll-Ross (CIR) process.

TABLE OF CONTENTS

	Page
List of Figures	iii
Chapter 1: Introduction	1
1.1 Background: Interest Rate and Overview	1
1.2 Fixed-Income Instrument	2
1.3 Risk-Neutral Pricing	5
1.4 Options and Implied Volatilities	8
1.5 Thesis Outline	12
Chapter 2: Modeling Short-Rate	14
2.1 Assumptions	14
2.2 Short-Rate and Bond Price	14
2.3 Affine Term-Structure Model	16
2.4 Quadratic Term-Structure Model	17
2.5 Pricing Option on Bonds	18
2.6 Pricing Options on Simple Forward Rates	20
2.7 Local Stochastic Volatility Model	22
Chapter 3: Asymptotic Option Pricing and Implied Volatility	31
3.1 Option Price Asymptotics	31
3.2 Option on Bonds Implied Volatility Asymptotics	35
3.3 Option on Forward Rates Implied Volatility Asymptotics	37
3.4 Example: Option on Bond Implied Volatility Under ATS Model	38
3.5 Example: Caplet Implied Volatility Under QTS Models	48
3.6 Example: Calibration to Market Data	51

Chapter 4: Optimal times to buy and sell a home	53
4.1 Introduction	53
4.2 The Relation Between Interest Rates and Home Values	55
4.3 Optimal Home Buying and Selling Problems	58
4.4 Expressions for the Value Function J and Optimal Stopping Time τ^*	62
4.5 Detailed Analysis: CIR Process Risk-Free Rate	64
4.6 Future Research	72
4.7 Conclusion	72
Chapter 5: Figures	73
Bibliography	92
Appendix A: Explicit Expressions for σ_0 , σ_1 and σ_2	99
Appendix B: Expressions for F , G_1 and G_2 in the Fong-Vasicek Setting	103
Appendix C: Relevant Expressions for u_+ , u_- , \hat{h}_s and \hat{h}_b	105
C.1 Expressions for u_+ and u_-	105
C.2 Expressions for \hat{h}_s and \hat{h}_b	107
C.3 Constant discount rate	112

LIST OF FIGURES

Figure Number	Page
5.1 For the Vasicek short-rate model described in Section 3.4.1, we plot implied volatility Σ as a function of t with the maturity date of the options fixed at $T = 0.5$ and with the maturity date of the underlying bond taking the following values $\bar{T} = \{1, 3, 5, 10\}$, which correspond to the blue, orange, green, and red curves, respectively. The following model parameters remained fixed: $\kappa = 0.9$, $\delta = \sqrt{0.033}$, and $\theta = \frac{0.08}{0.9}$	74
5.2 For the CIR short-rate model described in Section 3.4.2, we plot exact implied volatility Σ and approximate implied volatility $\bar{\Sigma}_n$ up to order $n = 2$ as a function of log-moneyness $k - x$ with the maturity date of the bond fixed at $\bar{T} = 2$ and with the maturity of the option taking the following values $T = \{\frac{1}{12}, \frac{1}{4}, \frac{1}{2}, \frac{3}{4}\}$. The zeroth, first, and second order approximate implied volatilities correspond to the orange, green and red curves, respectively, and the blue curve correspond to the exact implied volatility. The following parameters, which were taken from [26, Example 10.3.2.2], remained fixed $t = 0$, $\kappa = 0.9$, $\delta = \sqrt{0.033}$, $\theta = \frac{0.08}{0.9}$, $y = 0.08$	75
5.3 For the CIR short-rate model described in Section 3.4.2, we plot the absolute value of the relative error of our second order implied volatility approximation $ \bar{\Sigma}_2 - \Sigma /\Sigma$ as a function of log-moneyness $(k - x)$ and option maturity T . The horizontal axis represents log-moneyness $(k - x)$ and the vertical axis represents option maturity T . Ranging from darkest to lightest, the regions above represent relative errors in increments of 0.2% from $< 0.2\%$ to $> 1.4\%$. The maturity date of the bond is fixed at $\bar{T} = 2$. The following parameters, which were taken from [26, Example 10.3.2.2], remained fixed $t = 0$, $\kappa = 0.9$, $\delta = \sqrt{0.033}$, $\theta = \frac{0.08}{0.9}$, $y = 0.08$	76

- 5.4 For the 2-D CIR short-rate model described in Section 3.4.3, we plot exact implied volatility Σ and approximate implied volatility $\bar{\Sigma}_n$ up to order $n = 2$ as a function of log-moneyness $k - x$ with the maturity date of the bond fixed at $\bar{T} = 2$ and with the maturity of the option taking the following values $T = \{\frac{1}{12}, \frac{1}{4}, \frac{1}{2}, \frac{3}{4}\}$. The zeroth, first, and second order approximate implied volatilities correspond to the orange, green and red curves, respectively, and the blue curve correspond to the exact implied volatility. The following parameters remained fixed $t = 0$, $\kappa_1 = \kappa_2 = 0.9$, $\delta_1 = \delta_2 = \sqrt{0.033}$, $\theta_1 = \theta_2 = \frac{0.08}{0.9}$, $y_1 = y_2 = 0.04$ 77
- 5.5 For the 2-D CIR short-rate model described in Section 3.4.3, we plot the absolute value of the relative error of our second order implied volatility approximation $|\bar{\Sigma}_2 - \Sigma|/\Sigma$ as a function of log-moneyness ($k - x$) and option maturity T . The horizontal axis represents log-moneyness ($k - x$) and the vertical axis represents option maturity T . Ranging from darkest to lightest, the regions above represent relative errors in increments of 0.1% from $< 0.1\%$ to $> 0.8\%$. The maturity date of the bond is fixed at $\bar{T} = 2$. The following parameters remained fixed $t = 0$, $\kappa_1 = \kappa_2 = 0.9$, $\delta_1 = \delta_2 = \sqrt{0.033}$, $\theta_1 = \theta_2 = \frac{0.08}{0.9}$, $y_1 = y_2 = 0.04$ 78
- 5.6 For the Fong-Vasicek short-rate model described in Section 3.4.4, we plot the approximate implied volatility $\bar{\Sigma}_2$ as a function of log-moneyness $k - x$ with the maturity date of the bond fixed at $\bar{T} = 2$, with the maturity of the option taking the following values $T = \{\frac{1}{12}, \frac{1}{4}, \frac{1}{2}, \frac{3}{4}\}$ and with the correlation parameter taking values $\rho = \{-0.7, -0.3, 0.3, 0.7\}$ corresponding to the blue, orange, green and red curves respectively. The following model parameters remained fixed in all four plots $t = 0$, $\kappa_1 = \kappa_2 = 0.9$, $\delta_2 = \sqrt{0.08}$, $\theta_1 = \theta_2 = 0.08$, $y_2 = 0.08$ 79
- 5.7 For the QOU model described in Section 3.5, we plot exact implied volatility Σ and approximate implied volatility $\bar{\sigma}_n$ up to order $n = 2$ as a function of log-moneyness $k - x$ with the initial date and settlement date of the caplet is fixed at $t = 0$ and $\bar{T} = 2$, respectively, and with the reset date of the caplet taking the following values $T = \{\frac{1}{64}, \frac{1}{32}, \frac{1}{16}, \frac{1}{8}\}$. The zeroth, first, and second order approximate implied volatilities correspond to the orange, green and red curves, respectively, and the blue curve corresponds to the exact implied volatility. The following parameters remained fixed: $q = 0$, $\kappa = 0.9$, $\theta = \frac{0.25}{0.9}$, $\delta = 0.2$ 80

5.8 For the QOU model described in Section 3.5, we plot the exact implied volatility σ and approximate implied volatility $\bar{\sigma}_n$ up to order $n = 2$ as a function of log-moneyness $k - x$ with the initial date and settlement date of the caplet is fixed at $t = 0$ and $\bar{T} = 2$, respectively, and with the reset date of the caplet taking the following values $T = \{\frac{1}{64}, \frac{1}{32}, \frac{1}{16}, \frac{1}{8}\}$. The zeroth, first, and second order approximate implied volatilities correspond to the orange, green and red curves, respectively, and the blue curve corresponds to the exact implied volatility. The following parameters remained fixed: $\kappa = 0.045$, $\delta = \sqrt{0.035}$, $y = \sqrt{0.08}$, $\theta = q = 0$ 81

5.9 For the QOU model described in Section 3.5, we plot the absolute value of the relative error of our second order implied volatility approximation $|\bar{\sigma}_2 - \sigma|/\sigma$ as a function of log-moneyness $k - x$ and caplet reset date T . The horizontal axis represents log-moneyness $k - x$ and the vertical axis represents caplet reset date T . Ranging from darkest to lightest, the regions above represent relative errors in increments of 0.002 from < 0.002 to > 0.018 . The initial date and settlement date of the caplet is fixed at $t = 0$ and $\bar{T} = 2$, respectively. The following parameters remained fixed: $q = 0$, $\kappa = 0.9$, $\theta = \frac{0.25}{0.9}$, $\delta = 0.2$, $y = \sqrt{0.08}$ 82

5.10 For the QOU model described in Section 3.5, we plot the absolute value of the relative error of our second order implied volatility approximation $|\bar{\sigma}_2 - \sigma|/\sigma$ as a function of log-moneyness $k - x$ and caplet reset date T . The horizontal axis represents log-moneyness $k - x$ and the vertical axis represents caplet reset date T . Ranging from darkest to lightest, the regions above represent relative errors in increments of 0.005 from < 0.005 to 0.03. The initial date and settlement date of the caplet is fixed at $t = 0$ and $\bar{T} = 2$, respectively. The following parameters remained fixed: $\kappa = 0.045$, $\delta = \sqrt{0.035}$, $y = \sqrt{0.08}$, $\theta = q = 0$ 83

5.11 Using the parameters Φ^* given in (3.6), we plot the fitted simple forward rate curve $L_t^{T, T+\tau}(\Phi^*)$ along with L_i , the forward LIBOR curve data on the 18 November 2008 where $t = 0$ and $\tau = \frac{1}{2}$ are fixed. The horizontal axis represents T in years and the vertical axis represents the simple forward rate. 84

- 5.12 For the QOU model described in Section 3.5, we plot the exact implied volatility σ and approximate implied volatility $\bar{\sigma}_n$ up to order $n = 2$ as a function of log-moneyness $k - x$ with the initial date and settlement date of the caplet is fixed at $t = 0$ and $\bar{T} = 2$, respectively, and with the reset date of the caplet taking the following values $T = \{\frac{1}{64}, \frac{1}{32}, \frac{1}{16}, \frac{1}{8}\}$. The zeroth, first, and second order approximate implied volatilities correspond to the orange, green and red curves, respectively, and the blue curve corresponds to the exact implied volatility. The parameters $(\kappa, \theta, \delta, q, y) = (\kappa^*, \theta^*, \delta^*, q^*, y^*)$ are given by (3.6). 85
- 5.13 For the QOU model described in Section 3.5, we plot the absolute value of the relative error of our second order implied volatility approximation $|\bar{\sigma}_2 - \sigma|/\sigma$ as a function of log-moneyness $k - x$ and caplet reset date T . The horizontal axis represents log-moneyness $k - x$ and the vertical axis represents caplet reset date T . Ranging from darkest to lightest, the regions above represent relative errors in increments of 0.002 from < 0.002 to 0.012. The initial date and settlement date of the caplet is fixed at $t = 0$ and $\bar{T} = 2$, respectively. The parameters $(\kappa, \theta, \delta, q, y) = (\kappa^*, \theta^*, \delta^*, q^*, y^*)$ are given by (3.6). 86
- 5.14 We plot, from January 2019 to January 2021, the Monthly S&P/Case-Shiller U.S. National Home Price Index [1] in orange with the scale on the right vertical axis, and Weekly 30-Year Fixed Rate Mortgage Average in the United States [2] in blue with the scale on the left vertical axis. Note that decreasing the federal mortgage rate has an effect of increasing the home price index during this short-term period. 87
- 5.15 The graph shows, from January 2019 to January 2021, the Overnight Bank Funding Rate in percentage. Note the sharp drop in the funding rate in the shaded area. 88
- 5.16 We plot the optimal selling and buying functions $J_s(r)$ and $J_b(r)$ when the interest rate is modeled by CIR process using (4.28) and (4.31) as a function of risk-free rate of interest r where $0 < r < 1$ using parameters defined in (4.40). We numerically solved for the selling and buying threshold using (C.11) and (C.14) to obtain $r_s \approx 0.026$ and $r_b \approx 0.167$ which is shown as red points in each respective graph. 89
- 5.17 We plot the graphs of the functions $h_s(q)$ defined in (4.27) and its NCM $\hat{h}_s(q)$ defined in (C.12) using parameter (4.40) for $-2.5 < q < 0$. The red point shows the point q_s which is numerically solved from (C.9), and the orange point shows the inflection point q_s^* of h_s which is numerically solved using the expression of h_s'' in (4.26). 89

- 5.18 We plot the graphs of the functions $h_b(q)$ defined in (4.30) and its NCM $\widehat{h}_b(q)$ defined in (C.13) using parameter (4.40) for $-2.5 < q < 0$. The red point shows the critical point q_b of h_b which is solved numerically using the expression h'_b in (4.25) and orange point shows the inflection point q_b^* of h_b which is numerically solved using the expression of h''_b in (4.26). 90
- 5.19 The following plots used $r = 0.08$ and other parameters from (4.40). The selling and buying threshold r_s and r_b are calculated numerically using (C.11) and (C.14) to obtain $r_s \approx 0.026$ and $r_b \approx 0.167$. We plot the density of the length of time the investor waits before buying $p_{\tau_b^*}(t; r)$ defined in (4.33) for $0 < t < 20$ using the first 100 terms of the truncated infinite sum. The density of the length of time the investor waits before selling $p_{\tau_s^*}(t; r_b)$ defined in (4.34) for $0 < t < 30$ is also plotted using the first 100 terms of the truncated infinite sum. Lastly, the density of the total time the investor waits to buy and sell a home $p_{\tau_b^* + \tau_s^*}(t; r)$ defined in (4.39) for $0 < t < 50$ is plotted using the first 100 indices in the truncated double infinite sum, giving a total of 10000 terms for the approximation. The expectations for each of the random variable calculated in (4.41) are shown as a vertical red bar in the respective graphs. 91

ACKNOWLEDGMENTS

I want to express my heartfelt appreciation to my advisor, Professor Matthew Lorig. Beyond teaching me financial mathematics, Matt consistently emphasized the practical application of mathematics to real-world scenarios, stressing the importance of solving problems that have tangible connections to our everyday lives. Under his guidance, I have become more attentive to details and careful in my approach. Matt has a remarkable ability to simplify seemingly daunting problems, making them more accessible and manageable. During the challenging period of the COVID-19 pandemic, Matt's extraordinary patience and support were instrumental in helping me navigate difficulties. Even in the tough job market that followed, Matt's encouragement continued to bolster my spirits. His mentorship has fostered deep thinking and provided me with new perspectives after every meeting.

I am also immensely grateful to Teerapat Jenrungrot, a Ph.D. student in Computer Science & Engineering and a dear friend since our undergraduate days. His exceptional programming skills constantly amazed me, and his unwavering positivity has lifted me out of my darkest moments. Beyond coding, he is a food enthusiast and an outstanding cook. His advice and recommendations for tech job interviews have played a pivotal role in my accomplishments.

Furthermore, I extend my gratitude to all my friends in the Applied Mathematics Ph.D. cohort, especially Natalie Wellen, who has consistently radiated positivity. Natalie and I shared a mutual interest in financial mathematics and often engaged in discussions on various political topics. Her involvement in political issues is admirable, and her feedback on my general exam preparation has been invaluable. I am confident that Natalie will achieve great success post-Ph.D. with her optimistic outlook.

Lastly, I want to acknowledge my parents, who, despite being thousands of miles away, have always supported my decisions and continually remind me of the importance of pursuing mathematics and earning a Ph.D. Their unwavering encouragement from a young age has been a driving force behind my academic pursuits.

DEDICATION

I dedicate this Thesis to my parents, who never stopped believing in me.

Chapter 1

INTRODUCTION

1.1 Background: Interest Rate and Overview

The research problems we are discussing in this Thesis are centered around the concept of *interest rates*, which often refers to the additional rate at which the borrower of assets or money has to pay back to the loaner. The first recorded use of interest rate dates back to 3000 BC. The collection of old Sumerian documents shows that the systematic loans of metal and grain required the borrower to pay back a larger amount the longer the loan duration was. Once the concept of coins and money was invented, modern regimes deployed interest rates as a tool to govern the finance and economic growth of the realm. Today, interest rate plays a critical role in determining macroeconomic and microeconomic policies and is a large part of everyday decision making such as buying a house, car, etc.

Because of how important interest rates are, modeling their movements is a large area of research in mathematical finance. Mathematically modeling the movement of interest rate requires taking into account deterministic financial factors along with natural factors that fluctuate randomly. Thus, one of the best modeling choices is *stochastic modeling*, which assumes that the dynamics of interest rates consist of the *drift term* that is usually deterministic, and *volatility term* that is usually paired with Brownian motion, which represents random fluctuation through Gaussian normal distribution. An important family of stochastic interest rate models is a *short-rate model*. Some of the most influential and commonly known are Vasicek's model [82] and Cox–Ingersoll–Ross model [18]. We will explore the analytical and numerical differences among these models concerning the implied volatility approximation of options on bonds and forward rates, and house price dynamics in this Thesis.

1.2 Fixed-Income Instrument

A type of financial instruments called *fixed-income instruments* yields a fixed return to the buyer at a specific time. Many fixed-income instruments have their values linked to the movement of interest rates and are also the basis for understanding more complicated types of financial derivatives that we will be discussing in this Thesis. Thus, we begin with introducing the following types of fixed income instruments: *money market account* which represents the amount of money deposited in the saving account, *short-rate* which represents the rate of growth of money market account, *zero-coupon bond* which is a basic and safe long-term investment tool yielding a fix amount to the owner at maturity, and lastly *simple forward rate* which represents loan rates between banks.

1.2.1 Money Market Account and Short-Rate

In a market, we need a notion of how the money grows in a saving account over time. We denote the value of *money market account* by a *positive* stochastic process $M = (M_t)_{t \geq 0}$. Anyone can deposit money into the money market account and always make a profit as time goes on because otherwise there is no incentive for them to do so and keep their money as cash at home. Thus, we assume that M is *non-decreasing*, and for mathematical purposes, we assume additionally that M is *continuous*. These properties of M guarantee that there exists a non-negative process $R = (R_t)_{t \geq 0}$ called instantaneous *short-rate* of interest such that the dynamics of M are of the form

$$dM_t = R_t M_t dt, \quad \rightarrow \quad M_t = M_0 \exp \left(\int_0^t R_s ds \right) \quad (1.1)$$

The short-rate R represents the rate at which the money market account grows. Short-rate is one representation of interest rate and we may use the terms short-rate and interest rate interchangeably in this Thesis. Because the dynamics of R are different for each specific

problem we are discussing in this Thesis, they will be separately specified in the corresponding chapter.

1.2.2 Zero-Coupon Bond

We denote by $B^T = (B_t^T)_{0 \leq t \leq T}$ the value at time t of T -maturity zero-coupon bond or simply T -bond, which is a financial instrument that pays 1 unit of currency at time T called *maturity* to the buyer. As this is the only type of bond we will be discussing, we will frequently refer to zero-coupon bond simply as *bond*. Because the buyer is paid the fixed income at maturity regardless of the initial price, bonds provide a predictable income stream for the buyer and are regarded as a risk-averse investment. Additionally, bonds are ideal for long-term investment that requires a high degree of stability such as a retirement account. Every personal investment portfolio consists of stocks for risk-seeking investments and bonds for risk-averse ones.

Bonds can be issued by corporate entities or governments. Because the issuer may, for example, become bankrupt at maturity and unable to pay the bond owner, the zero-coupon bonds might not pay exactly 1 unit of currency at maturity. In this Thesis, we do not consider this event happening. It is also important to point out that the maturities are not always available at all times T because bonds are usually issued to mature in months or years. For example, the *United States Treasury Security* is the type of fixed income instruments issued by the Department of the Treasury which includes *United States Treasury Bond*. The treasury bond can have maturities up to 30 years and is one of the most stable and frequently traded type of bonds. While the treasury security also includes other types of fixed income instruments such as treasury notes and treasury bills, they are merely derivatives of bonds with different maturity. Thus, the mathematical results regarding bonds and option on bonds presented in this Thesis will naturally extend to all types of treasury securities.

For the computations going forward, we will assume that bonds are traded at all available maturities and pay exactly 1 unit of currency at maturities. Once we specify the dynamics

of short-rate, we will be able to write bond prices explicitly, which will be necessary to price options on bonds later in this Thesis.

1.2.3 Simple Forward Rate

With the goal of introducing *simple forward rate* in mind, let us first introduce *simple interest rate* from time t to T . To begin, suppose that an investor deposits N units of currency to the bank at time t . Then, a bank would pay, a fixed interest rate r during the period $[t, T]$, which means that at time T the investor obtains the extra deposit interest equaling to $Nr(T-t)$. In such case, the *simple interest rate from t to T* is defined by the ratio of the final withdrawal amount to the initial deposit amount

$$\text{Simple Interest Rate from } t \text{ to } T := \frac{N(1 + r(T - t))}{N} = 1 + r(T - t), \quad (1.2)$$

which can be considered as the interest gain at future time T that can be locked in at present time t . As the investor may want to consider a future investment window rather than a fixed time, an immediate question follows: *what is the simple interest rate from time T to time $\bar{T} > T$ that can be locked in at time t ?* To that end, suppose again that the investor begins with N units of currency and that the investor performs the following investments on T -bonds and \bar{T} -bonds at present time t :

- Sells N units of T -bonds, gaining NB_t^T units of currency.
- Buys $NB_t^T/B_t^{\bar{T}}$ units of \bar{T} -bonds, spending $(NB_t^T/B_t^{\bar{T}})(B_t^{\bar{T}}) = NB_t^T$ units of currency.

At time T , the investor needs to pay N units of currency for the amount of T -bonds he sold at time t , and at time \bar{T} will receive $NB_t^T/B_t^{\bar{T}}$ units of currency for the amount of \bar{T} -bonds he has bought at time t . In this case, the simple interest rate from T to \bar{T} is $\frac{NB_t^T/B_t^{\bar{T}}}{N} = B_t^T/B_t^{\bar{T}}$, and this amount must match the form of simple interest rate given by (1.2). Thus, if we denote the process $L^{T,\bar{T}} = (L_t^{T,\bar{T}})_{0 \leq t \leq T}$ as the simple interest rate from T to \bar{T} that can be locked in at time t , which is commonly known as *simple forward rate from T to \bar{T}* , we must

have that

$$1 + L_t^{T, \bar{T}}(\bar{T} - T) = \frac{B_t^T}{B_t^{\bar{T}}}, \quad \rightarrow \quad L_t^{T, \bar{T}} = \frac{1}{\bar{T} - T} \left(\frac{B_t^T}{B_t^{\bar{T}}} - 1 \right). \quad (1.3)$$

Because simple forward rate essentially represents the simple interest rate during a future period calculated at a present time, it is used to represent the rates at which deposits between banks are exchanged at a future period called *interbank rates*. One of the most standardized and commonly used interbank rate is *London Interbank Offered Rate (LIBOR)*, which served as the global benchmark of the rate that global banks lend to one another. The importance of LIBOR motivates the research done in this Thesis regarding option on simple forward rate.

Once we specify the dynamics of short-rate, we will be able to write simple forward rate explicitly. As simple forward rate is the only type of forward rate discussed in this Thesis, we will use the terms interchangeably.

1.3 Risk-Neutral Pricing

We will be pricing multiple assets, such as bonds, forward rates, and the corresponding options in this Thesis. In practice, accurately pricing assets at a future time is an impossible task as it requires knowing precisely the dynamics of all factors that drive the price in advance. Theoretically, however, asset prices can be written as functions of stochastic processes under appropriate probability measures. Many assumptions are required to ensure that theoretical pricing is possible. One of the most important assumptions is that the market is *fair* which is loosely defined as nobody in the market can always generate guaranteed profit with zero initial investment. The act of someone being able to perform such an investment is called an *arbitrage*. In any market that we want to price assets theoretically, we must first ensure that it has no arbitrage. To mathematically define arbitrage, we will first define what a *self-financing portfolio* is.

Definition 1.3.1. Suppose that the market consists of finite list of n assets, and the value of i -th asset at time t is given by the process $A^i = (A_t^i)_{t \geq 0}$, for $i = 1, 2, \dots, n$. A portfolio with

value represented by the process $X = (X_t)_{t \geq 0}$ is a *self-financing portfolio* if the following conditions are satisfied:

- The value of portfolio X at a time t is given by

$$X_t = \sum_{i=1}^n \Delta_t^i A_t^i,$$

where Δ_t^i represents the number of shares held at time t of i -th asset.

- The changes to the portfolio value are only due to the changes in asset values and not to any external factors, in other words,

$$dX_t = \sum_{i=1}^n \Delta_t^i dA_t^i.$$

This means that any gains or losses in a self-financing portfolio are not the results of, for example, an addition or removal of cash in the portfolio.

We are now able to introduce the mathematical definition of arbitrage as follows.

Definition 1.3.2. Suppose that a portfolio whose value is represented by a process $X = (X_t)_{t \geq 0}$ is a self-financing portfolio and that the financial market is associated with probability measure \mathbb{P} called *physical measure*. The portfolio X is an *arbitrage* if the following properties are satisfied:

- $X_0 = 0$
- $\mathbb{P}(X_T \geq 0) = 1$
- $\mathbb{P}(X_T > 0) > 0$

for some $T > 0$.

The market we are discussing in this Thesis will not have arbitrage. This condition is necessary for *the first fundamental theorem of asset pricing* which we will now introduce and will be applied repeatedly to price different types of assets throughout this Thesis.

Theorem 1.3.3 (The first fundamental theorem of asset pricing). *Suppose that a financial market is associated with a physical measure \mathbb{P} . For any positive self-financing portfolio $N = (N_t)_{t \geq 0}$, a market has no arbitrage if and only if there exists a probability measure $\tilde{\mathbb{P}}$ called the risk-neutral measure which is equivalent to \mathbb{P} such that for any self-financing portfolio X , X/N is a $\tilde{\mathbb{P}}$ -martingale, which means that*

$$\tilde{\mathbb{E}} \left(\frac{X_T}{N_T} \middle| \mathcal{F}_t \right) = \frac{X_t}{N_t}, \quad \text{for any } T \geq t, \quad (1.4)$$

where $\tilde{\mathbb{E}}$ is an expectation under $\tilde{\mathbb{P}}$ and the filtration \mathcal{F}_t represents the information observed in the market at or before time t such as the historical price of stocks or observed interest rate.

The proof can be found in, for example, [77, Theorem 5.4.7]. The self-financing portfolio N used in pricing equation (1.4) is generally called a *numéraire*. We will be using (1.4) repeatedly throughout this Thesis with appropriately chosen numéraire. As an example application of risk-neutral pricing, we will now price the bond.

Example 1.3.4. Define the T -bond $B^T = (B_t^T)_{t \geq 0}$ as in Section 1.2.2. We will use the money market account M given in (1.1), which is a self-financing portfolio, as the numéraire. In the absence of arbitrage, the process B^T/M must be a martingale under risk-neutral measure $\tilde{\mathbb{P}}$. Using (1.4) and with the shorthand $\tilde{\mathbb{E}}_t(\cdot) := \tilde{\mathbb{E}}(\cdot | \mathcal{F}_t)$ we have that

$$\frac{B_t^T}{M_t} = \tilde{\mathbb{E}}_t \left(\frac{B_T^T}{M_T} \right) = \tilde{\mathbb{E}}_t \left(\frac{1}{M_T} \right),$$

where we have used $B_T^T = 1$. Solving for B_t^T , we obtain

$$B_t^T = \tilde{\mathbb{E}}_t \left(\frac{M_t}{M_T} \right) = \tilde{\mathbb{E}}_t \left(e^{-\int_t^T R_{sds}} \right), \quad (1.5)$$

where we have used (1.1) in the second equality. The bond price is now given by an expectation under a risk-neutral measure of function of the short-rate, which will have a closed form once we specified the short-rate dynamics.

1.4 Options and Implied Volatilities

An *option* is defined as a contract between two parties where the buyer of the option owns the right to buy (*call* option) or sell (*put* option) an underlying asset at a certain price on or before a specified date in the future called *maturity* date. In this Thesis, we will limit ourselves to the European option which allows the option to be exercised only *exactly* at the maturity date. The call and put options have associated *strike* price, which is the agreed-upon price that the asset will be bought or sold at the maturity date, respectively. Thus, if the underlying asset price at maturity is larger than the sum of the current option price and the strike price, the call option buyer will earn a profit when they exercise the option. The same line of reasoning goes for put. Thus, an option is typically used to hedge risk in the future because the cost of buying/selling is never larger than the strike price.

If the underlying asset is digital, such as stock or bond, then there is no need to consider the logistics of transferring the underlying assets to the call owner. However, a very rare event happened when the oil price during COVID 2019 pandemic dropped very low and made the oil option value decreased to near zero. Due to the logistics of transporting oil to the owner of the call (which the call owner has to pay for), most investors cannot afford to have barrels of oil delivered to their residents and pay for shipment costs and maintenance. Thus, the calls had to price in these costs and the value of the call options became negative, meaning that the owner of the call would prefer to pay someone else to take the shipment of the oil. While such a scenario is possible, they are very rare and we will not consider shipment, maintenance, and transaction costs in this Thesis, thus the price of an option will always be non-negative.

At this point, we can formally price the European option as follow. Suppose that $S = (S_t)_{t \geq 0}$ denotes the value of an underlying asset of the option and $U = (U_t)_{0 \leq t \leq T}$ denotes the value of a European option written on S with strike price $K > 0$ that pays $\varphi(S_T)$ at time T for some function $\varphi : \mathbb{R} \rightarrow \mathbb{R}$. The function φ is called a *payoff function* and for a call and put

option are defined as

$$\text{Call option: } \varphi(s) = (s - K)^+, \quad \text{Put option: } \varphi(s) = (K - s)^+. \quad (1.6)$$

We will once again use the money market account M as a numéraire. With $\tilde{\mathbb{P}}$ as the risk-neutral measure, in the absence of arbitrage, the process U/M must be a $\tilde{\mathbb{P}}$ -martingale, we have from (1.4) that

$$\frac{U_t}{M_t} = \tilde{\mathbb{E}}_t\left(\frac{U_T}{M_T}\right) = \tilde{\mathbb{E}}_t\left(\frac{\varphi(S_T)}{M_T}\right), \quad \rightarrow \quad U_t = \tilde{\mathbb{E}}_t\left(\frac{M_t}{M_T}\varphi(S_T)\right). \quad (1.7)$$

Note that while we have chosen the money market account as a numéraire here, at other points we may use a different self-financing portfolio, such as a bond, as a numéraire.

1.4.1 Option on Bonds

Because bonds are a large part of any personal portfolio, it is important to protect the portfolio against unfavorable movements of bond price, which, as we have seen in (1.5), is directly related to interest rate movements. The bonds could have a long time until maturity, requiring the knowledge of long-term interest rate movements to invest appropriately. The options on those bonds, however, can mature at any time long before maturity. Thus, options on bonds can offer short-term protection against long-term interest rate movements. The payoff for the options written on \bar{T} -bond that matures at time T with strike price K are given by

$$\text{Call option on bonds: } \varphi(B_T^{\bar{T}}) = (B_T^{\bar{T}} - K)^+,$$

$$\text{Put option on bonds: } \varphi(B_T^{\bar{T}}) = (K - B_T^{\bar{T}})^+.$$

Options on bonds are offered as financial products from certain financial groups, such as CME group ¹ who offers options on treasury bond and ICAP's ² desks is a market maker for the global bond options markets.

¹CME Group Treasury Bonds Options, <https://www.cmegroup.com/markets/interest-rates/us-treasury/30-year-us-treasury-bond.quotes.options.html>

²Option on Bonds product, <https://www.icap.com/what-we-do/our-markets-and-products/products/bond-options.aspx>

1.4.2 Option on Simple Forward Rates

Call and put options on simple forward rates are known as *caplet* and *floorlet*, respectively, and are important fixed-income derivatives. The payoff for the option written on simple forward rate from time T to \bar{T} that matures at time T with strike price K are given by

$$\begin{aligned} \text{Caplet: } \varphi(L_T^{T,\bar{T}}) &= (\bar{T} - T)(L_T^{T,\bar{T}} - K)^+, \\ \text{Floorlet: } \varphi(L_T^{T,\bar{T}}) &= (\bar{T} - T)(K - L_T^{T,\bar{T}})^+. \end{aligned} \quad (1.8)$$

The form of caplet and floorlet payoff (1.8) show that the owner of a caplet gains profit from a rise in forward rates above the strike, which makes it so that caplet offers protection against a rising forward rate, and similarly, floorlet offers protection against falling forward rate.

1.4.3 Black-Scholes Option Price and Implied Volatility

In order to discuss the factors that affect option price, we first observe that the option price (1.7) is directly determined by the dynamics of underlying asset S and money market account M . To proceed, we will now specify their dynamics under *Black-Scholes Market Model* which assumes that the dynamics of S and M are given by the following system of stochastic differential equations (SDEs)

$$\left. \begin{aligned} dS_t &= rS_t dt + \Sigma S_t d\tilde{W}_t, \\ dM_t &= rM_t dt, \end{aligned} \right\} \quad (1.9)$$

which assumes that the dynamics of S are given by *Geometric Brownian Motion (GBM)* under risk-neutral measure $\tilde{\mathbb{P}}$ with drift r and volatility Σ , that r is also the constant short-rate and that \tilde{W} is a $\tilde{\mathbb{P}}$ -Brownian motion.

The GBM process is a well-known and frequently used model for the dynamics of risky assets for multiple reasons:

- Under GBM dynamics, the value of S is always nonnegative, which is the case for realistic asset pricing. For example, the stock price never goes below zero.

- The GBM process is a *Markov process* under $\tilde{\mathbb{P}}$, meaning that given the present value of the asset, the future value only depends on the present value and is independent of the values in the past. Mathematically, Markov property of S can be stated as follow. For any function $f : \mathbb{R} \rightarrow \mathbb{R}$,

$$\tilde{\mathbb{E}}(f(S_T)|\mathcal{F}_t) = \tilde{\mathbb{E}}(f(S_T)|S_t), \quad \text{for } T \geq t. \quad (1.10)$$

This property will be useful in calculating explicit Black-Scholes option prices.

- The asset value S has the following closed-form

$$S_t = S_0 \exp \left(\left(r - \frac{\Sigma^2}{2} \right) t + \Sigma \tilde{W}_t \right). \quad (1.11)$$

This closed form is useful for calculating explicit formulas related to risky asset pricing.

The model assumes in (1.9) that the short-rate R is a constant value $r > 0$, and thus, using (1.1), the form of M is deterministic and is given by $M_t = e^{rt} M_0$.

Next, we will present the *Black-Scholes call option price*, which is the unique call option price under Black-Scholes market model. The Black-Scholes price at time t of a call option with underlying asset S , maturity T and strike K denoted by C^{BS} , is given by

$$\begin{aligned} C^{\text{BS}}(t, S_t; T, K, \Sigma) &= \tilde{\mathbb{E}} \left(\frac{M_t}{M_T} (S_T - K)^+ \middle| \mathcal{F}_t \right) = \tilde{\mathbb{E}} \left(\frac{M_t}{M_T} (S_T - K)^+ \middle| S_t \right) \\ &= \left(S_t \Phi(d_+) - K \Phi(d_-) e^{-r(T-t)} \right), \\ d_{\pm} &:= \frac{1}{\Sigma \sqrt{T-t}} \left(\log \frac{S_t}{K} + \left(r \pm \frac{\Sigma^2}{2} \right) (T-t) \right), \\ \Phi(d) &:= \int_{-\infty}^d dx \frac{1}{\sqrt{2\pi}} e^{-x^2/2}, \end{aligned} \quad (1.12)$$

where the first equality of (1.12) followed from (1.6) and (1.7), the second equality followed from the Markov property (1.10) of S and the third equality is derived from applying (1.11) and Feynman–Kac formula and solve the corresponding PDE which is the details that we have omitted here but can be found in many sources such as [77, Section 5.2.5]. Note that

the call option price C^{BS} in (1.12) is a function of observable variables, namely, current time t , the price of asset S_t , the maturity T , strike price K and an unobservable variable *implied volatility* Σ . While Σ is unobserved, it can be calculated from the observed call price as follow. Suppose that $C^{Market}(T, K)$ is the observable price at time t of the call option at maturity T and strike K which is usually the way option price is listed in the market. Then, Σ is a unique positive solution to the equation

$$C^{BS}(t, S_t; T, K, \Sigma) = C^{Market}(T, K). \quad (1.13)$$

While (1.13) is guaranteed to have a unique positive solution for Σ , due to the complicated form of (1.12), there is no *closed form solution*. The importance of Σ established a large area of research in estimating the implied volatility efficiently and accurately. Our research will present one such estimation, namely, asymptotic approximation to implied volatility of options on bonds and forward rates. The Black-Scholes option price (1.12) is only a basis for introducing the concept of implied volatility. The form for the implied volatility of options on bond and on forward rate will be different. Most importantly, the short-rate R will *not* be a constant as it is in (1.9), but will be represented by an appropriate term-structure model. At this point, we have introduced all necessary basic definitions required to understand the purpose of this thesis. We will now provide an outline for each chapter.

1.5 Thesis Outline

The rest of this Thesis proceeds as follows: the first part of the Thesis discusses the asymptotic approximation of the implied volatility of option on bonds and caplets. In Chapter 2 we first give specifications for short-rates and use them to derive explicit expressions for the values of options on bonds and on simple forward rates. Next, we provide the connection between short-rate models and local-stochastic volatility models and determine these options prices as solutions to certain PDEs. In Chapter 3, we give an overview of how we obtain an asymptotic approximation to the solution of such PDEs. Then, we explored how the asymptotic approximation for these lends itself to that of the implied volatility and provide

numerical examples under certain term-structure models. These conclude the first part of the thesis.

The second part of the thesis is in Chapter 4 which discusses another problem of finding the optimal time to buy and sell a home. We take another look at interest rates and how they affect home prices. Next, we frame the optimal profit an investor would make by buying and selling a home as a nested optimal stopping problem. Lastly, we solved the nested optimal stopping problems and perform numerical examples under specific term-structure model.

Chapter 2

MODELING SHORT-RATE

As discussed in the introduction, our first step to obtaining the explicit form for bonds price, forward rates, and the corresponding option prices, is to specify a closed form for short-rate under a term-structure model. One of the most important and well known term-structure model is an *Affine Term-Structure (ATS)* model. This model allows the bond price to be written as an affine function of the factors that drive the short rate. Another model, *Quadratic Term-Structure (QTS)* model, allows the bond price to be written as a quadratic function of the factors that drive the short rate. The main focus of this chapter will be presenting bonds price, forward rates and the corresponding options price under these models.

2.1 Assumptions

To begin, we will impose certain assumptions that allows us to effectively use the tools introduced so far. We consider a financial market over a time horizon from zero to $\bar{T} < \infty$ with no arbitrage and no transaction costs, which enables the use the risk-neutral pricing formula per Theorem (1.3.3). We fix a complete probability space $(\Omega, \mathcal{F}, \tilde{\mathbb{P}})$ and a filtration $\mathbb{F} = (\mathcal{F}_t)_{0 \leq t \leq \bar{T}}$. The probability measure $\tilde{\mathbb{P}}$ represents risk-neutral measure taking the money market account $M = (M_t)_{0 \leq t \leq \bar{T}}$ as numéraire. The filtration \mathbb{F} represents the history of the market.

2.2 Short-Rate and Bond Price

We further suppose that the short-rate R defined in (1.1) is given by

$$R_t = r(Y_t), \tag{2.1}$$

for some function $r : \mathbb{R}^d \rightarrow \mathbb{R}_+$ and some Markov diffusion process $Y = (Y_t^{(1)}, Y_t^{(2)}, \dots, Y_t^{(d)})^\top$, where \top denotes the matrix transpose. The process Y represents the *auxiliary factors* that drive the short-rate, and we further suppose that Y is the unique strong solution of a stochastic differential equation (SDE) of the form

$$dY_t = \mu(t, Y_t)dt + \sigma(t, Y_t)d\widetilde{W}_t, \quad (2.2)$$

for some functions $\mu : [0, \bar{T}] \times \mathbb{R}^d \rightarrow \mathbb{R}^d$ and $\sigma : [0, \bar{T}] \times \mathbb{R}^d \rightarrow \mathbb{R}^{d \times d}$, where $\widetilde{W} = (\widetilde{W}_t^{(1)}, \widetilde{W}_t^{(2)}, \dots, \widetilde{W}_t^{(d)})_{t \geq 0}^\top$ is a d -dimensional $(\widetilde{\mathbb{P}}, \mathbb{F})$ -Brownian motion. Thus, the i th component of Y is given by

$$dY_t^{(i)} = \mu_i(t, Y_t)dt + \sum_{j=1}^d \sigma_{i,j}(t, Y_t)d\widetilde{W}_t^{(j)}. \quad (2.3)$$

Next, for any $T \leq \bar{T}$, let us define $\Gamma(\cdot, \cdot; T, \zeta) : [0, T] \times \mathbb{R}^d \rightarrow \mathbb{C}^d$ by

$$\Gamma(t, Y_t; T, \zeta) := \widetilde{\mathbb{E}}_t \exp \left(- \int_t^T r(Y_s)ds + \alpha(Y_T; \zeta) \right), \quad \alpha(Y_T; 0) = 0, \quad (2.4)$$

where $\widetilde{\mathbb{E}}_t$ is the \mathcal{F}_t -conditional expectation under $\widetilde{\mathbb{P}}$ and the parameter ζ and the function $\alpha(\cdot; \zeta) : \mathbb{R}^d \rightarrow \mathbb{C}^d$ for each term-structure model are defined by

$$\zeta := \nu, \quad \alpha(y; \nu) := \nu^\top y, \quad \text{for ATS model,} \quad (2.5)$$

$$\zeta := (\nu, \Omega), \quad \alpha(y; \nu, \Omega) := \nu^\top y + y^\top \Omega y, \quad \text{for QTS model,} \quad (2.6)$$

where $\nu \in \mathbb{C}^{d \times 1}$ and $\Omega \in \mathbb{C}^{d \times d}$. While we have used the parameter ν in both (2.5) and (2.6) the parameters from these two models will always be discussed separately. Note that the existence of the function Γ follows from the Markov property of Y .

Formally, Γ satisfies the Kolmogorov backward partial differential equation (PDE)

$$(\partial_t + \mathcal{A}(t) - r)\Gamma(t, \cdot; T, \zeta) = 0, \quad \Gamma(T, y; T, \zeta) = \exp(\alpha(y; \zeta)), \quad (2.7)$$

where the operator \mathcal{A} is the generator of Y under $\widetilde{\mathbb{P}}$. Explicitly, the generator \mathcal{A} is given by

$$\mathcal{A}(t) = \mu(t, y)^\top \nabla_y + \frac{1}{2} \text{Tr}(\sigma(t, y) \sigma^\top(t, y) \nabla_y \nabla_y^\top), \quad (2.8)$$

where $\nabla_y = (\partial_{y_1}, \partial_{y_2}, \dots, \partial_{y_d})^\top$, and “Tr” denotes the trace operator. Using (1.5), (2.1) and (2.4) the price of T -bond at time t is given by

$$B_t^T = \tilde{\mathbb{E}}_t \left(e^{-\int_t^T r(Y_s) ds} \right) = \Gamma(t, Y_t; T, 0). \quad (2.9)$$

To explicitly specify the bond price (2.9), it is left to obtain the solution Γ of the PDE (2.7). At the moment, the solution to (2.7) depends on the form of function r and of the functions μ and σ that define the generator (2.8). Thus, the functions (r, μ, σ) define the solution to (2.7). Because defining term-structure model also requires specifying the functions (r, μ, σ) , we are now in a position to introduce ATS and QTS models, and give the solution to PDE (2.7) for explicit bond price (2.9).

2.3 Affine Term-Structure Model

Affine term-structure models refer to a class of term-structure models in which the price of any zero-coupon bond can be expressed as the exponential of affine function of the instantaneous short-rate. Well-known affine term-structure models include the Vasicek [82], Cox-Ingersoll-Ross (CIR) [18], Hull-White [35] and Fong-Vasicek [27] models, as well as their multi-factor versions. Such models enjoy wide popularity among practitioners and academics alike because they show high degree of model flexibility due to the closed-form expression for bond prices.

Suppose that the short-rate R is described by an ATS model, meaning that the functions (r, μ, σ) defined in (2.1) and (2.2) satisfy

$$r(y) = q + \Xi^\top y, \quad \mu(t, y) = b(t) + \beta^\top(t)y, \quad \sigma(t, y)\sigma^\top(t, y) = \ell(t) + \sum_{i=1}^d \lambda_i(t)y_i, \quad (2.10)$$

for some constants $q \in \mathbb{R}$ and $\Xi \in \mathbb{R}^d$ and some functions $b, \beta_i : [0, \bar{T}] \rightarrow \mathbb{R}^{d \times 1}$ and $\ell, \lambda_i : [0, \bar{T}] \rightarrow \mathbb{R}^{d \times d}$. It can be confirmed by substitution that the function Γ for ATS model defined by (2.4) and (2.5) is given by

$$\Gamma(t, y; T, \nu) = \exp \left(-F(t; T, \nu) - G^\top(t; T, \nu)y \right), \quad (2.11)$$

where the functions $F(\cdot; T, \nu) : [0, T] \rightarrow \mathbb{C}$ and $G(\cdot; T, \nu) : [0, T] \rightarrow \mathbb{C}^{d \times 1}$ are the solution of the following system of coupled ordinary differential equations (ODEs)

$$\begin{aligned} \partial_t F(t; T, \nu) &= \frac{1}{2} G^\top(t; T, \nu) \ell(t) G(t; T, \nu) - b^\top(t) G(t; T, \nu) - q, \\ F(T; T, \nu) &= 0, \end{aligned} \tag{2.12}$$

$$\begin{aligned} \partial_t G_i(t; T, \nu) &= \frac{1}{2} G^\top(t; T, \nu) \lambda_i(t) G(t; T, \nu) - \beta_i^\top(t) G(t; T, \nu) - \Xi_i, \\ G_i(T; T, \nu) &= -\nu_i. \end{aligned} \tag{2.13}$$

The solution to the system (2.12)-(2.13) exists and is unique.

2.4 Quadratic Term-Structure Model

A somewhat lesser-known class of term-structure models are the *quadratic term-structure* (QTS) models, which, as the name suggests, model the short-rate as an quadratic function of the auxiliary factor process. QTS models include some ATS models as special cases and also offer some additional modeling flexibility due to the fact that the zero-coupon bond price can be written as exponential quadratic functions of the auxiliary factors. Moreover, empirical results from [3] indicate that QTS model better captures historical bond price than ATS models. Thus, in addition to ATS models, we consider QTS models for options on bonds and forward rates pricing in this Thesis.

We now define QTS model mathematically. Suppose that the short-rate R is described by a QTS model, meaning that the functions (r, μ, σ) defined in (2.1) and (2.2) satisfy (while we reuse some of the variables from (2.10) in (2.14), there will be no confusion for ATS and QTS models as we will always be specifying which models we are discussing)

$$r(y) = q + y^\top \Xi y, \quad \mu(t, y) = b + \beta^T y, \quad \sigma(t, y) = \ell, \tag{2.14}$$

for some constant $q \in \mathbb{R}_+$ and some matrix $\Xi \in \mathbb{R}^{d \times d}$ that is positive semidefinite and satisfies $\Xi_{i,i} = 1$ for $i = 1, 2, \dots, d$ (note that the restrictions on q and Ξ guarantee that the short-rate R is non-negative) and $b \in \mathbb{R}_+^{d \times 1}$ is a column vector, the matrix $\beta \in \mathbb{R}^{d \times d}$ is

diagonalizable and has negative real components of eigenvalues, the matrix $\ell \in \mathbb{R}^{d \times d}$. Then, following [3, Section 2], every equivalence class of QTS models can be written in this unique *canonical representation* form. Thus, it is sufficient to consider the form (2.14) to cover all possible QTS models.

It can be confirmed by substitution that Γ for QTS model defined by (2.4) and (2.6) is given by

$$\Gamma(t, y; T, \nu, \Omega) = \exp \left(-F(t; T, \nu, \Omega) - G^\top(t; T, \nu, \Omega)y - y^\top H(t; T, \nu, \Omega)y \right), \quad (2.15)$$

where, from [17, Theorem 3.6], the scalar-valued function $F(\cdot; T, \nu, \Omega) : [0, T] \rightarrow \mathbb{C}$, the vector-valued function $G(\cdot; T, \nu, \Omega) : [0, T] \rightarrow \mathbb{C}^{d \times 1}$ and the matrix-valued function $H(\cdot; T, \nu, \Omega) : [0, T] \rightarrow \mathbb{C}^{d \times d}$ solve the following system of ODEs

$$\begin{aligned} \partial_t F(t; T, \nu, \Omega) &= \frac{1}{2} G^\top(t; T, \nu, \Omega) \ell \ell^\top G(t; T, \nu, \Omega) \\ &\quad - \text{Tr}(\ell \ell^\top H(t; T, \nu, \Omega)) - G^\top(t; T, \nu, \Omega) b - q, \\ F(T; T, \nu, \Omega) &= 0, \end{aligned} \quad (2.16)$$

$$\begin{aligned} \partial_t G(t; T, \nu, \Omega) &= 2H^\top(t; T, \nu, \Omega) \ell \ell^\top G(t; T, \nu, \Omega) - \beta G(t; T, \nu, \Omega) \\ &\quad - 2H^\top(t; T, \nu, \Omega) b, \\ G(T; T, \nu, \Omega) &= -\nu, \end{aligned} \quad (2.17)$$

$$\begin{aligned} \partial_t H(t; T, \nu, \Omega) &= 2H^\top(t; T, \nu, \Omega) \ell \ell^\top H(t; T, \nu, \Omega) - \beta H(t; T, \nu, \Omega) \\ &\quad - H^\top(t; T, \nu, \Omega) \beta^\top - \Xi, \\ H(T; T, \nu, \Omega) &= -\Omega. \end{aligned} \quad (2.18)$$

The solution to the system (2.16),(2.17) and (2.18) exists and is unique.

2.5 Pricing Option on Bonds

In the sections that follow, for conciseness we will present the form of bond price and the corresponding option price that are applicable to both ATS and QTS models. To begin,

note that for ATS models, the functions (F, G) are used to express the form of Γ given in (2.11) and for QTS models, the functions (F, G, H) are used to express the form of Γ given in (2.15). With that in mind, we begin by introducing the shorthands

$$\mathfrak{F}(t; T) := \begin{cases} F(t; T, 0), & \text{for ATS model,} \\ F(t; T, 0, 0), & \text{for QTS model,} \end{cases}$$

and define $\mathfrak{G}(t; T)$ similarly. We also define $\mathfrak{H}(t; T) := H(t; T, 0, 0)$ for QTS model. Next, let us define

$$\chi(t; T) := \begin{cases} -\mathfrak{G}(t; T), & \text{for ATS model,} \\ (-\mathfrak{G}(t; T), -\mathfrak{H}(t; T)), & \text{for QTS model.} \end{cases}$$

Using the introduced shorthands, (2.5), (2.6), (2.11) and (2.15) we can rewrite the bond price (2.9) as

$$B_t^T = \exp \left(-\mathfrak{F}(t; T) + \alpha(Y_t; \chi(t; T)) \right). \quad (2.19)$$

With the expression of the bond price (2.19) that is applicable to both ATS and QTS models, we now proceed to give the expression for option on bond price.

Let $U = (U_t)_{0 \leq t \leq T}$ denotes the value of a European option that pays $\psi(\log B_T^T)$ at time T for some function $\psi : \mathbb{R}_- \rightarrow \mathbb{R}$. With the aim of finding U_t , let $\widehat{\psi} : \mathbb{C} \rightarrow \mathbb{C}$ denote the generalized Fourier transform of ψ , which is defined as follows

$$\widehat{\psi}(\omega) := \int_{-\infty}^{\infty} dx e^{-i\omega x} \psi(x), \quad \omega = \omega_r + i\omega_i, \quad \omega_r, \omega_i \in \mathbb{R}. \quad (2.20)$$

We can recover ψ from $\widehat{\psi}$ using the inverse Fourier transform

$$\psi(x) = \frac{1}{2\pi} \int_{-\infty}^{\infty} d\omega_r e^{i\omega_r x} \widehat{\psi}(\omega). \quad (2.21)$$

Now, noting that, in the absence of arbitrage, the process U/M must be a $(\widetilde{\mathbb{P}}, \mathbb{F})$ -martingale.

We have from (1.7) that

$$U_t = \widetilde{\mathbb{E}}_t \left(\frac{M_t}{M_T} \psi(\log B_T^T) \right).$$

Then, using the form of money market account (1.1), we obtain

$$U_t = \tilde{\mathbb{E}}_t \exp \left(- \int_t^T ds r(Y_s) \right) \psi(\log B_T^{\bar{T}}) \quad (2.22)$$

$$\begin{aligned} &= \frac{1}{2\pi} \int_{-\infty}^{\infty} d\omega_r \hat{\psi}(\omega) \tilde{\mathbb{E}}_t e^{-\int_t^T ds r(Y_s) + i\omega \log B_T^{\bar{T}}} \\ &= \frac{1}{2\pi} \int_{-\infty}^{\infty} d\omega_r \hat{\psi}(\omega) \tilde{\mathbb{E}}_t e^{-\int_t^T ds r(Y_s)} \tilde{\mathbb{E}}_t e^{i\omega \log B_T^{\bar{T}}} \\ &= \frac{1}{2\pi} \int_{-\infty}^{\infty} d\omega_r \hat{\psi}(\omega) e^{-i\omega \mathfrak{F}(T; \bar{T})} \tilde{\mathbb{E}}_t e^{-\int_t^T ds r(Y_s) + \alpha(Y_T; i\omega \chi(T; \bar{T}))} \\ &= \frac{1}{2\pi} \int_{-\infty}^{\infty} d\omega_r \hat{\psi}(\omega) e^{-i\omega \mathfrak{F}(T; \bar{T})} \Gamma(t, Y_t; T, i\omega \chi(T; \bar{T})) \end{aligned} \quad (2.23)$$

$$=: u(t, Y_t; T, \bar{T}), \quad (2.24)$$

where the fourth and fifth equalities follow from (2.4) and (2.19), respectively. In general, the inverse Fourier integral (2.23) that defines u must be computed numerically.

Example 2.5.1. For the particular case of a T -maturity European call option written on $B^{\bar{T}}$ we have

$$\psi(x) = (e^x - e^k)^+, \quad \hat{\psi}(\omega) = \frac{-e^{k-i\omega k}}{\omega^2 + i\omega}, \quad \omega_i < -1, \quad (2.25)$$

where k is the log of the strike. The option on bond price U_t can now be computed by inserting the expression (2.25) for $\hat{\psi}$ into (2.23) and evaluating the integral numerically.

Remark 2.5.2. As $\log B_T^{\bar{T}} \leq 0$ $\tilde{\mathbb{P}}$ -a.s., values of $\psi(x)$ for $x > 0$ do not affect the conditional expectation (2.22) and thus do not affect the value U_t of the option. The values of $\psi(x)$ for $x > 0$ do, however, affect convergence properties of the Fourier transform (2.20) and inverse Fourier transform (2.21). As such, it makes sense to choose values of $\psi(x)$ for $x > 0$ so that these integrals converge for some value of $\omega_i \in \mathbb{R}$.

2.6 Pricing Options on Simple Forward Rates

Let $V = (V_t)_{0 \leq t \leq T}$ denotes the value of a European forward rate option with *reset date* T and *settlement date* \bar{T} that pays $\varphi(\log L_T^{T, \bar{T}})$ at time \bar{T} for some function $\varphi : \mathbb{R} \rightarrow \mathbb{R}$ where $L^{T, \bar{T}}$

represents simple forward rate from T to \bar{T} defined in (1.3). Because the payoff $\varphi(\log L_T^{T,\bar{T}})$ to be made at time \bar{T} is known at time T we have

$$V_T = B_T^{\bar{T}} \varphi(\log L_T^{T,\bar{T}}). \quad (2.26)$$

To see this, simply note that $V_{\bar{T}} = B_{\bar{T}}^{\bar{T}} \varphi(\log L_T^{T,\bar{T}}) = \varphi(\log L_T^{T,\bar{T}})$. Using (1.3), $B_T^T = 1$, and with the shorthand $\bar{\tau} := \bar{T} - T$, we can express V_T as a function of $B_T^{\bar{T}}$ as follows

$$V_T = B_T^{\bar{T}} \varphi\left(\log \left[\frac{1}{\bar{\tau}} \left(\frac{1}{B_T^{\bar{T}}} - 1\right)\right]\right) = e^{\log B_T^{\bar{T}}} \varphi\left(\log \left[\frac{1}{\bar{\tau}} \left(e^{-\log B_T^{\bar{T}}} - 1\right)\right]\right) =: \psi(\log B_T^{\bar{T}}) \quad (2.27)$$

Thus, we can view a forward rate option on $L^{T,\bar{T}}$ with reset date T , settlement date \bar{T} and payoff $\varphi(\log L_T^{T,\bar{T}})$ as a European option on B^T with expiration date T and payoff $\psi(\log B_T^{\bar{T}})$, where ψ is defined in (2.27). It follows that

$$V_t = u(t, Y_t; T, \bar{T}), \quad \text{where} \quad \psi(x) = e^x \varphi\left(\log \left[\frac{1}{\bar{\tau}} \left(e^{-x} - 1\right)\right]\right), \quad (2.28)$$

with u given by (2.24).

Example 2.6.1. An important example of a European forward rate option is a *caplet*, which we introduced in Section 1.4.2 which has a payoff

$$\varphi(\log L_T^{T,\bar{T}}) = \bar{\tau} (e^{\log L_T^{T,\bar{T}}} - e^k)^+.$$

Here, $k := \log K$ is the log strike of the caplet. We have from (2.28) that

$$\psi(x) = (1 + \bar{\tau} e^k) \left(\frac{1}{1 + \bar{\tau} e^k} - e^x \right)^+,$$

and thus, from (2.20), the generalized Fourier transform of ψ is given by

$$\widehat{\psi}(\omega) = \frac{-(1 + \bar{\tau} e^k) i \omega}{\omega^2 + i \omega}, \quad \omega_i > 0. \quad (2.29)$$

The caplet price V_t can now be computed by inserting the expression (2.29) for $\widehat{\psi}$ into (2.23) and evaluating the integral numerically.

2.7 Local Stochastic Volatility Model

While (2.24) in conjunction with (2.25) can be used to compute option on bond prices, and (2.28) in conjunction with (2.29) can be used to compute option on forward rate prices, the resulting expression tells us very little about the corresponding implied volatilities. In this section, we will establish a precise relation between term-structure models and local-stochastic volatility models. This relation will be used in subsequent sections to find an explicit approximation for the corresponding implied volatilities.

We begin by deriving the dynamics of B^T/M . Using (1.1) and (2.19), we have by Itô's Lemma that

$$d\left(\frac{B_t^T}{M_t}\right) = \left(\frac{B_t^T}{M_t}\right)\gamma^\top(t, Y_t; T)d\widetilde{W}_t, \quad (2.30)$$

where we have introduced the vector-valued function $\gamma(\cdot, \cdot; T) : [0, T] \times \mathbb{R}^{d \times 1} \rightarrow \mathbb{R}^{d \times 1}$, which is defined as follows

$$\begin{aligned} \gamma(t, Y_t; T) &:= \sigma(t, Y_t)^\top \nabla_y \log \Gamma(t, Y_t; T, 0), \\ &= \begin{cases} -\sigma(t, Y_t)^\top \mathfrak{G}(t; T), & \text{for ATS model,} \\ -\sigma(t, Y_t)^\top \left(\mathfrak{G}(t; T) + \left(\mathfrak{H}(t; T) + \mathfrak{H}^\top(t; T) \right) Y_t \right), & \text{for QTS model.} \end{cases} \end{aligned} \quad (2.31)$$

Observe that B^T/M is a $(\widetilde{\mathbb{P}}, \mathbb{F})$ -martingale, as it must be.

Now, let us denote by $\widetilde{\mathbb{P}}^T$ the T -forward probability measure, whose relation to $\widetilde{\mathbb{P}}$ is given by the following Radon-Nikodym derivative

$$\frac{d\widetilde{\mathbb{P}}^T}{d\widetilde{\mathbb{P}}} := \frac{M_0 B_T^T}{B_0^T M_T} = \exp\left(-\frac{1}{2} \int_0^T \|\gamma(t, Y_t; T)\|^2 dt + \int_0^T \gamma^\top(t, Y_t; T) d\widetilde{W}_t\right), \quad (2.32)$$

where $\|\gamma\|^2 = \gamma^\top \gamma$. Observe that the last equality follows from (2.30). We note that, by Girsanov's theorem and (2.32), the process $\widetilde{W}^T := (\widetilde{W}_t^{T,(1)}, \widetilde{W}_t^{T,(2)}, \dots, \widetilde{W}_t^{T,(d)})_{0 \leq t \leq T}^\top$, defined as follows

$$\widetilde{W}_t^T := -\int_0^t \gamma(s, Y_s; T) ds + \widetilde{W}_t, \quad (2.33)$$

is a d -dimensional $(\widetilde{\mathbb{P}}^T, \mathbb{F})$ -Brownian motion. The following lemma will be useful.

Lemma 2.7.1. *Let $\Pi = (\Pi_t)_{0 \leq t \leq \bar{T}}$ denote the value of a self-financing portfolio and let $\Pi^T = (\Pi_t^T)_{0 \leq t \leq T}$, defined by $\Pi_t^T := \Pi_t/B_t^T$, be the T -forward price of Π . Then the process Π^T is a $(\tilde{\mathbb{P}}^T, \mathbb{F})$ -martingale.*

Proof. Define the Radon-Nikodym derivative process $Z = (Z_t)_{0 \leq t \leq T}$ by $Z_t := \tilde{\mathbb{E}}_t(d\tilde{\mathbb{P}}^T/d\mathbb{P})$. Using the fact that Π/M is a $(\tilde{\mathbb{P}}, \mathbb{F})$ -martingale as well as [77, Lemma 5.2.2] we have for any $0 \leq t \leq s \leq T$ that

$$\frac{\Pi_t}{M_t} = \tilde{\mathbb{E}}_t\left(\frac{\Pi_s}{M_s}\right) = Z_t \tilde{\mathbb{E}}_t^T\left(\frac{1}{Z_s} \frac{\Pi_s}{M_s}\right) = \frac{B_t^T}{M_t} \tilde{\mathbb{E}}_t^T\left(\frac{M_s}{B_s^T} \frac{\Pi_s}{M_s}\right), \quad (2.34)$$

where $\tilde{\mathbb{E}}^T$ denotes an expectation under $\tilde{\mathbb{P}}^T$. Dividing both sides of equation (2.34) by B_t^T and canceling common factors of M_t and M_s , we obtain

$$\Pi_t^T = \frac{\Pi_t}{B_t^T} = \tilde{\mathbb{E}}_t^T \frac{\Pi_s}{B_s^T} = \tilde{\mathbb{E}}_t^T \Pi_s^T,$$

which establishes that Π^T is a $(\tilde{\mathbb{P}}^T, \mathbb{F})$ -martingale, as claimed. \square

2.7.1 Option on bonds

Now, let us denote by $X = (X_t)_{0 \leq t \leq T}$ the log of the T -forward price of a \bar{T} -bond $B^{\bar{T}}$. We have from (2.19) that

$$X_t := \log\left(\frac{B_t^{\bar{T}}}{B_t^T}\right) = \mathfrak{F}(t; T) - \mathfrak{F}(t; \bar{T}) + \alpha(Y_t; \chi(t; \bar{T})) - \alpha(Y_t; \chi(t; T)). \quad (2.35)$$

Next, we derive the PDE for the price of option on T -forward price of a \bar{T} -maturity bond $B^{\bar{T}}$ under stochastic volatility settings in the next Proposition.

Proposition 2.7.2. *Let $V^T = V/B^T$ denote the T -forward price of an option that pays $\psi(\log B_T^{\bar{T}})$ at time T . Then there exists a function $v(\cdot, \cdot, \cdot; T, \bar{T}) : [0, T] \times \mathbb{R}_- \times \mathbb{R}^d \rightarrow \mathbb{R}$ such that*

$$V_t^T = v(t, X_t, Y_t; T, \bar{T}).$$

Moreover, the function v satisfies the following PDE

$$(\partial_t + \tilde{\mathcal{A}}(t))v(t, \cdot, \cdot; T, \bar{T}) = 0, \quad v(T, x, y; T, \bar{T}) = \psi(x), \quad (2.36)$$

where $\tilde{\mathcal{A}}$ is the generator of (X, Y) under $\tilde{\mathbb{P}}^T$. Explicitly, $\tilde{\mathcal{A}}$ is given by

$$\begin{aligned} \tilde{\mathcal{A}}(t) &= \frac{1}{2} \|\gamma(t, y; \bar{T}) - \gamma(t, y; T)\|^2 (\partial_x^2 - \partial_x) \\ &\quad + \left(\mu(t, y) + \sigma(t, y) \gamma(t, y; T) \right)^\top \nabla_y + \frac{1}{2} \text{Tr} \left(\sigma(t, y) \sigma^\top(t, y) \nabla_y \nabla_y^\top \right) \\ &\quad + \left(\sigma(t, y) (\gamma(t, y; \bar{T}) - \gamma(t, y; T)) \right)^\top \nabla_y \partial_x. \end{aligned} \quad (2.37)$$

Proof. Noting that V^T is a $(\tilde{\mathbb{P}}^T, \mathbb{F})$ -martingale, we have

$$V_t^T = \frac{V_t}{B_t^{\bar{T}}} = \tilde{\mathbb{E}}_t^T \left(\frac{V_T}{B_T^{\bar{T}}} \right) = \tilde{\mathbb{E}}_t^T \psi(\log B_T^{\bar{T}}) = \tilde{\mathbb{E}}_t^T \psi(X_T) =: v(t, X_t, Y_t; T, \bar{T}),$$

where the existence of the function v follows from the Markov property of (X, Y) . The function v satisfies the Kolmogorov backward PDE (2.36) where $\tilde{\mathcal{A}}$ denotes the generator of (X, Y) under $\tilde{\mathbb{P}}^T$. Thus, we have from (2.3), (2.31) and (2.33) that

$$dY_t = \left(\mu(t, Y_t) + \sigma(t, Y_t) \gamma(t, Y_t; T) \right) dt + \sigma(t, Y_t) d\tilde{W}_t^T. \quad (2.38)$$

Similarly, using (2.30) and (2.35), we find using Itô's Lemma that

$$d \left(\frac{B_t^{\bar{T}}}{B_t^T} \right) = \left(\frac{B_t^{\bar{T}}}{B_t^T} \right) \left(\gamma(t, Y_t; \bar{T}) - \gamma(t, Y_t; T) \right)^\top d\tilde{W}_t^T$$

thus,

$$dX_t = -\frac{1}{2} \|\gamma(t, Y_t; \bar{T}) - \gamma(t, Y_t; T)\|^2 dt + \left(\gamma(t, Y_t; \bar{T}) - \gamma(t, Y_t; T) \right)^\top d\tilde{W}_t^T. \quad (2.39)$$

The explicit expression (2.37) for the generator $\tilde{\mathcal{A}}$ follows from (2.38) and (2.39). \square

Remark 2.7.3. We note using (2.35) that

$$X_t = \mathfrak{F}(t; T) - \mathfrak{F}(t; \bar{T}) + \alpha(Y_t; \chi(t; \bar{T})) - \alpha(Y_t; \chi(t; T)) =: \xi(t, Y_t; T, \bar{T}). \quad (2.40)$$

Let $\tilde{Y} := (Y_t^{(2)}, Y_t^{(3)}, \dots, Y_t^{(d)})_{0 \leq t \leq T}^\top$. In the case of ATS models, the function $\xi(t, y; T, \bar{T})$ defined in (2.40) is invertible with respect to y_1 . Thus, we can write $Y_t^{(1)} = \eta(t, X_t, \tilde{Y}_t; T, \bar{T})$ where η is the inverse of ξ with respect to y_1 . The process (X, \tilde{Y}) is a d -dimensional Markov process with a non-singular instantaneous covariance matrix and thus, a uniformly elliptic generator. We present in Proposition 2.7.5 the steps to reducing the dimension of $\tilde{\mathcal{A}}$ to only involve (X, \tilde{Y}) , which effectively eliminates the need of $Y^{(1)}$.

Remark 2.7.4. In the case of QTS models, however, the function $\xi(t, y; T, \bar{T})$ defined in (2.40) is *not* invertible with respect to any y_j for $j \in \{1, 2, \dots, d\}$. Thus, the generator $\tilde{\mathcal{A}}$ defined in (2.42) is not uniformly elliptic. The setting here is similar to the settings in [44] and [8] where the authors use the approximation methods described in Chapter 3 to find explicit approximations of implied volatility for options on leveraged exchange traded funds and the volatility index, respectively. As the authors of those papers point out, the lack of a uniformly elliptic generator does *not* complicate the construction of a formal implied volatility approximation.

As mentioned in Remark 2.7.3 we will use the fact that ξ is invertible in the case of ATS models, to rewrite the generator $\tilde{\mathcal{A}}$ given in (2.37) more efficiently in the following Proposition 2.7.5.

Proposition 2.7.5. *Suppose that the short rate R given in (2.1) is defined under ATS model (2.10). Let $V^T = V/B^T$ denote the T -forward price of an option that pays $\psi(\log B_T^{\bar{T}})$ at time T . Then there exists a function $v(\cdot, \cdot, \cdot; T, \bar{T}) : [0, T] \times \mathbb{R}_- \times \mathbb{R}^{d-1} \rightarrow \mathbb{R}$ such that*

$$V_t^T = v(t, X_t, \tilde{Y}_t; T, \bar{T}).$$

Moreover, the function v satisfies the following PDE

$$(\partial_t + \tilde{\mathcal{A}}(t))v(t, \cdot, \cdot; T, \bar{T}) = 0, \quad v(T, x, \tilde{y}; T, \bar{T}) = \psi(x), \quad (2.41)$$

where $\tilde{\mathcal{A}}$ is the generator of $(X, \tilde{Y}) := (X_t, Y_t^{(2)}, \dots, Y_t^{(d)})_{0 \leq t \leq T}$ under $\tilde{\mathbb{P}}^T$. Explicitly, $\tilde{\mathcal{A}}$ is

given by

$$\begin{aligned}
\tilde{\mathcal{A}}(t) &= \frac{1}{2} \|\tilde{\sigma}^\top(t, x, \tilde{y}; T, \bar{T})(\mathfrak{G}(t; T) - \mathfrak{G}(t; \bar{T}))\|^2 (\partial_x^2 - \partial_x) \\
&+ \sum_{i=2}^d \left(\tilde{\mu}_i(t, x, \tilde{y}; T, \bar{T}) - \sum_{j=1}^d \left(\tilde{\sigma}(t, x, \tilde{y}; T, \bar{T}) \tilde{\sigma}^\top(t, x, \tilde{y}; T, \bar{T}) \right)_{i,j} \mathfrak{G}_j(t; T) \right) \partial_{y_i} \\
&+ \frac{1}{2} \sum_{i=2}^d \sum_{j=2}^d \left(\tilde{\sigma}(t, x, \tilde{y}; T, \bar{T}) \tilde{\sigma}^\top(t, x, \tilde{y}; T, \bar{T}) \right)_{i,j} \partial_{y_i} \partial_{y_j} \\
&+ \sum_{i=2}^d \sum_{j=1}^d \left(\tilde{\sigma}(t, x, \tilde{y}; T, \bar{T}) \tilde{\sigma}^\top(t, x, \tilde{y}; T, \bar{T}) \right)_{i,j} \left(\mathfrak{G}_j(t; T) - \mathfrak{G}_j(t; \bar{T}) \right) \partial_x \partial_{y_i}, \quad (2.42)
\end{aligned}$$

where the functions $\tilde{\mu}(\cdot, \cdot, \cdot; T, \bar{T}) : [0, T] \times \mathbb{R}_- \times \mathbb{R}^{d-1} \rightarrow \mathbb{R}^d$ and $\tilde{\sigma}(\cdot, \cdot, \cdot; T, \bar{T}) : [0, T] \times \mathbb{R}_- \times \mathbb{R}^{d-1} \rightarrow \mathbb{R}^{d \times d}$ are given by

$$\begin{aligned}
\tilde{\mu}(t, x, \tilde{y}; T, \bar{T}) &:= \mu(t, \eta(t, x, \tilde{y}; T, \bar{T}), \tilde{y}), \\
\tilde{\sigma}(t, x, \tilde{y}; T, \bar{T}) &:= \sigma(t, \eta(t, x, \tilde{y}; T, \bar{T}), \tilde{y}), \quad (2.43)
\end{aligned}$$

the function $\eta(\cdot, \cdot, \cdot; T, \bar{T}) : [0, T] \times \mathbb{R}_- \times \mathbb{R}^{d-1} \rightarrow \mathbb{R}$ is defined as follows

$$\eta(t, x, \tilde{y}; T, \bar{T}) = \frac{\mathfrak{F}(t; T) - \mathfrak{F}(t; \bar{T}) - x + \sum_{i=2}^d (\mathfrak{G}_i(t; T) - \mathfrak{G}_i(t; \bar{T})) y_i}{\mathfrak{G}_1(t; \bar{T}) - \mathfrak{G}_1(t; T)}, \quad (2.44)$$

and the functions \mathfrak{F} and \mathfrak{G}_i satisfy the system of coupled ODEs (2.12) and (2.13).

Proof. Noting that V^T is a $(\tilde{\mathbb{P}}^T, \mathbb{F})$ -martingale, we have

$$V_t^T = \frac{V_t}{B_t^T} = \tilde{\mathbb{E}}_t^T \left(\frac{V_T}{B_T^T} \right) = \tilde{\mathbb{E}}_t^T \psi(\log B_T^T) = \tilde{\mathbb{E}}_t^T \psi(X_T) =: v(t, X_t, \tilde{Y}_t; T, \bar{T}),$$

where the existence of the function v follows from the Markov property of (X, \tilde{Y}) . The function v satisfies the Kolmogorov backward PDE (2.41) where $\tilde{\mathcal{A}}$ denotes the generator of (X, \tilde{Y}) under $\tilde{\mathbb{P}}^T$. Thus, we have from equations (2.3), (2.31) and (2.33) that

$$\begin{aligned}
dY_t &= \left(\mu(t, Y_t) - \sigma(t, Y_t) \sigma^\top(t, Y_t) \mathfrak{G}(t; T) \right) dt + \sigma(t, Y_t) d\tilde{W}_t^T. \\
&= \left(\tilde{\mu}(t, X_t, \tilde{Y}_t; T, \bar{T}) - \tilde{\sigma}(t, X_t, \tilde{Y}_t; T, \bar{T}) \tilde{\sigma}^\top(t, X_t, \tilde{Y}_t; T, \bar{T}) \mathfrak{G}(t; T) \right) dt \\
&\quad + \tilde{\sigma}(t, X_t, \tilde{Y}_t; T, \bar{T}) d\tilde{W}_t^T. \quad (2.45)
\end{aligned}$$

where, in the the second equality, we have used $Y_t^{(1)} = \eta(t, X_t, \tilde{Y}_t; T, \bar{T})$, which follows from (2.44). Similarly, using (2.30) and (2.35), we find using Itô's Lemma that

$$\begin{aligned}
dX_t &= -\frac{1}{2}\|\sigma^\top(t, Y_t)(\mathfrak{G}(t; T) - \mathfrak{G}(t; \bar{T}))\|^2 dt \\
&\quad + \sigma^\top(t, Y_t)(\mathfrak{G}(t; T) - \mathfrak{G}(t; \bar{T}))d\tilde{W}_t^T \\
&= -\frac{1}{2}\|\tilde{\sigma}^\top(t, X_t, \tilde{Y}_t; T, \bar{T})(\mathfrak{G}(t; T) - \mathfrak{G}(t; \bar{T}))\|^2 dt \\
&\quad + \tilde{\sigma}^\top(t, X_t, \tilde{Y}_t; T, \bar{T})(\mathfrak{G}(t; T) - \mathfrak{G}(t; \bar{T}))d\tilde{W}_t^T.
\end{aligned} \tag{2.46}$$

The explicit expression (2.42) for the generator $\tilde{\mathcal{A}}$ follows from (2.45) and (2.46). \square

Observe that $e^X = B^{\bar{T}}/B^T$ is a strictly positive $(\tilde{\mathbb{P}}^T, \mathbb{F})$ -martingale. Thus, the process (X, \tilde{Y}) has the same form as a local-stochastic volatility model where X represents the log of the T -forward price of a risky asset (e.g., stock, index, etc.) and \tilde{Y} represents $(d-1)$ non-local factors of volatility.

Example 2.7.6. Consider a one-factor ATS model ($d = 1$). Then X has the form of a (pure) local volatility model with generator (2.42) simplified to

$$\tilde{\mathcal{A}}(t) = c(t, x)(\partial_x^2 - \partial_x), \quad c(t, x) := \frac{1}{2}\tilde{\sigma}^2(t, x; T, \bar{T})\left(\mathfrak{G}(t; T) - \mathfrak{G}(t; \bar{T})\right)^2, \tag{2.47}$$

where we have omitted the argument \tilde{y} as it plays no role.

Example 2.7.7. Consider a two-factor ATS model ($d = 2$). Then the process $(X, Y^{(2)})$ has the form of a local-stochastic volatility model with a single non-local factor of volatility. The generator (2.42) in this case, is given by

$$\tilde{\mathcal{A}}(t) = c(t, x, y_2)(\partial_x^2 - \partial_x) + f(t, x, y_2)\partial_{y_2} + g(t, x, y_2)\partial_{y_2}^2 + h(t, x, y_2)\partial_x\partial_{y_2}, \tag{2.48}$$

where the functions c , f , g and h are given by

$$\begin{aligned}
c(t, x, y_2) &:= \frac{1}{2} \left(\tilde{\sigma}_{1,1}^2(t, x, y_2; T, \bar{T}) + \tilde{\sigma}_{1,2}^2(t, x, y_2; T, \bar{T}) \right) \left(\mathfrak{G}_1(t; T) - \mathfrak{G}_1(t; \bar{T}) \right)^2 \\
&\quad + \left(\tilde{\sigma}_{1,1}(t, x, y_2; T, \bar{T}) \tilde{\sigma}_{2,1}(t, x, y_2; T, \bar{T}) + \tilde{\sigma}_{1,2}(t, x, y_2; T, \bar{T}) \tilde{\sigma}_{2,2}(t, x, y_2; T, \bar{T}) \right) \\
&\quad \times \left(\mathfrak{G}_1(t; T) - \mathfrak{G}_1(t; \bar{T}) \right) \left(\mathfrak{G}_2(t; T) - \mathfrak{G}_2(t; \bar{T}) \right) \\
&\quad + \frac{1}{2} \left(\tilde{\sigma}_{2,1}^2(t, x, y_2; T, \bar{T}) + \tilde{\sigma}_{2,2}^2(t, x, y_2; T, \bar{T}) \right) \left(\mathfrak{G}_2(t; T) - \mathfrak{G}_2(t; \bar{T}) \right)^2, \\
f(t, x, y_2) &:= \tilde{\mu}_2(t, x, y_2; T, \bar{T}) - \left(\tilde{\sigma}_{2,1}^2(t, x, y_2; T, \bar{T}) + \tilde{\sigma}_{2,2}^2(t, x, y_2; T, \bar{T}) \right) \mathfrak{G}_2(t; T) \\
&\quad - \left(\tilde{\sigma}_{1,1}(t, x, y_2; T, \bar{T}) \tilde{\sigma}_{2,1}(t, x, y_2; T, \bar{T}) \right. \\
&\quad \left. + \tilde{\sigma}_{1,2}(t, x, y_2; T, \bar{T}) \tilde{\sigma}_{2,2}(t, x, y_2; T, \bar{T}) \right) \mathfrak{G}_1(t; T), \\
g(t, x, y_2) &:= \frac{1}{2} \left(\tilde{\sigma}_{2,1}^2(t, x, y_2; T, \bar{T}) + \tilde{\sigma}_{2,2}^2(t, x, y_2; T, \bar{T}) \right), \\
h(t, x, y_2) &:= \left(\tilde{\sigma}_{2,1}^2(t, x, y_2; T, \bar{T}) + \tilde{\sigma}_{2,2}^2(t, x, y_2; T, \bar{T}) \right) \left(\mathfrak{G}_2(t; T) - \mathfrak{G}_2(t; \bar{T}) \right) \\
&\quad + \left(\tilde{\sigma}_{1,1}(t, x, y_2; T, \bar{T}) \tilde{\sigma}_{2,1}(t, x, y_2; T, \bar{T}) \right. \\
&\quad \left. + \tilde{\sigma}_{1,2}(t, x, y_2; T, \bar{T}) \tilde{\sigma}_{2,2}(t, x, y_2; T, \bar{T}) \right) \left(\mathfrak{G}_1(t; T) - \mathfrak{G}_1(t; \bar{T}) \right).
\end{aligned}$$

2.7.2 Option on Forward Rates

Note from (1.3) that $L^{T, \bar{T}}$ is the \bar{T} -forward price of a static portfolio consisting of $1/\bar{\tau}$ shares of B^T and $-1/\bar{\tau}$ shares of $B^{\bar{T}}$. As such, we have from Lemma 2.7.1 that $L^{T, \bar{T}}$ is a $(\tilde{\mathbb{P}}^{\bar{T}}, \mathbb{F})$ -martingale.

It will be helpful to write the dynamics of $L^{T, \bar{T}}$ under the \bar{T} -forward measure $\tilde{\mathbb{P}}^{\bar{T}}$. Using Itô's Lemma, (1.3), (2.30) and (2.33), we obtain

$$\begin{aligned}
dL_t^{T, \bar{T}} &= \frac{1}{\bar{\tau}} d \left(\frac{B_t^T}{B_t^{\bar{T}}} \right) = \frac{1}{\bar{\tau}} d \left(\frac{B_t^T / M_t}{B_t^{\bar{T}} / M_t} \right) \\
&= \frac{1}{\bar{\tau}} \left(\frac{B_t^T}{B_t^{\bar{T}}} \right) \left(\gamma^\top(t, Y_t; T) - \gamma^\top(t, Y_t; \bar{T}) \right) d\tilde{W}_t^{\bar{T}} \\
&= \left(L_t^{T, \bar{T}} + \frac{1}{\bar{\tau}} \right) \left(\gamma^\top(t, Y_t; T) - \gamma^\top(t, Y_t; \bar{T}) \right) d\tilde{W}_t^{\bar{T}}. \tag{2.49}
\end{aligned}$$

Now, let us denote by $\tilde{X} = (\tilde{X}_t)_{0 \leq t \leq T}$ the log of the simple forward rate from T to \bar{T} , that is

$$\tilde{X}_t := \log L_t^{T, \bar{T}}.$$

Next, we derive the PDE for the price of option on simple forward rate under stochastic volatility settings in the next Proposition.

Proposition 2.7.8. *As in Section 2.6, let $V = (V_t)_{0 \leq t \leq T}$ denote the value of a European forward rate option with reset date T and settlement date \bar{T} that pays $\varphi(\log L_T^{T, \bar{T}}) = \varphi(\tilde{X}_T)$ at time \bar{T} for some function $\varphi : \mathbb{R} \rightarrow \mathbb{R}$. Let $V^{\bar{T}} = (V_t^{\bar{T}})_{0 \leq t \leq T}$ denote the \bar{T} -forward price of V . Then, there exists a function $v(\cdot, \cdot, \cdot; T, \bar{T}) : [0, T] \times \mathbb{R} \times \mathbb{R}^{d \times 1} \rightarrow \mathbb{R}$ such that*

$$V_t^{\bar{T}} = v(t, \tilde{X}_t, Y_t; T, \bar{T}).$$

Moreover, the function v satisfies the following PDE

$$(\partial_t + \tilde{\mathcal{A}}(t))v(t, \cdot, \cdot; T, \bar{T}) = 0, \quad v(T, x, y; T, \bar{T}) = \varphi(x), \quad (2.50)$$

where the operator $\tilde{\mathcal{A}}$ is given by

$$\begin{aligned} \tilde{\mathcal{A}}(t) &= \frac{1}{2} \left(1 + \frac{e^{-x}}{\bar{\tau}}\right)^2 \|\gamma(t, y; T) - \gamma(t, y; \bar{T})\|^2 (\partial_x^2 - \partial_x) \\ &\quad + \left(\mu(t, y) + \sigma(t, y) \gamma(t, y; \bar{T})\right)^\top \nabla_y + \frac{1}{2} \text{Tr} \left(\sigma(t, y)^\top \sigma(t, y) \nabla_y \nabla_y^\top\right) \\ &\quad + \left(1 + \frac{e^{-x}}{\bar{\tau}}\right) \left(\sigma(t, y) (\gamma(t, y; T) - \gamma(t, y; \bar{T}))\right)^\top \nabla_y \partial_x. \end{aligned} \quad (2.51)$$

Proof. We begin by writing the dynamics of \tilde{X} and Y under the \bar{T} -forward probability measure $\tilde{\mathbb{P}}^{\bar{T}}$. First, using Itô's Lemma and (2.49), we obtain

$$\begin{aligned} d\tilde{X}_t &= -\frac{1}{2} \left(1 + \frac{e^{-\tilde{X}_t}}{\bar{\tau}}\right)^2 \|\gamma(t, Y_t; T) - \gamma(t, Y_t; \bar{T})\|^2 dt \\ &\quad + \left(1 + \frac{e^{-\tilde{X}_t}}{\bar{\tau}}\right) \left(\gamma^\top(t, Y_t; T) - \gamma^\top(t, Y_t; \bar{T})\right) d\tilde{W}_t^{\bar{T}}. \end{aligned}$$

Next, using (2.2) and (2.33), we find

$$dY_t = \left(\mu(t, Y_t) + \sigma(t, Y_t) \gamma(t, Y_t; \bar{T})\right) dt + \sigma(t, Y_t) d\tilde{W}_t^{\bar{T}}.$$

The pair (\tilde{X}, Y) is a Markov process whose generator $\tilde{\mathcal{A}}$ under $\tilde{\mathbb{P}}^{\bar{T}}$ is given by (2.51). Now, using the fact that \bar{T} -forward prices are $(\tilde{\mathbb{P}}^{\bar{T}}, \mathbb{F})$ -martingales and the fact that the process (\tilde{X}, Y) is Markov, there exists a function v such that

$$V_t^{\bar{T}} = \frac{V_t}{B_t^{\bar{T}}} = \tilde{\mathbb{E}}_t^{\bar{T}} \frac{V_T}{B_T^{\bar{T}}} = \tilde{\mathbb{E}}_t^{\bar{T}} \varphi(\tilde{X}_T) = v(t, \tilde{X}_t, Y_t; T, \bar{T}), \quad (2.52)$$

where, in the third equality, we have used (2.26). We have from (2.52) that the function v satisfies the Kolmogorov backward PDE (2.50). \square

Remark 2.7.9. Under ATS model setting, we can follow the same process introduced in Remark 2.7.3 and shown in detailed in Proposition 2.7.5 to obtain the simplified form of the generator $\tilde{\mathcal{A}}$ given by (2.51) with Y_1 eliminated for ATS model.

Remark 2.7.10. The Remark 2.7.4 also applies to the generator $\tilde{\mathcal{A}}$ given by (2.51). As such, while the generator is not uniformly elliptic under the QTS model, this fact does not complicate the construction of a formal implied volatility approximation.

Remark 2.7.11. As $L^{T, \bar{T}} = e^{\tilde{X}}$ is a positive $(\tilde{\mathbb{P}}^{\bar{T}}, \mathbb{F})$ -martingale, the process (\tilde{X}, Y) can be seen as a classical LSV model, where Y represents non-local factors of volatility. For example, under QTS model and for $d = 1$ we have from (2.51) that

$$\tilde{\mathcal{A}}(t) = c(t, x, y)(\partial_x^2 - \partial_x) + f(t, x, y)\partial_y + g(t, x, y)\partial_y^2 + h(t, x, y)\partial_x\partial_y, \quad (2.53)$$

where the functions c , f , g and h are given by

$$\begin{aligned} c(t, x, y) &= \frac{1}{2}\ell^2 \left(1 + \frac{e^{-x}}{\bar{\tau}}\right)^2 \left(\mathfrak{G}(t; \bar{T}) - \mathfrak{G}(t; T) + 2\left(\mathfrak{H}(t; \bar{T}) - \mathfrak{H}(t; T)\right)y\right)^2, \\ f(t, x, y) &= b + \beta y - \ell^2 \left(\mathfrak{G}(t; \bar{T}) + 2\mathfrak{H}(t; \bar{T})y\right), \\ g(t, x, y) &= \frac{1}{2}\ell^2, \\ h(t, x, y) &= \ell^2 \left(1 + \frac{e^{-x}}{\bar{\tau}}\right) \left(\mathfrak{G}(t; \bar{T}) - \mathfrak{G}(t; T) + 2\left(\mathfrak{H}(t; \bar{T}) - \mathfrak{H}(t; T)\right)y\right). \end{aligned}$$

Chapter 3

ASYMPTOTIC OPTION PRICING AND IMPLIED VOLATILITY

While we have obtained the PDEs that the value of option on bonds and forward rates satisfy, there is no closed form for the solution of those PDEs. Thus, we will present the asymptotic approximation to the solution of those PDEs, which is based on [68] and subsequently extended to d -dimensional diffusions in [55, 59]. The asymptotic approximation of price can be extended to that of the implied volatility, as we will see in the later part of this chapter.

3.1 Option Price Asymptotics

We have from (2.41) and (2.50) that the function v satisfies a parabolic PDE of the form

$$(\partial_t + \tilde{\mathcal{A}}(t))v(t, \cdot) = 0, \quad \tilde{\mathcal{A}}(t) = \sum_{|\alpha| \leq 2} a_\alpha(t, z) \partial_z^\alpha, \quad v(T, \cdot) = \varphi, \quad (3.1)$$

where, for brevity, we have omitted the dependence on T and \bar{T} . Note that we have introduced standard multi-index notation

$$\alpha = (\alpha_1, \alpha_2, \dots, \alpha_{d+1}), \quad \partial_z^\alpha = \prod_{i=1}^{d+1} \partial_{z_i}^{\alpha_i}, \quad z^\alpha = \prod_{i=1}^{d+1} z_i^{\alpha_i}, \quad |\alpha| = \sum_{i=1}^{d+1} \alpha_i, \quad \alpha! = \prod_{i=1}^{d+1} \alpha_i!$$

In general, there is no explicit solution to PDEs of the form (3.1). In this section, we will show in a formal manner how an explicit approximation of v can be obtained by using a simple Taylor series expansion of the coefficients $(a_\alpha)_{|\alpha| \leq 2}$ of $\tilde{\mathcal{A}}$. The method described below was introduced for scalar diffusions in [68] and subsequently extended to d -dimensional diffusions in [59, 55].

To begin, for any $\varepsilon \in [0, 1]$ and $\bar{z} : [0, T] \rightarrow \mathbb{R}^{d+1}$, let v^ε be the unique classical solution to

$$0 = (\partial_t + \tilde{\mathcal{A}}^\varepsilon(t))v^\varepsilon(t, \cdot), \quad v^\varepsilon(T, \cdot) = \varphi, \quad (3.2)$$

where the operator $\tilde{\mathcal{A}}^\varepsilon$ is defined as follows

$$\tilde{\mathcal{A}}^\varepsilon(t) := \sum_{|\alpha| \leq 2} a_\alpha^\varepsilon(t, z) \partial_z^\alpha, \quad \text{with} \quad a_\alpha^\varepsilon := a_\alpha(t, \bar{z}(t) + \varepsilon(z - \bar{z}(t))),$$

Observe that $\tilde{\mathcal{A}}^\varepsilon|_{\varepsilon=1} = \tilde{\mathcal{A}}$ and thus $v^\varepsilon|_{\varepsilon=1} = v$. We will seek an approximate solution of (3.2) by expanding v^ε and $\tilde{\mathcal{A}}^\varepsilon$ in powers of ε . Our approximation for v will be obtained by setting $\varepsilon = 1$ in our approximation for v^ε . We have

$$v^\varepsilon = \sum_{n=0}^{\infty} \varepsilon^n v_n, \quad \tilde{\mathcal{A}}^\varepsilon(t) = \sum_{n=0}^{\infty} \varepsilon^n \tilde{\mathcal{A}}_n(t), \quad (3.3)$$

where the functions $(v_n)_{n \geq 0}$ are, at the moment, unknown, and the operators $(\tilde{\mathcal{A}}_n)_{n \geq 0}$ are given by

$$\tilde{\mathcal{A}}_n(t) = \frac{d^n}{d\varepsilon^n} \tilde{\mathcal{A}}^\varepsilon|_{\varepsilon=0} = \sum_{|\alpha| \leq 2} a_{\alpha,n}(t, z) \partial_z^\alpha, \quad a_{\alpha,n} = \sum_{|\eta|=n} \frac{1}{\eta!} (z - \bar{z}(t))^\eta \partial_z^\eta a_\alpha(t, \bar{z}(t)).$$

Note that $a_{\alpha,n}(t, \cdot)$ is the sum of the n th order terms in the Taylor series expansion of $a_\alpha(t, \cdot)$ about the point $\bar{z}(t)$. Inserting the expansions from (3.3) for v^ε and $\tilde{\mathcal{A}}^\varepsilon$ into PDE (3.2) and collecting terms of like order in ε we obtain

$$\mathcal{O}(\varepsilon^0) : \quad 0 = (\partial_t + \tilde{\mathcal{A}}_0(t))v_0(t, \cdot), \quad v_0(T, \cdot) = \varphi, \quad (3.4)$$

$$\mathcal{O}(\varepsilon^n) : \quad 0 = (\partial_t + \tilde{\mathcal{A}}_0(t))v_n(t, \cdot) + \sum_{k=1}^n \tilde{\mathcal{A}}_k(t)v_{n-k}(t, \cdot), \quad v_n(T, \cdot) = 0. \quad (3.5)$$

Now, observe that the coefficients $(a_{\alpha,0})_{|\alpha| \leq 2}$ of $\tilde{\mathcal{A}}_0$ do not depend on z . Thus, $\tilde{\mathcal{A}}_0$ is the generator of a $(d+1)$ -dimensional Brownian motion with a time-dependent drift vector and covariance matrix. As such, v_0 is given by

$$v_0(t, z) = \mathcal{P}_0(t, T)\varphi(z) = \int_{\mathbb{R}^{d+1}} dz' p_0(t, z; T, z')\varphi(z'). \quad (3.6)$$

where \mathcal{P}_0 is the semigroup generated by $\tilde{\mathcal{A}}_0$ and p_0 is the associated transition density (i.e., the solution to (3.4) with $\varphi = \delta_\zeta$). Explicitly, we have

$$p_0(t, z; T, \zeta) = \frac{1}{\sqrt{(2\pi)^{d+1} |\mathbf{C}(t, T)|}} \exp\left(-\frac{1}{2}(\zeta - z - \mathbf{m}(t, T))^\top \mathbf{C}^{-1}(t, T)(\zeta - z - \mathbf{m}(t, T))\right),$$

where \mathbf{m} and \mathbf{C} are given by

$$\mathbf{m}(t, T) := \int_t^T ds m(s), \quad \mathbf{C}(t, T) := \int_t^T ds A(s), \quad (3.7)$$

and m and A are, respectively, the instantaneous drift vector and covariance matrices

$$m(s) := \begin{pmatrix} a_{(1,0,\dots,0),0}(s) \\ a_{(0,1,\dots,0),0}(s) \\ \vdots \\ a_{(0,0,\dots,1),0}(s) \end{pmatrix}, \quad A(s) := \begin{pmatrix} 2a_{(2,0,\dots,0),0}(s) & a_{(1,1,\dots,0),0}(s) & \cdots & a_{(1,0,\dots,1),0}(s) \\ a_{(1,1,\dots,0),0}(s) & 2a_{(0,2,\dots,0),0}(s) & \cdots & a_{(0,1,\dots,1),0}(s) \\ \vdots & \vdots & \ddots & \vdots \\ a_{(1,0,\dots,1),0}(s) & a_{(0,1,\dots,1),0}(s) & \cdots & 2a_{(0,0,\dots,2),0}(s) \end{pmatrix}.$$

By Duhamel's principle, the solution v_n of (3.5) is

$$\begin{aligned} v_n(t, z) &= \sum_{k=1}^n \int_t^T dt_1 \mathcal{P}_0(t, t_1) \tilde{\mathcal{A}}_k(t_1) v_{n-k}(t_1, z) \\ &= \sum_{k=1}^n \sum_{i \in I_{n,k}} \int_t^T dt_1 \int_{t_1}^T dt_2 \cdots \int_{t_{k-1}}^T dt_k \\ &\quad \mathcal{P}_0(t, t_1) \mathcal{A}_{i_1}(t_1) \mathcal{P}_0(t_1, t_2) \mathcal{A}_{i_2}(t_2) \cdots \mathcal{P}_0(t_{k-1}, t_k) \mathcal{A}_{i_k}(t_k) \mathcal{P}_0(t_k, T) \varphi(z), \end{aligned} \quad (3.8)$$

$$I_{n,k} = \{i = (i_1, i_2, \dots, i_k) \in \mathbb{N}^k : i_1 + i_2 + \cdots + i_k = n\}. \quad (3.9)$$

While the expression (3.8) for v_n is explicit, it is not easy to compute as written because operating on a function with \mathcal{P}_0 requires performing a $(d+1)$ -dimensional integral. The following proposition establishes that v_n can be expressed as a differential operator acting on v_0 .

Proposition 3.1.1. *The solution v_n of PDE (3.5) is given by*

$$v_n(t, z) = \mathcal{L}_n(t, T) v_0(t, z), \quad (3.10)$$

where \mathcal{L} is a linear differential operator, which is given by

$$\mathcal{L}_n(t, T) = \sum_{k=1}^n \sum_{i \in I_{n,k}} \int_t^T dt_1 \int_{t_1}^T dt_2 \cdots \int_{t_{k-1}}^T dt_k \mathcal{G}_{i_1}(t, t_1) \mathcal{G}_{i_2}(t, t_2) \cdots \mathcal{G}_{i_k}(t, t_k),$$

the index set $I_{n,k}$ is as defined in (3.9) and the operator \mathcal{G}_i is given by

$$\mathcal{G}_i(t, t_k) := \sum_{|\alpha| \leq 2} a_{\alpha, i}(t_k, \mathcal{Z}(t, t_k)) \partial_z^\alpha, \quad \mathcal{Z}(t, t_k) := z + \mathbf{m}(t, t_k) + \mathbf{C}(t, t_k) \nabla_z. \quad (3.11)$$

Proof. The proof, which is given in [59, Theorem 2.6], relies on the fact that, for any $0 \leq t \leq t_k < \infty$ the operator \mathcal{G}_i in (3.11) satisfies

$$\mathcal{P}_0(t, t_k) \mathcal{A}_i(t_k) = \mathcal{G}_i(t, t_k) \mathcal{P}_0(t, t_k). \quad (3.12)$$

Using (3.12), as well as the semigroup property $\mathcal{P}_0(t_1, t_2) \mathcal{P}_0(t_2, t_3) = \mathcal{P}_0(t_1, t_3)$, we have that

$$\begin{aligned} & \mathcal{P}_0(t, t_1) \mathcal{A}_{i_1}(t_1) \mathcal{P}_0(t_1, t_2) \mathcal{A}_{i_2}(t_2) \cdots \mathcal{P}_0(t_{k-1}, t_k) \mathcal{A}_{i_k}(t_k) \mathcal{P}_0(t_k, T) \varphi(z) \\ &= \mathcal{G}_{i_1}(t, t_1) \mathcal{G}_{i_2}(t, t_2) \cdots \mathcal{G}_{i_k}(t, t_k) \mathcal{P}_0(t, t_1) \mathcal{P}_0(t_1, t_2) \cdots \mathcal{P}_0(t_{k-1}, t_k) \mathcal{P}_0(t_k, T) \varphi \\ &= \mathcal{G}_{i_1}(t, t_1) \mathcal{G}_{i_2}(t, t_2) \cdots \mathcal{G}_{i_k}(t, t_k) \mathcal{P}_0(t, T) \varphi \\ &= \mathcal{G}_{i_1}(t, t_1) \mathcal{G}_{i_2}(t, t_2) \cdots \mathcal{G}_{i_k}(t, t_k) v_0(t, \cdot), \end{aligned} \quad (3.13)$$

where, in the last equality we have used $\mathcal{P}_0(t, T) \varphi = v_0(t, \cdot)$. Inserting (3.13) into (3.8) yields (3.10). \square

Having obtained expressions for the functions $(v_n)_{n \geq 0}$ as differential operators $(\mathcal{L}_n)_{n \geq 0}$ acting on v_0 , we define \bar{v} , the n th order approximation of v , as follows

$$\bar{v}_n := \sum_{k=0}^n v_k.$$

Note that \bar{v}_n depends on the choice of \bar{z} . In general, if one is interested in the value of $v(t, z)$ a good choice for \bar{z} is $\bar{z}(t) = z$.

3.2 Option on Bonds Implied Volatility Asymptotics

Throughout this section, we fix a short rate model (2.1)-(2.2), an initial date t , an option maturity date $T > t$, a bond maturity date $\bar{T} > T$, the initial values $(X_t = \log(B_t^{\bar{T}}/B_t^T), Y_t) = (x, y)$ and a Call payoff $\psi(X_T) = (e^{X_T} - e^k)^+$. Our goal is to find an approximation of implied volatility for *this particular option on bond*. To ease notation, we will sometimes hide the dependence on $(t, x, y; T, \bar{T}, k)$. However, the reader should keep in mind that the implied volatility of the caplet under consideration does depend on $(t, x, y; T, \bar{T}, k)$, even if this is not explicitly indicated. Below, we remind the reader of the *Black model* and provide definitions of the *Black price* and *Black implied volatility*, which will be used throughout this section.

In the *Black model*, the dynamics of T -forward price of $B^{\bar{T}}$ which is $B_t^{\bar{T}}/B_t^T = e^{X_t}$ are given by

$$d\left(\frac{B_t^{\bar{T}}}{B_t^T}\right) = \Sigma\left(\frac{B_t^{\bar{T}}}{B_t^T}\right)d\widetilde{W}_t^T, \quad \text{and thus} \quad dX_t = -\frac{1}{2}\Sigma^2 dt + \Sigma d\widetilde{W}_t^T, \quad (3.14)$$

where $\Sigma > 0$ is the *Black volatility* and \widetilde{W}^T is a scalar $(\widetilde{\mathbb{P}}^T, \mathbb{F})$ -Brownian motion. Equation (3.14) leads to the following definitions.

Definition 3.2.1. The T -forward *Black price* of an option on bond, denoted v^{BS} , is defined as follows

$$v^{\text{BS}}(t, x; T, \bar{T}, k, \Sigma) := \widetilde{\mathbb{E}}^T[(e^{X_T} - e^k)^+ | X_t = x] = \left(e^x \Phi(d_+) - e^k \Phi(d_-)\right), \quad (3.15)$$

where the dynamics of X are given by (3.14) and

$$d_{\pm} := \frac{1}{\Sigma\sqrt{T-t}} \left(x - k \pm \frac{\Sigma^2(T-t)}{2}\right), \quad \Phi(d) := \int_{-\infty}^d dx \frac{1}{\sqrt{2\pi}} e^{-x^2/2}.$$

Definition 3.2.2. The *Black implied volatility* corresponding to the T -forward price v of an option on bond is the unique positive solution Σ of the equation

$$v^{\text{BS}}(t, x; T, \bar{T}, k, \Sigma) = v. \quad (3.16)$$

where the Black price v^{BS} is given by (3.15).

As in the previous section, we will seek an approximation of the implied volatility Σ^ε corresponding to v^ε by expanding Σ^ε in power of ε . Our approximation of Σ will then be obtained by setting $\varepsilon = 1$. We have

$$\Sigma^\varepsilon = \Sigma_0 + \delta\Sigma^\varepsilon, \quad \delta\Sigma^\varepsilon = \sum_{n=1}^{\infty} \varepsilon^n \Sigma_n.$$

Next, expanding $v^{\text{BS}}(\Sigma^\varepsilon)$ in powers of ε we obtain

$$\begin{aligned} v^{\text{BS}}(\Sigma^\varepsilon) &= v^{\text{BS}}(\Sigma_0 + \delta\Sigma^\varepsilon) \\ &= \sum_{k=0}^{\infty} \frac{1}{k!} (\delta\Sigma^\varepsilon \partial_\Sigma)^k v^{\text{BS}}(\Sigma_0) \\ &= v^{\text{BS}}(\Sigma_0) + \sum_{k=1}^{\infty} \frac{1}{k!} \sum_{n=1}^{\infty} \varepsilon^n \sum_{I_{n,k}} \left(\prod_{j=1}^k \Sigma_{i_j} \right) \partial_\Sigma^k v^{\text{BS}}(\Sigma_0) \\ &= v^{\text{BS}}(\Sigma_0) + \sum_{n=1}^{\infty} \varepsilon^n \sum_{k=1}^{\infty} \frac{1}{k!} \sum_{I_{n,k}} \left(\prod_{j=1}^k \Sigma_{i_j} \right) \partial_\Sigma^k v^{\text{BS}}(\Sigma_0) \\ &= v^{\text{BS}}(\Sigma_0) + \sum_{n=1}^{\infty} \varepsilon^n \left(\Sigma_n \partial_\Sigma + \sum_{k=2}^{\infty} \frac{1}{k!} \sum_{I_{n,k}} \left(\prod_{j=1}^k \Sigma_{i_j} \right) \partial_\Sigma^k \right) v^{\text{BS}}(\Sigma_0), \end{aligned}$$

where $I_{n,k}$ is given by (3.9). Inserting the expansions for v^ε and $v^{\text{BS}}(\Sigma^\varepsilon)$ into $v^\varepsilon = v^{\text{BS}}(\Sigma^\varepsilon)$ and collecting terms of like order in ε we obtain

$$\mathcal{O}(\varepsilon^0) \quad v_0 = v^{\text{BS}}(\Sigma_0), \quad (3.17)$$

$$\mathcal{O}(\varepsilon^n) \quad v_n = \left(\Sigma_n \partial_\Sigma + \sum_{k=2}^{\infty} \frac{1}{k!} \sum_{I_{n,k}} \left(\prod_{j=1}^k \Sigma_{i_j} \right) \partial_\Sigma^k \right) v^{\text{BS}}(\Sigma_0). \quad (3.18)$$

Now, from (3.6) we have

$$v_0 = v^{\text{BS}} \left(\sqrt{\mathbf{C}_{1,1}(t, T)/(T-t)} \right),$$

where \mathbf{C} is defined in (3.7). Thus, it follows from (3.17) that

$$\Sigma_0 = \sqrt{\mathbf{C}_{1,1}(t, T)/(T-t)}. \quad (3.19)$$

Having identified Σ_0 , we can use (3.18) to obtain Σ_n recursively for every $n \geq 1$. We have

$$\Sigma_n = \frac{1}{\partial_{\Sigma} v^{\text{BS}}(\Sigma_0)} \left(v_n - \sum_{k=2}^{\infty} \frac{1}{k!} \sum_{I_{n,k}} \left(\prod_{j=1}^k \Sigma_{i_j} \right) \partial_{\Sigma}^k v^{\text{BS}}(\Sigma_0) \right). \quad (3.20)$$

Using the expression given in (3.10) for v_n , one can show that Σ_n is an n th order polynomial in log-moneyness $k - x$ with coefficients that depend on (t, T) ; see [59, Section 3] for details. We provide explicit expressions for Σ_0 , Σ_1 , and Σ_2 for the cases $d = \{1, 2\}$ in Appendix A.

Having obtained expressions for (Σ_n) , we define $\bar{\Sigma}_n$, the n th order approximation of Σ , as follows

$$\bar{\Sigma}_n := \sum_{k=0}^n \Sigma_k.$$

Note that $\bar{\Sigma}_n$ depends on the choice of \bar{z} . In general, the best choice for \bar{z} is $\bar{z}(t) = (x, y)$. In this case, we have under mild conditions on the generator $\tilde{\mathcal{A}}$ that

$$|\Sigma(t, x, y; T, \bar{T}, k) - \bar{\Sigma}_n(t, x, y; T, \bar{T}, k)| = \mathcal{O}((T - t)^{(n+1)/2}), \quad \text{as } |k - x| = \mathcal{O}(\sqrt{T - t}).$$

by [69, Theorem 5.1].

3.3 Option on Forward Rates Implied Volatility Asymptotics

Throughout this section, we fix a short rate model (2.1)-(2.2), an initial date t , a reset date $T > t$, a settlement date $\bar{T} > T$, the initial values $(\tilde{X}_t = \log L_t^{T, \bar{T}}, Y_t) = (x, y)$ and a caplet payoff $\varphi(\tilde{X}_T) = \bar{\tau}(e^{\tilde{X}_T} - e^k)^+$. Our goal is to find an approximation of implied volatility for *this particular caplet*. To ease notation, we will sometimes hide the dependence on $(t, x, y; T, \bar{T}, k)$. However, the reader should keep in mind that the implied volatility of the caplet under consideration does depend on $(t, x, y; T, \bar{T}, k)$, even if this is not explicitly indicated. Below, we remind the reader of the *Black model* and provide definitions of the *Black price* and *Black implied volatility*, which will be used throughout this section.

In the *Black model*, the dynamics of the simple forward rate $L^{T, \bar{T}} = e^{\tilde{X}}$ are given by

$$dL_t^{T, \bar{T}} = \Sigma L_t^{T, \bar{T}} d\tilde{W}_t^{\bar{T}}, \quad \text{and thus} \quad d\tilde{X}_t = -\frac{1}{2}\Sigma^2 dt + \Sigma d\tilde{W}_t^{\bar{T}}, \quad (3.21)$$

where $\Sigma > 0$ is the *Black volatility* and $\widetilde{W}^{\bar{T}}$ is a scalar $(\widetilde{\mathbb{P}}^{\bar{T}}, \mathbb{F})$ -Brownian motion. Equation (3.21) leads to the following definitions.

Definition 3.3.1. The \bar{T} -forward *Black price* of a caplet, denoted v^{BS} , is defined as follows

$$v^{\text{BS}}(t, x; T, \bar{T}, k, \Sigma) := \bar{\tau} \widetilde{\mathbb{E}}^{\bar{T}}[(e^{\widetilde{X}_T} - e^k)^+ | \widetilde{X}_t = x] = \bar{\tau} \left(e^x \Phi(d_+) - e^k \Phi(d_-) \right), \quad (3.22)$$

where the dynamics of \widetilde{X} are given by (3.21) and

$$d_{\pm} := \frac{1}{\Sigma \sqrt{T-t}} \left(x - k \pm \frac{\Sigma^2(T-t)}{2} \right), \quad \Phi(d) := \int_{-\infty}^d dx \frac{1}{\sqrt{2\pi}} e^{-x^2/2}.$$

Definition 3.3.2. The *Black implied volatility* corresponding to the \bar{T} -forward price v of a caplet is the unique positive solution Σ of the equation

$$v^{\text{BS}}(t, x; T, \bar{T}, k, \Sigma) = v.$$

where the Black price v^{BS} is given by (3.22).

Now, suppose that $v \equiv v(t, x, y; T, \bar{T}, k)$ is the \bar{T} -forward price of a caplet corresponding to a short rate model, where we have now indicated the dependence on the log strike k explicitly. We can now proceed similarly to 3.2 to obtain the approximation (3.20). If we set $\bar{z}(t) = (x, y)$ in the price approximation, then the corresponding implied volatility approximation (3.20) satisfies the following asymptotic accuracy result that, as $(T, k) \rightarrow (t, x)$,

$$|\Sigma(t, x, y; T, \bar{T}, k) - \bar{\Sigma}_n(t, x, y; T, \bar{T}, k)| = \mathcal{O}((T-t)^{(n+1)/2}), \quad (3.23)$$

within the parabolic region $\{(T, k) : |k - x| \leq \ell \sqrt{T-t}\}$ for some $\ell > 0$. The proof of (3.23) is a direct consequence of [8, Theorem 3.10].

3.4 Example: Option on Bond Implied Volatility Under ATS Model

In this section we use the results from Section 3.2 to compute approximate implied volatilities for T -forward Call prices written on $B^{\bar{T}}$ for the following four ATS models:

- Section 3.4.1: Vasicek model,

- Section 3.4.2: Cox-Ingersoll-Ross model,
- Section 3.4.3: Two-factor Cox-Ingersoll-Ross model,
- Section 3.4.4: Fong-Vasicek model.

Note that, given $(X_t, \tilde{Y}_t) = (x, \tilde{y})$, exact T -forward Call prices can be computed using

$$v(t, x, \tilde{y}; T, \bar{T}) = \frac{u(t, y; T, \bar{T})}{\Gamma(t, y; T, 0)}, \quad y_1 = \eta(t, x, \tilde{y}; T, \bar{T}), \quad (3.24)$$

where Γ , u and η are given in (2.4), (2.24)-(2.25) and (2.44), respectively. The corresponding “exact” implied volatilities can be obtained by inserting (3.24) into (3.16) and solving for Σ numerically. We will use this in what follows below in order to gauge the numerical accuracy of our implied volatility approximation $\bar{\Sigma}_n$.

3.4.1 Vasicek

In the short-rate model developed in [82], the dynamics of $R = r(Y)$ are given by

$$dY_t = \kappa(\theta - Y_t)dt + \delta d\tilde{W}_t, \quad R_t = Y_t. \quad (3.25)$$

Comparing (3.25) with (2.1) and (2.3), we see that the functions r , μ , and σ are given by

$$r(y) = y, \quad \mu(t, y) = \kappa(\theta - y), \quad \sigma(t, y) = \delta, \quad (3.26)$$

and comparing (3.26) with (2.10) we identify

$$q = 0, \quad \Xi = 1, \quad b(t) = \kappa\theta, \quad \beta(t) = -\kappa, \quad \ell(t) = \delta^2, \quad \lambda(t) = 0,$$

where we have dropped the subscripts from Ξ , β and λ as $d = 1$. With the above parameters, the solution G of ODE (2.13) is

$$G(t; T, \nu) = -e^{-\kappa(T-t)}\nu + \frac{1 - e^{-\kappa(T-t)}}{\kappa}. \quad (3.27)$$

While the solution F of ODE (2.12) is needed to compute exact Call option prices, we shall see that it is not needed to compute implied volatilities in the Vasicek setting. As such, we do not provide a formula for F here. From (2.43), (2.44), and (3.26), we have

$$\tilde{\sigma}(t, x; T, \bar{T}) := \delta. \quad (3.28)$$

And thus, using (2.47), (3.27) and (3.28), the generator $\tilde{\mathcal{A}}$ is given by

$$\tilde{\mathcal{A}}(t) = c(t, x)(\partial_x^2 - \partial_x), \quad c(t, x) = \frac{1}{2}\delta^2 \left(\frac{1 - e^{-\kappa(T-t)}}{\kappa} - \frac{1 - e^{-\kappa(\bar{T}-t)}}{\kappa} \right)^2.$$

The explicit implied volatility approximation $\bar{\Sigma}_n$ up to order $n = 2$ can now be computed using the formulas in Appendix A. Because the coefficient c does not depend on x in the Vasicek setting, the zeroth order implied volatility approximation is exact

$$\begin{aligned} \Sigma = \Sigma_0 &= \sqrt{\frac{1}{T-t} \int_t^T ds \delta^2 \left(\frac{1 - e^{-\kappa(T-s)}}{\kappa} - \frac{1 - e^{-\kappa(\bar{T}-s)}}{\kappa} \right)^2} \\ &= \frac{\delta}{\kappa^{3/2}} \sqrt{\frac{e^{2\kappa T} - e^{2\kappa t}}{2(T-t)}} \left(e^{-\kappa T} - e^{-\kappa \bar{T}} \right). \end{aligned}$$

From the above, it is easy to identify the following limits

$$\lim_{t \rightarrow T} \Sigma = \frac{\delta}{\kappa} \left(1 - e^{-\kappa(\bar{T}-T)} \right), \quad \lim_{T \rightarrow \bar{T}} \Sigma = 0, \quad \lim_{\bar{T} \rightarrow \infty} \Sigma = \frac{\delta}{\kappa^{3/2}} \sqrt{\frac{1 - e^{-2\kappa(T-t)}}{2(T-t)}}, \quad \lim_{t \rightarrow T, \bar{T} \rightarrow \infty} \Sigma = \frac{\delta}{\kappa}.$$

In Figure 5.1 we plot Σ as a function of t for various valued of \bar{T} with T fixed.

3.4.2 Cox-Ingersoll-Ross

In the Cox-Ingersoll-Ross (CIR) short-rate model developed in [18], the dynamics of $R = r(Y)$ are given by

$$dY_t = \kappa(\theta - Y_t)dt + \delta\sqrt{Y_t}\tilde{dW}_t, \quad R_t = Y_t. \quad (3.29)$$

Comparing (3.29) with (2.1) and (2.3), we see that the functions r , μ , and σ are given by

$$r(y) = y, \quad \mu(t, y) = \kappa(\theta - y), \quad \sigma(t, y) = \delta\sqrt{y}, \quad (3.30)$$

and comparing (3.30) with (2.10) we identify

$$q = 0, \quad \Xi = 1, \quad b(t) = \kappa\theta, \quad \beta(t) = -\kappa, \quad \ell(t) = 0, \quad \lambda(t) = \delta^2,$$

where we have dropped the subscripts from Ξ , β and λ as $d = 1$. With the above parameters, the solutions F and G of coupled ODEs (2.12) and (2.13) are

$$F(t; T, \nu) = -\frac{2\kappa\theta}{\delta^2} \log \left(\frac{2\Lambda \exp((\Lambda + \kappa)\tau/2)}{-\delta^2\nu(\exp(\Lambda\tau) - 1) + \Lambda(\exp(\Lambda\tau) + 1) + \kappa(\exp(\Lambda\tau) - 1)} \right),$$

$$\tau := T - t,$$

$$G(t; T, \nu) = \frac{2(\exp(\Lambda\tau) - 1) - (\Lambda(\exp(\Lambda\tau) + 1) - \kappa(\exp(\Lambda\tau) - 1))\nu}{-\delta^2\nu(\exp(\Lambda\tau) - 1) + \Lambda(\exp(\Lambda\tau) + 1) + \kappa(\exp(\Lambda\tau) - 1)},$$

$$\Lambda := \sqrt{\kappa^2 + 2\delta^2}.$$

From (2.43), (2.44), and (3.30), we have

$$\tilde{\sigma}(t, x; T, \bar{T}) = \delta \sqrt{\frac{\mathfrak{F}(t; T) - \mathfrak{F}(t; \bar{T}) - x}{\mathfrak{G}(t; \bar{T}) - \mathfrak{G}(t; T)}}, \quad (3.31)$$

And thus, using (2.47) and (3.31), the generator $\tilde{\mathcal{A}}$ is given by

$$\tilde{\mathcal{A}}(t) = c(t, x)(\partial_x^2 - \partial_x), \quad c(t, x) = \frac{\delta^2}{2} \left(\mathfrak{F}(t; T) - \mathfrak{F}(t; \bar{T}) - x \right) \left(\mathfrak{G}(t; \bar{T}) - \mathfrak{G}(t; T) \right).$$

Introducing the short-hand notation $c_j(t, x) := \partial_x^j c(t, x)/j!$, we have

$$c_0(t, x) = \frac{\delta^2}{2} \left(\mathfrak{F}(t; T) - \mathfrak{F}(t; \bar{T}) - x \right) \left(\mathfrak{G}(t; \bar{T}) - \mathfrak{G}(t; T) \right),$$

$$c_1(t, x) \equiv c_1(t) = -\frac{\delta^2}{2} \left(\mathfrak{G}(t; \bar{T}) - \mathfrak{G}(t; T) \right),$$

$$c_n(t, x) = 0, \quad n \geq 2.$$

The explicit implied volatility approximation $\bar{\Sigma}_n$ can now be computed up to order $n = 2$ using the formulas in Appendix A. We have

$$\begin{aligned}\Sigma_0 &= \sqrt{\frac{2}{\tau} \int_t^T ds c_0(s, x)}, \\ \Sigma_1 &= \frac{2(k-x)}{\Sigma_0^3 \tau^2} \int_t^T ds c_1(s, x) \int_t^s dq c_0(q, x), \\ \Sigma_2 &= \frac{6(k-x)^2}{\Sigma_0^7 \tau^4} \left(-2 \left(\int_t^T ds c_1(s) \int_t^s dq c_0(q, x) \right)^2 + \Sigma_0^2 \tau \int_t^T ds_1 \int_{s_1}^T ds_2 c_1(s_1) c_1(s_2) \right. \\ &\quad \times \left. \int_t^{s_1} dq c_0(q, x) \right) + \frac{(\Sigma_0^2 \tau + 12)}{2 \Sigma_0^5 \tau^3} \left(\left(\int_t^T ds c_1(s) \int_t^s dq c_0(q, x) \right)^2 \right. \\ &\quad \left. - \Sigma_0^2 \tau \int_t^T ds_1 \int_{s_1}^T ds_2 c_1(s_1) c_1(s_2) \int_t^{s_1} dq c_0(q, x) \right).\end{aligned}$$

In Figure 5.2 we plot our explicit approximation of implied volatility $\bar{\Sigma}_n$ up to order $n = 2$ as a function of log-moneyness $k - x$ with $t = 0$ and $\bar{T} = 2$ fixed and with option maturities ranging over $T = \{\frac{1}{12}, \frac{1}{4}, \frac{1}{2}, \frac{3}{4}\}$. For comparison, we also plot the exact implied volatility Σ . We observe that the second order approximation $\bar{\Sigma}_2$ accurately matches the level, slope, and convexity of the exact implied volatility Σ near-the-money for all four option maturity dates. In Figure 5.3 we plot the absolute value of the relative error of our second order approximation $|\bar{\Sigma}_2 - \Sigma|/\Sigma$ as a function of log-moneyness $k - x$ and option maturity T . We observe that the error decreases as we approach the origin in both directions of $k - x$ and T and the best approximation region is within 0.2% of the exact implied volatility.

3.4.3 Two-factor Cox-Ingersoll-Ross

In the Two-factor Cox-Ingersoll-Ross (2-D CIR) short-rate model developed in [18], the dynamics of $R = r(Y)$ are given by

$$\begin{aligned}dY_t^{(1)} &= \kappa_1(\theta_1 - Y_t^{(1)})dt + \delta_1 \sqrt{Y_t^{(1)}} d\widetilde{W}_t^{(1)}, \\ dY_t^{(2)} &= \kappa_2(\theta_2 - Y_t^{(2)})dt + \delta_2 \sqrt{Y_t^{(2)}} d\widetilde{W}_t^{(2)}, \\ R_t &= Y_t^{(1)} + Y_t^{(2)}.\end{aligned}\tag{3.32}$$

Comparing (3.32) with (2.1) and (2.3), we see that the functions r , μ , and σ are given by

$$\begin{aligned} r(y_1, y_2) &= y_1 + y_2, \\ \mu(t, y_1, y_2) &= \begin{pmatrix} \kappa_1(\theta_1 - y_1) \\ \kappa_2(\theta_2 - y_2) \end{pmatrix}, \quad \sigma(t, y_1, y_2) = \begin{pmatrix} \delta_1\sqrt{y_1} & 0 \\ 0 & \delta_2\sqrt{y_2} \end{pmatrix}, \end{aligned} \quad (3.33)$$

and comparing (3.33) with (2.10) we identify

$$\begin{aligned} q &= 0, \quad \Xi = \begin{pmatrix} 1 \\ 1 \end{pmatrix}, \quad b(t) = \begin{pmatrix} \kappa_1\theta_1 \\ \kappa_2\theta_2 \end{pmatrix}, \quad \beta_1(t) = -\begin{pmatrix} \kappa_1 \\ 0 \end{pmatrix}, \\ \beta_2(t) &= -\begin{pmatrix} 0 \\ \kappa_2 \end{pmatrix}, \quad \ell(t) = 0, \quad \lambda_1(t) = \begin{pmatrix} \delta_1^2 & 0 \\ 0 & 0 \end{pmatrix}, \quad \lambda_2(t) = \begin{pmatrix} 0 & 0 \\ 0 & \delta_2^2 \end{pmatrix}. \end{aligned}$$

With the above parameters, the solutions F and $G = (G_1, G_2)$ of coupled ODEs (2.12) and (2.13) are

$$\begin{aligned} F(t; T, \nu) &= -\sum_{i=1}^2 \frac{2\kappa_i\theta_i}{\delta_i^2} \log \left(\frac{2\Lambda_i \exp((\Lambda_i + \kappa_i)\tau/2)}{-\delta_i^2\nu_i(\exp(\Lambda_i\tau) - 1) + \Lambda_i(\exp(\Lambda_i\tau) + 1) + \kappa_i(\exp(\Lambda_i\tau) - 1)} \right), \\ G_i(t; T, \nu) &= \frac{2(\exp(\Lambda_i\tau) - 1) - (\Lambda_i(\exp(\Lambda_i\tau) + 1) - \kappa_i(\exp(\Lambda_i\tau) - 1))\nu_i}{-\delta_i^2\nu_i(\exp(\Lambda_i\tau) - 1) + \Lambda_i(\exp(\Lambda_i\tau) + 1) + \kappa_i(\exp(\Lambda_i\tau) - 1)}, \\ i &= \{1, 2\}, \\ \Lambda_i &:= \sqrt{\kappa_i^2 + 2\delta_i^2}. \end{aligned}$$

From (2.43), (2.44), and (3.33), we have

$$\begin{aligned} \eta(t, x, y_2; T, \bar{T}) &= \frac{\mathfrak{F}(t; T) - \mathfrak{F}(t; \bar{T}) - x + (\mathfrak{G}_2(t; T) - \mathfrak{G}_2(t; \bar{T}))y_2}{\mathfrak{G}_1(t; \bar{T}) - \mathfrak{G}_1(t; T)}, \\ \tilde{\sigma}(t, x, y_2; T, \bar{T}) &= \begin{pmatrix} \delta_1\sqrt{\eta(t, x, y_2; T, \bar{T})} & 0 \\ 0 & \delta_2\sqrt{y_2} \end{pmatrix}, \end{aligned} \quad (3.34)$$

and thus, using (2.48) and (3.34), the generator $\tilde{\mathcal{A}}$ is given by

$$\tilde{\mathcal{A}}(t) = c(t, x, y_2)(\partial_x^2 - \partial_x) + f(t, x, y_2)\partial_{y_2} + g(t, x, y_2)\partial_{y_2}^2 + h(t, x, y_2)\partial_x\partial_{y_2},$$

where the functions c , f , g and h are given by

$$\begin{aligned}
c(t, x, y_2) &= \frac{1}{2}\delta_1^2 \left(\mathfrak{F}(t; T) - \mathfrak{F}(t; \bar{T}) - x + \left(\mathfrak{G}_2(t; T) - \mathfrak{G}_2(t; \bar{T}) \right) y_2 \right) \\
&\quad \times \left(\mathfrak{G}_1(t; \bar{T}) - \mathfrak{G}_1(t; T) \right) + \frac{1}{2}\delta_2^2 \left(\mathfrak{G}_2(t; T) - \mathfrak{G}_2(t; \bar{T}) \right)^2 y_2, \\
f(t, x, y_2) &= \kappa_2(\theta_2 - y_2) - \delta_2^2 y_2 \mathfrak{G}_2(t; T), \\
g(t, x, y_2) &= \frac{1}{2}\delta_2^2 y_2, \\
h(t, x, y_2) &= \delta_2^2 y_2 \left(\mathfrak{G}_2(t; T) - \mathfrak{G}_2(t; \bar{T}) \right).
\end{aligned}$$

Introducing the notation $\chi_{i,j}(t, x, y_2) := \partial_x^i \partial_{y_2}^j \chi(t, x, y_2) / (i!j!)$ where $\chi \in \{c, f, g, h\}$, we compute

$$\begin{aligned}
\chi_{0,0}(t, x, y_2) &= \chi(t, x, y_2), \\
c_{1,0}(t, x, y_2) &= -\frac{1}{2}\delta_1^2 \left(\mathfrak{G}_1(t; \bar{T}) - \mathfrak{G}_1(t; T) \right), \\
c_{0,1}(t, x, y_2) &= \frac{1}{2}\delta_1^2 \left(\mathfrak{G}_2(t; T) - \mathfrak{G}_2(t; \bar{T}) \right) \left(\mathfrak{G}_1(t; \bar{T}) - \mathfrak{G}_1(t; T) \right) \\
&\quad + \frac{1}{2}\delta_2^2 \left(\mathfrak{G}_2(t; T) - \mathfrak{G}_2(t; \bar{T}) \right)^2, \\
f_{0,1}(t, x, y_2) &= -(\kappa_2 + \delta_2^2) \mathfrak{G}_2(t; T), \\
g_{0,1}(t, x, y_2) &= \frac{1}{2}\delta_2^2, \\
h_{0,1}(t, x, y_2) &= \delta_2^2 \left(\mathfrak{G}_2(t; T) - \mathfrak{G}_2(t; \bar{T}) \right),
\end{aligned}$$

and $\chi_{i,j}(t, x, y_2) = 0$, for any term not given above. The explicit implied volatility approximation $\bar{\Sigma}_n$ can now be computed up to order $n = 2$ using the formulas in Appendix A. We have

$$\begin{aligned}
\Sigma_0 &= \sqrt{\frac{2}{\tau} \int_t^T ds c_{0,0}(s, x, y_2)}, \\
\Sigma_1 &= \frac{(k-x)}{\tau^2 \Sigma_0^3} \left(2 \int_t^T ds c_{1,0}(s, x, y_2) \int_t^s dq c_{0,0}(q, x, y_2) + \int_t^T ds c_{0,1}(s, x, y_2) \int_t^s dq h_{0,0}(q, x, y_2) \right) \\
&\quad + \frac{1}{2\tau \Sigma_0} \int_t^T ds c_{0,1}(s, x, y_2) \left(2 \int_t^s dq f_{0,0}(q, x, y_2) + \int_t^s dq h_{0,0}(q, x, y_2) \right),
\end{aligned}$$

where we have omitted the 2nd order term Σ_2 due to its considerable length.

In Figure 5.4 we plot our explicit approximation of implied volatility $\bar{\Sigma}_n$ up to order $n = 2$ as a function of log-moneyness $k - x$ with $t = 0$ and $\bar{T} = 2$ fixed and with option maturities ranging over $T = \{\frac{1}{12}, \frac{1}{4}, \frac{1}{2}, \frac{3}{4}\}$. For comparison, we also plot the the exact implied volatility Σ . As is the case with the (1-D) CIR model, we observe in the 2-D CIR model that the second order approximation $\bar{\Sigma}_2$ accurately matches the level, slope, and convexity of the exact implied volatility Σ near-the-money for all four option maturity dates. In Figure 5.5 we plot the absolute value of the relative error of our second order approximation $|\bar{\Sigma}_2 - \Sigma|/\Sigma$ as a function of log-moneyness $k - x$ and option maturity T . We observe that the error decreases as we approach the origin in both directions of $k - x$ and T and the best approximation region is within 0.1% of the exact implied volatility.

3.4.4 Fong-Vasicek

In the Fong-Vasicek short-rate model developed in [27], the dynamics of $R = r(Y)$ are given by

$$\begin{aligned} dY_t^{(1)} &= \kappa_1(\theta_1 - Y_t^{(1)})dt + \sqrt{Y_t^{(2)}}d\widetilde{W}_t^{(1)}, \\ dY_t^{(2)} &= \kappa_2(\theta_2 - Y_t^{(2)})dt + \delta_2\rho\sqrt{Y_t^{(2)}}d\widetilde{W}_t^{(1)} + \delta_2\bar{\rho}\sqrt{Y_t^{(2)}}d\widetilde{W}_t^{(2)}, \quad \bar{\rho} = \sqrt{1 - \rho^2} \\ R_t &= Y_t^{(1)}. \end{aligned} \tag{3.35}$$

Comparing (3.35) with (2.1) and (2.3), we see that the functions r , μ , and σ are given by

$$r(y_1, y_2) = y_1, \quad \mu(t, y_1, y_2) = \begin{pmatrix} \kappa_1(\theta_1 - y_1) \\ \kappa_2(\theta_2 - y_2) \end{pmatrix}, \quad \sigma(t, y_1, y_2) = \begin{pmatrix} \sqrt{y_2} & 0 \\ \delta_2\rho\sqrt{y_2} & \delta_2\bar{\rho}\sqrt{y_2} \end{pmatrix}, \tag{3.36}$$

and comparing (3.36) with (2.10) we identify

$$\begin{aligned} q &= 0, & \Xi &= \begin{pmatrix} 1 \\ 0 \end{pmatrix}, & b(t) &= \begin{pmatrix} \kappa_1\theta_1 \\ \kappa_2\theta_2 \end{pmatrix}, & \beta_1(t) &= - \begin{pmatrix} \kappa_1 \\ 0 \end{pmatrix}, \\ \beta_2(t) &= - \begin{pmatrix} 0 \\ \kappa_2 \end{pmatrix}, & \ell(t) &= 0, & \lambda_1(t) &= \begin{pmatrix} 0 & 0 \\ 0 & 0 \end{pmatrix}, & \lambda_2(t) &= \begin{pmatrix} 1 & \delta_2\rho \\ \delta_2\rho & \delta_2^2 \end{pmatrix}. \end{aligned}$$

With the above parameters, we find using (2.12) and (2.13) that the ODEs satisfied by F and $G = (G_1, G_2)$ are

$$\begin{aligned}\partial_t F(t; T, \nu) &= -\kappa_1 \theta_1 G_1(t; T, \nu) - \kappa_2 \theta_2 G_2(t; T, \nu), \\ F(T; T, \nu) &= 0,\end{aligned}\tag{3.37}$$

$$\begin{aligned}\partial_t G_1(t; T, \nu) &= \kappa_1 G_1(t; T, \nu) - 1, \\ G_1(T; T, \nu) &= -\nu_1,\end{aligned}\tag{3.38}$$

$$\begin{aligned}\partial_t G_2(t; T, \nu) &= \frac{1}{2} \delta_2^2 G_2^2(t; T, \nu) + \left(\delta_2 \rho G_1(t; T, \nu) + \kappa_2 \right) G_2(t; T, \nu) \\ &\quad + \frac{1}{2} G_1^2(t; T, \nu), \\ G_2(T; T, \nu) &= -\nu_2.\end{aligned}\tag{3.39}$$

Although one can obtain explicit expressions for $F(t; T, \nu)$, $G_1(t; T, \nu)$ and $G_2(t; T, \nu)$, these expressions are given in terms of *confluent hypergeometric functions* (CHFs). As numerical evaluation of CHFs is time-consuming, computing explicit Call prices using (3.24) is not practical because it involves integrals with respect to ν . By contrast, in order to compute our explicit approximation of implied volatility $\bar{\Sigma}_n$, we need only expressions for $\mathfrak{F}(t; T)$, $\mathfrak{G}_1(t; T)$ and $\mathfrak{G}_2(t; T)$, which we provide in Appendix B.

From (2.43), (2.44), and (3.36), we have

$$\begin{aligned}\eta(t, x, y_2; T, \bar{T}) &= \frac{\mathfrak{F}(t; T) - \mathfrak{F}(t; \bar{T}) - x + \left(\mathfrak{G}_2(t; T) - \mathfrak{G}_2(t; \bar{T}) \right) y_2}{\mathfrak{G}_1(t; \bar{T}) - \mathfrak{G}_1(t; T)}, \\ \tilde{\sigma}(t, x, y_2; T, \bar{T}) &= \begin{pmatrix} \sqrt{y_2} & 0 \\ \delta_2 \rho \sqrt{y_2} & \delta_2 \bar{\rho} \sqrt{y_2} \end{pmatrix},\end{aligned}\tag{3.40}$$

And thus, using (2.48) and (3.40), the generator $\tilde{\mathcal{A}}$ is given by

$$\tilde{\mathcal{A}}(t) = c(t, x, y_2)(\partial_x^2 - \partial_x) + f(t, x, y_2)\partial_{y_2} + g(t, x, y_2)\partial_{y_2}^2 + h(t, x, y_2)\partial_x\partial_{y_2},$$

where the functions c , f , g and h are given by

$$\begin{aligned}
c(t, x, y_2) &= \frac{1}{2}y_2 \left(\mathfrak{G}_1(t; T) - \mathfrak{G}_1(t; \bar{T}) \right)^2 + \rho\delta_2 y_2 \left(\mathfrak{G}_1(t; T) - \mathfrak{G}_1(t; \bar{T}) \right) \\
&\quad \times \left(\mathfrak{G}_2(t; T) - \mathfrak{G}_2(t; \bar{T}) \right) + \frac{1}{2}\delta_2^2 y_2 \left(\mathfrak{G}_2(t; T) - \mathfrak{G}_2(t; \bar{T}) \right)^2, \\
f(t, x, y_2) &= \kappa_2(\theta_2 - y_2) - \delta_2^2 y_2 \mathfrak{G}_2(t; T) - \rho\delta_2 y_2 \mathfrak{G}_1(t; T), \\
g(t, x, y_2) &= \frac{1}{2}\delta_2^2 y_2, \\
h(t, x, y_2) &= \delta_2^2 y_2 \left(\mathfrak{G}_2(t; T) - \mathfrak{G}_2(t; \bar{T}) \right) + \rho\delta_2 y_2 \left(\mathfrak{G}_1(t; T) - \mathfrak{G}_1(t; \bar{T}) \right).
\end{aligned}$$

Once again using the short-hand notation $\chi_{i,j}(t, x, y_2) := \partial_x^i \partial_{y_2}^j \chi(t, x, y_2) / (i!j!)$ where $\chi \in \{c, f, g, h\}$, we compute

$$\begin{aligned}
\chi_{0,0}(t, x, y_2) &= \chi(t, x, y_2), \\
c_{0,1}(t, x, y_2) &= \frac{1}{2} \left(\mathfrak{G}_1(t; T) - \mathfrak{G}_1(t; \bar{T}) \right)^2 + \rho\delta_2 \left(\mathfrak{G}_1(t; T) - \mathfrak{G}_1(t; \bar{T}) \right) \\
&\quad \times \left(\mathfrak{G}_2(t; T) - \mathfrak{G}_2(t; \bar{T}) \right) + \frac{1}{2}\delta_2^2 \left(\mathfrak{G}_2(t; T) - \mathfrak{G}_2(t; \bar{T}) \right)^2, \\
f_{0,1}(t, x, y_2) &= -\kappa_2 - \delta_2^2 \mathfrak{G}_2(t; T) - \rho\delta_2 \mathfrak{G}_1(t; T), \\
g_{0,1}(t, x, y_2) &= \frac{1}{2}\delta_2^2, \\
h_{0,1}(t, x, y_2) &= \delta_2^2 \left(\mathfrak{G}_2(t; T) - \mathfrak{G}_2(t; \bar{T}) \right) + \rho\delta_2 \left(\mathfrak{G}_1(t; T) - \mathfrak{G}_1(t; \bar{T}) \right),
\end{aligned}$$

where $\chi_{i,j}(t, x, y_2) = 0$ for any term not given above. The explicit implied volatility approximation $\bar{\Sigma}_n$ can now be computed up to order $n = 2$ using the formulas in Appendix A. We have

$$\begin{aligned}
\Sigma_0 &= \sqrt{\frac{2}{\tau} \int_t^T ds c_{0,0}(s, x, y_2)}, \\
\Sigma_1 &= \frac{k-x}{\tau^2 \Sigma_0^3} \left(\int_t^T ds c_{0,1}(s, x, y_2) \int_t^s dq h_{0,0}(q, x, y_2) \right) \\
&\quad + \frac{1}{2\tau \Sigma_0} \int_t^T ds c_{0,1}(s, x, y_2) \left(2 \int_t^s dq f_{0,0}(q, x, y_2) + \int_t^s dq h_{0,0}(q, x, y_2) \right). \quad (3.41)
\end{aligned}$$

where we have omitted the second order term Σ_2 due to its considerable length.

In Figure 5.6 we plot our second order approximation of implied volatility $\bar{\Sigma}_2$ as a function of

log-moneyness $k - x$ with the maturity date of the bond fixed at $\bar{T} = 2$, the maturity date of the option taking the following values $T = \{\frac{1}{12}, \frac{1}{4}, \frac{1}{2}, \frac{3}{4}\}$ and the correlation parameter taking the following values $\rho = \{-0.7, -0.3, 0.3, 0.7\}$. We can see the convexity near-the-money changes from concave to convex as we increase ρ . From the expression of Σ_1 in (3.41) we observe that the slope of Σ_1 with respect to $k - x$ is controlled by the sign of $c_{0,1}$ and $h_{0,0}$. As $G(t; T, 0)$ is an increasing function in T , the expression $G_i(t; T, 0) - G_i(t; \bar{T}, 0)$ is negative, which means that, fixing all other parameters, ρ controls the sign of $c_{0,1}$ and $h_{0,0}$. As a result, as we change ρ from -1 to 1 the slope of Σ_1 changes accordingly. A similar analysis can be done on the sign of coefficients of $(k - x)^2$ of Σ_2 to show that ρ controls the convexity of Σ_2 with respect to $k - x$. This is in contrast to the CIR and 2-D CIR models, where the implied volatility curve near-the-money is concave.

3.5 Example: Caplet Implied Volatility Under QTS Models

Throughout this section, we consider a QTS model, whose dynamics are as follows

$$dY_t = \kappa(\theta - Y_t)dt + \delta d\widetilde{W}_t, \quad R_t = r(Y_t) = q + Y_t^2, \quad (3.42)$$

where the constants κ, δ are positive and θ, q are nonnegative. Noting that Y is an Ornstein-Uhlenbeck process, we refer to the model (3.42) as the *Quadratic Ornstein-Uhlenbeck* (QOU) model.

Remark 3.5.1. If we consider the special case $\theta = q = 0$. then we have by Itô's lemma that

$$dR_t = 2\kappa\left(\frac{\delta^2}{2\kappa} - R_t\right)dt + 2\delta\sqrt{R_t}d\widetilde{W}_t. \quad (3.43)$$

Note that (3.43) is a *Cox-Ingersoll-Ross* (CIR) process with a mean $\frac{\delta^2}{2\kappa}$, rate of mean-reversion 2κ and volatility 2δ . Thus, the QOU model contains as a special case, some (but not all) CIR short-rate models.

Comparing (3.42) with (2.2) and (2.14) we obtain

$$b = \kappa\theta, \quad \beta = -\kappa, \quad \ell = \delta, \quad \Xi = 1.$$

Next, we can obtain from (2.16), (2.17), and (2.18) that (F, G, H) satisfies the following system of ODEs

$$\left. \begin{aligned} \partial_t F(t; T, \nu, \Omega) &= \frac{1}{2}\delta^2 G^2(t; T, \nu, \Omega) - \delta^2 H(t; T, \nu, \Omega) - \kappa\theta G(t; T, \nu, \Omega) - q, \\ F(T; T, \nu, \Omega) &= 0, \\ \partial_t G(t; T, \nu, \Omega) &= (2\delta^2 H(t; T, \nu, \Omega) + \kappa)G(t; T, \nu, \Omega) - 2\kappa\theta H(t; T, \nu, \Omega), \\ G(T; T, \nu, \Omega) &= -\nu, \\ \partial_t H(t; T, \nu, \Omega) &= 2\delta^2 H^2(t; T, \nu, \Omega) + 2\kappa H(t; T, \nu, \Omega) - 1, \\ H(T; T, \nu, \Omega) &= -\Omega. \end{aligned} \right\} \quad (3.44)$$

Solving (3.44), we obtain

$$\begin{aligned} F(t; T, \nu, \Omega) &= \int_T^t ds \left(\frac{1}{2}\delta^2 G^2(s; T, \nu, \Omega) - \delta^2 H(s; T, \nu, \Omega) - \kappa\theta G(s; T, \nu, \Omega) - q \right), \quad (3.45) \\ G(t; T, \nu, \Omega) &= -\frac{Q_1(T-t)\nu + Q_2(T-t)\Omega + Q_3(T-t)}{Q_4(T-t)\Omega + Q_5(T-t)}, \\ H(t; T, \nu, \Omega) &= -\frac{Q_6(T-t)\Omega + Q_7(T-t)}{Q_4(T-t)\Omega + Q_5(T-t)}, \end{aligned} \quad (3.46)$$

where the functions $Q_i(t)$ for $i \in \{1, 2, \dots, 7\}$ are given by

$$\begin{aligned} Q_1(t) &:= 2\mu e^{\frac{1}{2}\mu t}, \\ Q_2(t) &:= \frac{8\delta^2}{\mu} \left(e^{\frac{1}{2}\mu t} - 1 \right)^2 \left(\frac{-\kappa^2\theta}{\delta^2} \right) - \frac{\kappa\theta Q_4(t)}{\delta^2}, \\ Q_3(t) &:= -\frac{\kappa\theta}{\delta^2} \left(\frac{\kappa}{\mu} Q_7 \left(\frac{t}{2} \right) Q_5 \left(\frac{t}{2} \right) - Q_1(t) + Q_5(t) \right), \\ Q_4(t) &:= 4\delta^2(1 - e^{\mu t}), \\ Q_5(t) &:= \mu(e^{\mu t} + 1) + 2\kappa(e^{\mu t} - 1), \\ Q_6(t) &:= \mu(e^{\mu t} + 1) - 2\kappa(e^{\mu t} - 1), \\ Q_7(t) &:= 2(1 - e^{\mu t}), \\ \mu &:= 2\sqrt{\kappa^2 + 2\delta^2}. \end{aligned}$$

Next, from (2.53) we have the form of the generator

$$\tilde{\mathcal{A}}(t) = c(t, x, y)(\partial_x^2 - \partial_x) + f(t, x, y)\partial_y + g(t, x, y)\partial_y^2 + h(t, x, y)\partial_x\partial_y,$$

where the functions c , f , g and h are given by

$$\begin{aligned} c(t, x, y) &= \frac{1}{2}\delta^2\left(1 + \frac{e^{-x}}{\bar{\tau}}\right)^2\left(\mathfrak{G}(t; \bar{T}) - \mathfrak{G}(t; T) \right. \\ &\quad \left. + 2\left(\mathfrak{H}(t; \bar{T}) - \mathfrak{H}(t; T)\right)y\right)^2, \\ f(t, x, y) &= \kappa\theta - \kappa y - \delta^2\left(\mathfrak{G}(t; \bar{T}) + 2\mathfrak{H}(t; \bar{T})y\right), \\ g(t, x, y) &= \frac{1}{2}\delta^2, \\ h(t, x, y) &= \delta^2\left(1 + \frac{e^{-x}}{\bar{\tau}}\right)\left(\mathfrak{G}(t; \bar{T}) - \mathfrak{G}(t; T) + 2\left(\mathfrak{H}(t; \bar{T}) - \mathfrak{H}(t; T)\right)y\right). \end{aligned}$$

Introducing the notation

$$\chi_{i,j}(t, x, y) := \frac{1}{i!j!}\partial_x^i\partial_y^j\chi(t, x, y) \quad \text{where} \quad \chi \in \{c, f, g, h\},$$

the explicit implied volatility approximation $\bar{\sigma}_n$ can now be computed up to order $n = 2$ using the formulas in Appendix A. We have

$$\begin{aligned} \sigma_0 &= \sqrt{\frac{2}{T-t}\int_t^T ds c_{0,0}(s, x, y_2)}, \\ \sigma_1 &= \frac{(k-x)}{(T-t)^2\sigma_0^3}\left(2\int_t^T ds c_{1,0}(s, x, y_2)\int_t^s dq c_{0,0}(q, x, y_2) \right. \\ &\quad \left. + \int_t^T ds c_{0,1}(s, x, y_2)\int_t^s dq h_{0,0}(q, x, y_2)\right) \\ &\quad + \frac{1}{2(T-t)\sigma_0}\int_t^T ds c_{0,1}(s, x, y_2)\left(2\int_t^s dq f_{0,0}(q, x, y_2) + \int_t^s dq h_{0,0}(q, x, y_2)\right), \end{aligned}$$

where we have omitted the 2nd order term σ_2 due to its considerable length.

In Figures 5.7 and 5.8, using different parameters for $(\kappa, \theta, \delta, q, y)$, we plot our explicit approximation of implied volatility $\bar{\sigma}_n$ up to order $n = 2$ as a function of log-moneyness $k - x$ with $t = 0$ and $\bar{T} = 2$ fixed and with reset date ranging over $T = \{\frac{1}{64}, \frac{1}{32}, \frac{1}{16}, \frac{1}{8}\}$. For comparison, we also plot the “exact” implied volatility σ , which can be computed using \bar{T} -forward caplet prices using (2.28) and inverting the Black formula (3.22) numerically. In both figures, we observe that the second order approximation $\bar{\sigma}_2$ accurately matches the level, slope, and convexity of the exact implied volatility σ near-the-money for all four reset dates.

In Figures 5.9 and 5.10, using the same values for $(\kappa, \theta, \delta, q, y)$ as in Figures 5.7 and 5.8, respectively, we plot the absolute value of the relative error of our second order approximation $|\bar{\sigma}_2 - \sigma|/\sigma$ as a function of log-moneyness $k - x$ and reset date T . Consistent with the asymptotic accuracy results (3.23), we observe that the errors decrease as we approach the origin in both directions of $k - x$ and T .

3.6 Example: Calibration to Market Data

In this section we show how to calibrate the QOU model, described in Section 3.5, to market data. To this end, let

$$L_t^{T, \bar{T}} \equiv L_t^{T, \bar{T}}(\Phi), \quad \Phi := (\kappa, \theta, \delta, q, y).$$

denote simple forward rate (1.3) as computed in the QOU model using the unobservable model parameters Φ . Note that $L_t^{T, \bar{T}}(\Phi)$ can be computed explicitly using (1.3), (2.9), (3.45) and (3.46). Next, let

$$L_i := L_t^{T_i, T_i + \tau}, \quad \tau = 0.5 \text{ years}, \quad T_i := t + \tau i,$$

denote the *Forward LIBOR Curve data on the 18 November 2008*, which we obtained from [26, Table 11.3]. We define the *optimal parameter set* Φ^* as the minimizer of the following least-squares optimization

$$\Phi^* := \operatorname{argmin}_{\Phi} \sum_{i=1}^n \left(L_t^{T_i, T_i + \tau}(\Phi) - L_i \right)^2.$$

Using Wolfram Mathematica's `NonlinearModelFit`¹, we obtain

$$\Phi^* \equiv (\kappa^*, \theta^*, \delta^*, q^*, y^*) = (0.158, 1.451, 0.008, -2.041, 1.437),$$

In Figure 5.11, we plot the fitted simple forward rate curve using the optimal parameter set $L_t^{T, T+\tau}(\Phi^*)$ as well as the market data L_i .

¹The function performs nonnegative least square fit using Levenberg-Marquardt variant of the Gauss-Newton method. The documentation can be found in <https://reference.wolfram.com/language/ref/NonlinearModelFit.html>

In order to see how well our implied volatility approximation performs using the calibrated parameters Φ^* , we plot in Figure 5.12 our explicit approximation of implied volatility $\bar{\sigma}_n$ up to order $n = 2$ as a function of log-moneyness $k - x$ with $t = 0$ and $\bar{T} = 2$ fixed and with reset date ranging over $T = \{\frac{1}{64}, \frac{1}{32}, \frac{1}{16}, \frac{1}{8}\}$. For comparison, we also plot the “exact” implied volatility σ , which can be computed using \bar{T} -forward caplet prices using (2.28) and inverting the Black formula (3.22) numerically. We observe that the second order approximation $\bar{\sigma}_2$ accurately matches the level, slope, and convexity of the exact implied volatility σ near-the-money for all four reset dates.

In Figure 5.13 we plot the absolute value of the relative error of our second order approximation $|\bar{\sigma}_2 - \sigma|/\sigma$ as a function of log-moneyness $k - x$ and reset date T . Consistent with the asymptotic accuracy results (3.23), we observe that the errors decrease as we approach the origin in both directions of $k - x$ and T .

Chapter 4

OPTIMAL TIMES TO BUY AND SELL A HOME

4.1 Introduction

While many consider a home merely as a place to live, it is also financial asset, the purchase and subsequent sale of which can generate a significant profit. The problem of buying and/or selling a home in order to minimize purchase price and/or maximize sale price or profit has been widely studied in academic literature. Various mathematical tools have been used to solve this problem, including multivariate probability theory, game theory, and optimal stopping theory. For example, [12] assumes home prices follow a specific probability distribution, and derives the optimal stopping rules for buying and selling homes. [6] derives an optimal stopping strategy from the perspective of a representative-home buyer who is observing multiple other homes to purchase. [23] and [11] use an optimal stopping approach to optimize the profit in a home bidding process. [4] considers house buying and selling in game theoretic framework and derive prices at equilibrium. And [40] use a housing market search model to derive prices at equilibrium.

When deriving the optimal home-buying or home-selling strategy, one must consider a number of factors such as, e.g., interest rates, transaction costs, an investor's discount rate, the demand and supply of homes in certain locations, quality of nearby schools, etc.. Among the many factors one might consider, perhaps the most important is the interest rate. To illustrate the important role interest rates play in home prices, in Figure 5.14, we plot the Monthly S&P/Case-Shiller U.S. National Home Price Index ¹ and the Weekly 30-Year Fixed

¹S&P Dow Jones Indices LLC, S&P/Case-Shiller U.S. National Home Price Index, Jan 2022, <https://fred.stlouisfed.org/series/CSUSHPINSA>

Rate Mortgage Average in the U.S.² and in Figure 5.15 the Overnight Bank Funding Rate in the U.S. from January 2019 to January 2021.³ The figures clearly shows during this period that home prices were inversely related to interest rates and overnight bank funding rate. This data is consistent with the theoretical results of [40] who show that, in equilibrium, home prices are inversely related to interest rates.

In the present paper, we present a framework that describes how the risk-free rate of interest affects home prices. Briefly, we suppose that home prices are set by a representative home-buyer, who can afford to pay only a fixed cash-flow per unit time for housing. The cash-flow is a fraction of the representative home-buyer's salary, which grows at a rate that is proportional to the risk-free rate of interest. As a result, in the long-run, higher interest rates lead to faster growth of home prices. The representative home-buyer finances the purchase of a home by taking out a mortgage. The mortgage rate paid by the home-buyer is fixed at the time of purchase and equal to the risk-free rate of interest plus a positive constant. As the home-buyer can only afford to pay a fixed cash-flow per unit time, a higher mortgage rate limits the size of the loan the home-buyer can take out. As a result, the short-term effect of higher interest rates is to lower the value of homes. In this setting, we consider an investor that wishes to maximize his expected discounted profit from buying a home and selling it at a later time. As the optimal time to buy a home depends on the optimal time to sell a home, this leads to a *nested optimal stopping problem*. The main purpose of this paper is to solve this nested optimal stopping problem by providing an explicit characterization of the optimal buying and selling times when the risk-free rate of interest is modeled as a Markov diffusion and to provide a detailed study of the case in which the risk-free rate of interest is modeled as a Cox-Ingersoll-Ross (CIR) process.

Mathematically, our problem formulation falls within a class of optimal stopping problems

²Freddie Mac, 30-Year Fixed Rate Mortgage Average in the U.S., Jan 2022, <https://fred.stlouisfed.org/series/MORTGAGE30US>

³Overnight Bank Funding Rate in the U.S. from January 2019 to January 2021., Jan 2022, <https://fred.stlouisfed.org/series/OBFR>

with stochastic discounting studied in [19]. To obtain the investor's value function, we use the nonnegative concave majorant approach developed by [19]. This approach has been applied to a variety of optimal stopping problems. For instance, [42] uses this approach to derive optimal strategies for the problem of starting-stopping a CIR process. And [41] uses this approach to derive the optimal timing for trading with transaction costs where the trading price spread between two assets is modeled by an Ornstein–Uhlenbeck (OU) process.

The rest of this chapter proceeds as follows. In Section 4.2 we present a model for how the risk-free rate of interest affects home values. Next, in Section 4.3, we define the investor's optimal home-buying and home-selling problems. The optimal home-buying and home-selling problems fall into a larger class of optimal stopping problems with stochastic discounting. We provide a general solution to these optimal stopping problems in Section 4.4. In Section 3.4.2 we focus specifically on the case in which the risk-free rate of interest is described by a CIR process. We derive expressions for the value functions and optimal stopping times that correspond to the investor's optimal buying and selling problems. Additionally, we calculate the expected time the investor waits to buy and then holds a home before selling, assuming he follows the optimal buying and selling strategies. Lastly, in Section 4.7, we offer some thoughts on future directions of research.

4.2 *The Relation Between Interest Rates and Home Values*

Throughout this chapter, we fix a probability space $(\Omega, \mathcal{F}, \mathbb{P})$ and a filtration $\mathbb{F} = (\mathcal{F}_t)_{t \geq 0}$. The probability measure \mathbb{P} represents the physical probability measure. In this setting, let $R = (R_t)_{t \geq 0}$ denote the risk-free rate of interest. We shall suppose that R is a regular diffusion that lives on an interval $\mathcal{J} := (x, y)$, where the end points x and y are natural and satisfy $0 \leq x < y \leq \infty$. Specifically, we suppose that R is the unique strong solution to an SDE that is of the form

$$dR_t = \mu(R_t)dt + \sigma(R_t)dW_t, \tag{4.1}$$

where $W = (W_t)_{t \geq 0}$ is a one-dimensional (\mathbb{P}, \mathbb{F}) -Brownian motion and the functions μ and σ satisfy

$$\mu : \mathcal{J} \rightarrow \mathbb{R}, \quad \sigma : \mathcal{J} \rightarrow \mathbb{R}_{++},$$

with $\mathbb{R}_{++} := (0, \infty)$.

The aim of this section is to develop a framework that captures how the dynamics of R affect home values. To this end, we consider a representative home-buyer seeking to purchase a primary residence, whose actions capture the typical home-buyer within a given economic class in the broader population. At time t , we suppose the home-buyer can afford to pay a cash flow of $(C_t)_{t \geq 0}$ per unit time for housing. As time passes, the home-buyer's wages will increase and, as such, so will the amount of money he can afford to pay for housing. To capture this effect, we suppose that the dynamics of the cash flows are as follows

$$C_t = C e^{\gamma \int_0^t R_s ds}, \quad C > 0, \quad \gamma > 0. \quad (4.2)$$

Equation (4.2) assumes that the amount of money the representative home-buyer can allocate to housing per unit time grows at a rate γR that is proportional to the risk-free rate of interest. If one considers the risk-free rate R to be a proxy for inflation, then γ captures how quickly the home-buyer's wages grow in real (as opposed to nominal) terms. If $\gamma > 1$ the home-buyer's wages grow faster than inflation and he is getting richer over time. On the other hand, if $\gamma < 1$ the home-buyer's wages are not keeping up with inflation and, over time, he is becoming poorer.

Now, suppose that, at time t , the representative home-buyer has found a home he wishes to purchase. In order to finance this purchase, he takes out a loan from a bank with a repayment period of T years at a fixed interest rate $R_t + \rho$ where $\rho > 0$. The constant ρ captures the fact that home-buyer may default on his loan payments and, thus, should be charged an interest rate that is higher than the risk-free rate of interest. As, at time t , the representative home-buyer can only afford to pay a cash-flow of C_t per unit time, the

maximum value of the home he can afford is

$$\int_t^{t+T} C_t e^{-(R_t+\rho)(u-t)} du = \frac{C_t}{R_t + \rho} \left(1 - e^{-(R_t+\rho)T}\right).$$

Although home-buyers of different economic classes will be able to afford different cash-flows for housing, the relationship between the value of a home and the interest rate R will be the same for all homes in the economy. Thus, the value $V = (V_t)_{t \geq 0}$ of any homes in the economy is given by

$$V_t = v(R_t) e^{\gamma \int_0^t R_s ds}, \quad v(R_t) := \frac{C}{R_t + \rho} \left(1 - e^{-(R_t+\rho)T}\right), \quad (4.3)$$

where C is a constant that captures the relative expense of a particular home; it will play no role in the analysis that follows. It is important to notice that the interest rate R has both a long-term and a short-term effect on the value V of a home. In the long-term, higher interest rates have the effect of raising the value of a home due to the term $e^{\gamma \int_0^t R_s ds}$. In the short-term, the effect of interest rates on home values is captured by $v(R_t)$. Using the fact that $e^x > 1 + x$ for any $x > 0$, we have that

$$v'(r) = -\frac{C e^{-(r+\rho)T}}{(r + \rho)^2} \left(e^{(r+\rho)T} - 1 - (r + \rho)T\right) < 0. \quad (4.4)$$

This means that $v(r)$ is a decreasing function of r , and that in the short-term, higher interest rates have the effect of lowering the value of a home. The dynamics of V is given by

$$dV_t = \left(\gamma R_t + \frac{1}{v(R_t)} \left(\mu(R_t) v'(R_t) + \frac{1}{2} \sigma^2(R_t) v''(R_t) \right) \right) V_t dt + \frac{v'(R_t) \sigma(R_t)}{v(R_t)} V_t dW_t.$$

Note that while V alone is not a Markov process, the pair (R, V) is Markov.

Remark 4.2.1. Note that we have modeled the mortgage rate obtained by the home-buyer as an affine function of the short rate: $R_t + \rho$. An alternative choice would be to model the mortgage rate as a function the forward rate $F_t^{t, t+T}$ where

$$F_t^{T_1, T_2} := \frac{1}{T_2 - T_1} \left(\frac{B_t^{T_1}}{B_t^{T_2}} - 1 \right),$$

and B_t^T is the value at time t of a zero-coupon bond that matures at time T . Note that, as we have assumed that R is a time-homogeneous diffusion process, the price of a bond is given by a function of R_t and the time to maturity $T - t$, that is, $B_t^T = B(T - t, R_t)$ for some function B . As such, the forward rate at the time a home is purchased

$$F_t^{t,t+T} = \frac{1}{T} \left(\frac{1}{B(T, R_t)} - 1 \right),$$

is simply a function of R_t . Thus, a more general modeling framework, which would allow for the mortgage rate to be a function of either the forward rate or the short rate would be to set the mortgage rate equal to some arbitrary function of the short-rate R_t .

4.3 *Optimal Home Buying and Selling Problems*

Having described the relationship between the risk-free rate of interest R and home values V , we now consider an investor who wishes to buy and then sell a home in order to maximize the present value of these transactions. Note that the investor's profit-maximizing aim is different from that of a representative home-buyer in the broader population, who typically purchases a home as a primary residence. In this sense, the investor can be considered an outlier in the population. As such, his actions do not affect home prices.

Note that, as short-selling of homes is not allowed, we will not consider cases in which the investor first sells and then later buys back a home. We will suppose that for a payment P_t received at time t the investor assigns a present value of $\mathbb{E}(e^{-\chi \int_0^t R_s ds} P_t)$, where $\chi > 0$ is a discount rate that is specific to the investor. The larger the value of χ , the more heavily the investor discounts future payments. One can alternatively consider constant discounting of the form $\mathbb{E}(e^{-\chi t} P_t)$. This case is discussed in Appendix C.3.

Let us denote by τ_b and τ_s , respectively, the times at which the investor buys and sells a home. In general, τ_b and τ_s will be (random) \mathbb{F} -stopping times. Because the investor is not purchasing a primary residence, the interest rate he would pay were he to take out a loan for a home would be very high. As such, we will suppose that the investor pays cash for a

home. The amount of money the investor will need to pay at time τ_b to buy a home will be

$$\begin{aligned} \text{Cost of home purchase} &= V_{\tau_b}(1 + \delta_b) + K_{b,\tau_b}, & \delta_b &> 0, \\ K_{b,t} &:= K_b e^{\gamma \int_0^t R_s ds}, & K_b &> 0, \end{aligned} \quad (4.5)$$

where δ_b represents a transaction cost that is proportional to the value of a home price (e.g., a fee to a realtor) and K_{b,τ_b} represents fixed transaction costs (e.g., fees paid to a title company). Note that the fixed transaction cost K_{b,τ_b} grows over time due to inflation whereas the proportional transaction cost $\delta_b V_{\tau_b}$ scales with the value of a home. Similarly, when the investor sells a home he has purchased, he will receive

$$\begin{aligned} \text{Revenue from home sale} &= V_{\tau_s}(1 - \delta_s) - K_{s,\tau_s}, & \delta_s &> 0, \\ K_{s,t} &:= K_s e^{\gamma \int_0^t R_s ds}, & K_s &> 0, \end{aligned} \quad (4.6)$$

where δ_s and K_{s,τ_s} capture proportional and fixed transaction costs, respectively.

Although chronologically, the investor must buy a home before he sells it, we will consider the optimal selling problem first. Let \mathcal{T} be the set of \mathbb{F} -stopping times. For a fixed selling strategy $\tau_s \in \mathcal{T}$ the expected discounted revenue the investor will receive from selling the home is

$$J_s^{\tau_s}(r) := \mathbb{E} \left[e^{-\chi \int_0^{\tau_s} R_s ds} (V_{\tau_s}(1 - \delta_s) - K_{s,\tau_s}) \middle| R_0 = r \right].$$

Recalling the relationship (4.3) between V and R , and introducing the process $\Lambda = (\Lambda_t)_{t \geq 0}$, defined by

$$\Lambda_t := (\chi - \gamma) \int_0^t R_s ds, \quad (4.7)$$

we can re-write $J_s^{\tau_s}(r)$ more compactly as follows

$$J_s^{\tau_s}(r) = \mathbb{E} \left[e^{-\Lambda_{\tau_s}} f_s(R_{\tau_s}) \middle| R_0 = r \right], \quad f_s(r) := v(r)(1 - \delta_s) - K_s. \quad (4.8)$$

In order to maximize the present value of the revenue received from selling a home, the investor will need to maximize $J_s^{\tau_s}$ over all stopping times $\tau_s \in \mathcal{T}$. We therefore define the

selling value function J_s and *optimal selling strategy* τ_s^* (assuming it exists) as follows

$$J_s(r) := \sup_{\tau_s \in \mathcal{T}} J_s^{\tau_s}(r) =: J_s^{\tau_s^*}(r). \quad (4.9)$$

Now, let us assume that the investor will follow the optimal selling strategy τ_s^* . Then, for a fixed buying strategy τ_b , the expected discounted profit he will receive from buying and then selling a home is given by

$$J_b^{\tau_b}(r) := \mathbb{E} \left[e^{-\chi \int_0^{\tau_b} R_s ds} J_s(R_{\tau_b}) - e^{-\chi \int_0^{\tau_b} R_s ds} (V_{\tau_b}(1 + \delta_b) + K_{b,\tau_b}) \middle| R_0 = r \right].$$

Recalling the relationship (4.3) between V and R , the definition (4.7) of Λ and the definition (4.9) of J_s , we can express $J_b^{\tau_b}(r)$ more compactly as follows

$$J_b^{\tau_b}(r) = \mathbb{E} \left[e^{-\Lambda \tau_b} f_b(R_{\tau_b}) \middle| R_0 = r \right], \quad f_b(r) := J_s(r) - (v(r)(1 + \delta_b) + K_b). \quad (4.10)$$

In order to maximize the present value of the purchase and sale of a home, the investor will need to maximize $J_b^{\tau_b}$ over all stopping times $\tau_b \in \mathcal{T}$. We therefore define the *buying value function* J_b and the *optimal buying strategy* τ_b^* (assuming it exists) as follows

$$J_b(r) := \sup_{\tau_b \in \mathcal{T}} J_b^{\tau_b}(r) =: J_b^{\tau_b^*}(r). \quad (4.11)$$

Note that J_s and J_b are the special cases of a class of *optimal stopping problems with stochastic discounting* of the form

$$J(r) := \sup_{\tau \in \mathcal{T}} J^\tau(r) =: J^{\tau^*}(r), \quad J^\tau(r) := \mathbb{E} \left[e^{-\Lambda \tau} f(R_\tau) \middle| R_0 = r \right]. \quad (4.12)$$

Note also that, in order for a nontrivial optimal stopping time of (4.12) to exist, we must have $\Lambda > 0$. Thus, we assume that $\chi > \gamma$ throughout this paper. We shall refer to J and τ^* (with no subscripts) as the *value function* and *optimal stopping time*, respectively. For ease of notation, in the sections that follow, we will use J in an expression that holds true for both J_b and J_s , τ^* in an expression that holds true for τ_b^* and τ_s^* and f in an expression that holds true for f_b and f_s .

Before deriving explicit characterizations of the optimal buying and selling times, let us

examine qualitatively what τ_b^* and τ_s^* should look like. Recall that the short-term effect of the risk free rate of interest R on home prices is captured by $v(R_t)$, which is a decreasing function of R_t . As the investor will want to buy a home when prices are relatively low, we expect that the optimal buying strategy τ_b^* will involve waiting until interest rates R rise to a value r_b called the *buying threshold*. Similarly, as the investor will want to sell when home prices are relatively high, we expect that the optimal selling strategy τ_s^* will involve waiting until the risk-free rate of interest R falls to a value r_s call the *selling threshold*, where $r_s < r_b$. In other words, we expect the optimal buying and selling strategies to be of the form

$$\tau_b^* := \inf\{t \geq 0 : R_t \geq r_b\}, \quad \tau_s^* := \inf\{t \geq 0 : R_t \leq r_s\}, \quad (4.13)$$

where $x < r_s < r_b < y$.

As typically happens in optimization problems, we have neglected to include some features from our modeling framework in order to make the problem analytically tractable. A few of the features we have omitted are listed in the following remarks.

Remark 4.3.1. In our framework, we have not included the possibility of the investor renting out the home he as purchased. There is, however, an important reason for why the investor may not wish to rent out his home for additional income. Consider the form of the optimal selling strategy given in (4.8)-(4.9). We can see that optimal selling time τ_s^* is heavily influenced by the movement of the risk-free rate of interest R . As we can see from Figure 5.14 and 5.15, the mortgage rate and overnight bank funding rate in the United States during a period of a year could fall quickly. Because rental contracts are usually signed for a fixed period (e.g., one year), if the investor were to rent out his home, it is likely that the optimal selling time τ_s^* would overlap with the time in which the home is being rented out, leading to the investor missing the opportunity to sell the home at the optimal time. Moreover, because renter-occupied homes sell for less than homes that are vacant (and staged for sale), if this investor tried to sell the home while the renter was occupying it, he would receive a lower price for the home than he would have had the home not been occupied.

Remark 4.3.2. Note that, as the investor acts to maximize his utility of terminal wealth, we have implicitly assumed that his utility function is linear and that he is not risk-averse. While it would perhaps be more realistic to consider a risk-averse investor with a non-linear utility function, this assumption would preclude framing the investor's optimal buying and selling strategy as the (analytically tractable) solution of a nested optimal stopping problem.

Remark 4.3.3. A possible alternative model for the dynamics of the cash flow C is

$$C_t = Ce^{\gamma t + \int_0^t ds R_s}.$$

In this case, $\gamma > 0$ means that the home-buyer's wages grow faster than inflation, and $\gamma < 0$ means the opposite. These alternative cash-flow dynamics can be recast into the framework previously discussed with a modified interest rate process $\bar{R} = (\bar{R}_t)_{t \geq 0}$. To see this, observe that

$$C_t = Ce^{\gamma \int_0^t ds (1 + \frac{1}{\gamma} R_s)} = Ce^{\gamma \int_0^t ds \bar{R}_s},$$

where we have defined $\bar{R}_t := 1 + \frac{1}{\gamma} R_t$. If we now set

$$\bar{\mu}(r) := \frac{1}{\gamma} \mu(\gamma(r - 1)), \quad \bar{\sigma}(r) := \frac{1}{\gamma} \sigma(\gamma(r - 1)),$$

then the dynamics of \bar{R} are given by

$$d\bar{R}_t = \bar{\mu}(\bar{R}_t)dt + \bar{\sigma}(\bar{R}_t)dW_t.$$

Thus, by replacing R by \bar{R} we are able to analyze the home-buying problem in the framework outline above.

4.4 Expressions for the Value Function J and Optimal Stopping Time τ^*

In this section, we present the expressions for the value function J and optimal stopping time τ^* , which are defined in (4.12). The expressions can be applied to the optimal selling problem (4.9) and optimal buying problem (4.11).

To begin, let \mathcal{A} denote the infinitesimal generator of the risk-free rate of interest process R .

We have

$$\mathcal{A} = \mu(r)\partial_r + \frac{1}{2}\sigma^2(r)\partial_r^2. \quad (4.14)$$

Consider the following ordinary differential equation (ODE) for a function $u : \mathcal{J} \rightarrow \mathbb{R}$

$$\left(\mathcal{A} - (\chi - \gamma)r\right)u(r) = 0. \quad (4.15)$$

Suppose that (4.15) has two independent solutions $u = (u_+, u_-)$ such that u_+ is positive and strictly increasing and u_- is positive and strictly decreasing. It is well-known (see [19, Equation (5)], for instance) that the functions u_+ and u_- are related to the hitting times of the process R as follows

$$\mathbb{E}\left[e^{-\Lambda\tau_c} \mid R_0 = r\right] = \begin{cases} u_+(r)/u_+(c) & r \leq c \\ u_-(r)/u_-(c) & r > c \end{cases}, \quad \tau_c := \inf\{t \geq 0 : R_t = c\},$$

where $c, r \in \mathcal{J}$.

Next, we define the functions $g : \mathcal{J} \rightarrow g(\mathcal{J})$ and $h : g(\mathcal{J}) \rightarrow \mathbb{R}$, which will be used in the expression of J by

$$g(r) := -\frac{u_-(r)}{u_+(r)}, \quad r \in \mathcal{J}, \quad h(q) := \frac{f(g^{-1}(q))}{u_+(g^{-1}(q))}, \quad q \in g(\mathcal{J}). \quad (4.16)$$

We define h_b and h_s from f_b and f_s , respectively, in the same way we define h from f . To ease the notation, we use h to represent expressions that hold true for both h_b and h_s . Because u_+ is strictly positive increasing and u_- is strictly positive decreasing, g is strictly negative increasing, which means that g^{-1} is well defined. The following proposition shows that the value function J can be written in terms of u_+ , u_- , g , and h .

Proposition 4.4.1. *Suppose that the risk-free rate of interest R is defined by (4.1) on an interval $\mathcal{J} = (x, y)$ where x and y are natural boundaries. Let the functions f , u_+ , u_- , g and h be as defined in (4.12), (4.15) and (4.16). If both of the following limits are finite*

$$\ell_x := \lim_{r \rightarrow x^+} \frac{f^+(r)}{u_-(r)}, \quad \ell_y := \lim_{r \rightarrow y^-} \frac{f^+(r)}{u_+(r)}, \quad f^+(r) := \max(f(r), 0),$$

then the value function J defined in (4.12) can be written as

$$J(r) = u_+(r)\widehat{h}(g(r)), \quad r \in \mathcal{J}, \quad (4.17)$$

where \widehat{h} is the smallest decreasing nonnegative concave majorant (NCM) of h .

Proof. See [19, Proposition 3.4]. □

It is well-known (see, for instance [76, Appendix D]) that the optimal stopping time τ^* can be computed from J as follows

$$\tau^* := \inf\{t \geq 0 : R_t \notin \mathcal{C}\}, \quad \text{where} \quad \mathcal{C} := \{r \in \mathcal{J} : J(r) > f(r)\}. \quad (4.18)$$

We refer to the set \mathcal{C} as the *continuation region*.

4.5 Detailed Analysis: CIR Process Risk-Free Rate

In this section, we derive the expressions of J and τ^* when the risk-free rate of interest is modeled by a CIR process. Specifically, suppose that the dynamics of risk-free rate of interest R is given by

$$dR_t = \kappa(\theta - R_t)dt + \sigma\sqrt{R_t}dW_t, \quad (4.19)$$

where $\kappa, \theta, \sigma > 0$. We shall assume the Feller's condition $2\kappa\theta \geq \sigma^2$ is satisfied, which guarantees that R never reaches zero. Note that R is regular on $\mathcal{J} = (0, \infty)$ and both boundaries 0 and ∞ are natural. Using (4.14), the infinitesimal generator \mathcal{A} of the CIR process is given by

$$\mathcal{A} = \kappa(\theta - r)\partial_r + \frac{1}{2}\sigma^2 r\partial_r^2. \quad (4.20)$$

Using this specific infinitesimal generator (4.20), the ODE (4.15) can be written as

$$\left(\kappa(\theta - r)\partial_r + \frac{1}{2}\sigma^2 r\partial_r^2 - (\chi - \gamma)r\right)u(r) = 0. \quad (4.21)$$

In Appendix C.1, we derive explicit expressions for positive increasing and positive decreasing solutions, u_+ and u_- , of (4.21), which are given by

$$u_+(r) = e^{-\nu r} M(\alpha, \beta, \zeta r), \quad u_-(r) = e^{-\nu r} U(\alpha, \beta, \zeta r), \quad (4.22)$$

where the constants $(\alpha, \beta, \xi, \zeta, \nu)$ are defined as follows

$$\begin{aligned} \alpha &:= \frac{\kappa\theta}{\sigma^2} \left(1 - \frac{\kappa}{\xi}\right), & \beta &:= \frac{2\kappa\theta}{\sigma^2}, & \xi &:= \sqrt{\kappa^2 + 2\sigma^2(\chi - \gamma)}, \\ \zeta &:= \frac{2\xi}{\sigma^2}, & \nu &:= \frac{\alpha\zeta}{\beta} = \frac{\xi - \kappa}{\sigma^2}, \end{aligned} \quad (4.23)$$

and where M and U are the confluent hypergeometric function of the first kind and second kind, respectively, as defined in (C.3). As $\kappa, \theta, \sigma > 0$ and $\chi > \gamma$, all parameters in (4.23) are positive, which allows us to write the following limit properties of u_+ and u_-

$$\lim_{r \rightarrow 0^+} u_+(r) = 0, \quad \lim_{r \rightarrow \infty} u_+(r) = \infty, \quad \lim_{r \rightarrow 0^+} u_-(r) = \infty, \quad \lim_{r \rightarrow \infty} u_-(r) = 0. \quad (4.24)$$

We will use the limits in (4.24) to verify the limit conditions of Proposition 4.4.1.

In order to apply Proposition 4.4.1 to determine the expressions for the value function J , it is necessary to determine \widehat{h} , the NCM of h . To that end, we need to know the sign of the slope and convexity of h throughout $g(\mathcal{J})$. Using the definition of h in (4.16) directly, the first and second derivative of h are given by (with the shorthand $r := g^{-1}(q)$)

$$h'(q) = \frac{1}{g'(r)} \frac{u_+(r)f'(r) - u'_+(r)f(r)}{(u_+(r))^2}, \quad (4.25)$$

$$h''(q) = \frac{2}{\sigma^2 r u_+(r) (g'(r))^2} (\mathcal{A} - (\chi - \gamma)r) f(r). \quad (4.26)$$

Equations (4.25) and (4.26) will be used to identify the critical and inflection points of h , which will then be used to calculate \widehat{h} , the NCM of h . We now have the necessary tools to derive the expressions for buying and selling value functions.

4.5.1 Optimal Home Selling Problem

Although chronologically the investor will have to buy a home before being able to sell it, the optimal selling problem must be solved before the optimal buying problem due to the

fact that the form of f_b in (4.10) requires having known the selling value function J_s . To derive the expression of J_s , we first define h_s from f_s the same way we define h from f in (4.16) by

$$h_s(q) := \frac{f_s(g^{-1}(q))}{u_+(g^{-1}(q))}, \quad q < 0. \quad (4.27)$$

It is straightforward to check using (4.8) and (4.24) that

$$\lim_{r \rightarrow 0^+} \frac{f_s^+(r)}{u_-(r)} = 0, \quad \lim_{r \rightarrow \infty} \frac{f_s^+(r)}{u_+(r)} = 0.$$

This shows that the limit conditions in Proposition 4.4.1 are satisfied. Next, we need to identify \widehat{h}_s , the NCM of h_s , which is done in Appendix C.2.1. We have from (C.12) that

$$\widehat{h}_s(q) = \begin{cases} h_s(q), & q \leq q_s \\ q \frac{h_s(q_s)}{q_s}, & q > q_s \end{cases}, \quad q_s := g(r_s),$$

where the selling threshold r_s is the unique positive solution to equation (C.11), which we repeat here for the reader's convenience

$$\frac{u'_-(r_s)}{u_-(r_s)} = \frac{f'_s(r_s)}{f_s(r_s)}.$$

Having confirmed that the limit conditions are satisfied and identified the NCM of h_s , we now apply Proposition (4.4.1) to explicitly write J_s using (4.17) and (C.12) as

$$J_s(r) = u_+(r)\widehat{h}_s(g(r)) = \begin{cases} u_+(r)h_s(g(r)) = f_s(r) & r \leq r_s \\ u_+(r)g(r)\frac{h_s(g(r_s))}{g(r_s)} = f_s(r_s)\frac{u_-(r)}{u_-(r_s)} & r > r_s \end{cases}. \quad (4.28)$$

Next, from (4.18) we can calculate the selling continuation region and optimal selling time as

$$\mathcal{C}_s := \{r : J_s(r) > f_s(r)\} = (r_s, \infty), \quad \tau_s^* := \inf\{t \geq 0 : R_t \leq r_s\}. \quad (4.29)$$

In words, the investor's optimal selling strategy is to sell his home the first time the risk-free rate of interest is at or below r_s . Note that the form of τ_s^* agrees with our previous speculation of the form of the optimal selling strategy in (4.13).

4.5.2 Optimal Home Buying Problem

Having obtained the optimal selling strategy τ_s^* , we now turn our attention to finding the optimal buying strategy τ_b^* . To begin, we define h_b from f_b in the same way we define h from f in (4.16) by

$$h_b(q) := \frac{f_b(g^{-1}(q))}{u_+(g^{-1}(q))}, \quad q < 0. \quad (4.30)$$

Using the form of f_b (4.10), the limit expressions (4.24), and the explicit form of J_s (4.28), it is straightforward to confirm that

$$\lim_{r \rightarrow 0^+} \frac{f_b^+(r)}{u_-(r)} = 0, \quad \lim_{r \rightarrow \infty} \frac{f_b^+(r)}{u_+(r)} = 0.$$

Thus, the limit conditions in Proposition 4.4.1 are satisfied. Next we need to identify \widehat{h}_b , the NCM of h_b , which is done in Appendix C.2.2. We have from (C.13) that

$$\widehat{h}_b(q) = \begin{cases} h_b(q_b) & q \leq q_b \\ h_b(q) & q > q_b \end{cases}, \quad q_b := g(r_b),$$

where the buying threshold is the unique positive solution to the following equation (C.14), which we repeat here for the reader's convenience

$$\frac{u'_+(r_b)}{u_+(r_b)} = \frac{f'_b(r_b)}{f_b(r_b)}.$$

Having confirmed that the limit conditions are satisfied and identified the NCM of h_b , we now apply Proposition 4.4.1 to explicitly write J_b using (4.17) and (C.13) as

$$J_b(r) = u_+(r)\widehat{h}_b(g(r)) = \begin{cases} u_+(r)h_b(g(r_b)) = f_b(r_b)\frac{u_+(r)}{u_+(r_b)} & r \leq r_b \\ u_+(r)h_b(g(r)) = f_b(r) & r > r_b \end{cases}. \quad (4.31)$$

Next, from (4.18) we calculate the buying continuation region and the optimal buying time as

$$\mathcal{C}_b := \{r : J_b(r) > f_b(r)\} = (0, r_b), \quad \tau_b^* := \inf\{t \geq 0 : R_t \geq r_b\}. \quad (4.32)$$

In other words, the investor's optimal buying strategy is to purchase a home the first time the risk-free rate of interest is at or above r_b . Note again that the form of the optimal buying rule agrees with our speculation of the optimal buying strategy as described in (4.13).

4.5.3 Density of Waiting Time

The goal of this section is to derive the densities and expected values of the optimal selling and buying times τ_s^* and τ_b^* , which are characterized by (4.29) and (4.32), respectively. These quantities are important because, for example, if the expected value of either τ_b^* or τ_s^* are on the order of 100s of years, then it would not be practical for an investor to implement the optimal buying and/or selling strategies.

To begin our analysis, let us define the probability density functions of τ_b^* and τ_s^* . We have

$$\begin{aligned} p_{\tau_b^*}(t; r) &:= \frac{d}{dt} \mathbb{P}(\tau_b^* \leq t | R_0 = r), & r < r_b, \\ p_{\tau_s^*}(t; r) &:= \frac{d}{dt} \mathbb{P}(\tau_s^* \leq t | R_0 = r), & r > r_s. \end{aligned}$$

Note that we have restricted the definitions of $p_{\tau_b^*}$ and $p_{\tau_s^*}$ to cases in which $r < r_b$ and $r > r_s$ because if $r \geq r_b$ we have trivially that $\tau_b^* = 0$ and if $r \leq r_s$ we have trivially that $\tau_s^* = 0$. Note also that $p_{\tau_b^*}$ is the density of the first hitting time of R to level r_b from below and $p_{\tau_s^*}$ is the density of the first hitting time of R to level r_s from above. The first hitting time densities for the CIR process are computed explicitly in [46, Proposition 1], which we present below using the notation of the present paper.

Proposition 4.5.1. *Suppose that the risk-free rate of interest $(R_t)_{t \geq 0}$ is a CIR process defined in (4.19) with parameters (κ, θ, σ) that satisfies Feller's condition. Suppose that the initial interest rate r , the buying threshold r_b , and the selling threshold r_s are such that $r_s < r < r_b$. Let $(k_{b,n}(r_b))_{n \geq 1}$, $(k_{s,n}(r_s))_{n \geq 1}$ be the decreasing negative sequences that are all negative roots of the equations*

$$M(k_{b,n}(r_b), \beta, \omega r_b) = 0, \quad U(k_{s,n}(r_s), \beta, \omega r_s) = 0, \quad \beta := \frac{2\kappa\theta}{\sigma^2}, \quad \omega := \frac{\beta}{\theta},$$

respectively, and $(m_{b,n}(r, r_b))_{n \geq 1}$, $(m_{s,n}(r, r_s))_{n \geq 1}$ by

$$m_{b,n}(r, r_b) := -\frac{M(k_{b,n}(r_b), \beta, \omega r)}{k_{b,n}(r_b) \frac{\partial}{\partial k} M(k, \beta, \omega r_b)|_{k=k_{b,n}(r_b)}},$$

$$m_{s,n}(r, r_s) := -\frac{U(k_{s,n}(r_s), \beta, \omega r)}{k_{s,n}(r_s) \frac{\partial}{\partial k} U(k, \beta, \omega r_s)|_{k=k_{s,n}(r_s)}}.$$

Then the probability density functions of τ_b^* and τ_s^* are given by

$$p_{\tau_b^*}(t; r) = -\kappa \sum_{n=1}^{\infty} m_{b,n}(r, r_b) k_{b,n}(r_b) e^{\kappa k_{b,n}(r_b) t}, \quad (4.33)$$

$$p_{\tau_s^*}(t; r) = -\kappa \sum_{n=1}^{\infty} m_{s,n}(r, r_s) k_{s,n}(r_s) e^{\kappa k_{s,n}(r_s) t}, \quad (4.34)$$

respectively. The uniform convergence of the infinite series (4.33) and (4.34) are proven in [46, Proposition 2].

From [46, Equation 19 and 20] the coefficients $k_{b,n}(r_b)$ and $m_{b,n}(r, r_b)$ have the following large- n asymptotics

$$k_{b,n}(r_b) = \mathcal{O}(-n^2), \quad |m_{b,n}(r, r_b)| = \mathcal{O}\left(\frac{1}{n}\right), \quad (4.35)$$

and using [46, Equation 23 and 24], the coefficients $k_{s,n}(r_s)$ and $m_{s,n}(r, r_s)$ have the following large- n asymptotics

$$k_{s,n}(r_s) = \mathcal{O}(-n), \quad |m_{s,n}(r, r_s)| = \mathcal{O}\left(\frac{1}{n}\right). \quad (4.36)$$

The large- n asymptotics of the coefficients in (4.35) and (4.36) guarantee that the infinite sums in the computation of expectations, which we perform below in (4.37), (4.38) and (4.41), converge absolutely. Thus, the infinite sums and integrals can be exchanged.

Using Proposition 4.5.1 we can compute the expected length of time the investor will wait prior to buying a home assuming he follows the optimal buying strategy. We have

$$\begin{aligned} \mathbb{E}\left(\tau_b^* \mid R_0 = r < r_b\right) &= \int_0^{\infty} t p_{\tau_b^*}(t; r) dt = -\kappa \sum_{n=1}^{\infty} \int_0^{\infty} m_{b,n}(r, r_b) k_{b,n}(r_b) t e^{\kappa k_{b,n}(r_b) t} dt \\ &= -\frac{1}{\kappa} \sum_{n=1}^{\infty} \frac{m_{b,n}(r, r_b)}{k_{b,n}(r_b)}. \end{aligned} \quad (4.37)$$

Similarly, the expected length of time the investor will wait prior to selling a home after buying it assuming he follows the optimal buying and selling strategies is

$$\begin{aligned} \mathbb{E}\left(\tau_s^* \mid R_0 = r_b\right) &= \int_0^\infty t p_{\tau_s^*}(t; r_b) dt = -\kappa \sum_{n=1}^\infty \int_0^\infty m_{s,n}(r_b, r_s) k_{s,n}(r_s) t e^{\kappa k_{s,n}(r_s) t} dt \\ &= -\frac{1}{\kappa} \sum_{n=1}^\infty \frac{m_{s,n}(r_b, r_s)}{k_{s,n}(r_s)}. \end{aligned} \quad (4.38)$$

Lastly, we are interested to know the probability density function of $\tau_b^* + \tau_s^*$ the total time the investor waits to buy and then sell a home, assuming he follows the optimal buying and selling strategies. The probability density function of $\tau_b^* + \tau_s^*$, given by

$$p_{\tau_b^* + \tau_s^*}(t; r) := \frac{d}{dt} \mathbb{P}(\tau_b^* + \tau_s^* \leq t \mid R_0 = r),$$

can be calculated as a convolution of the two probability densities (4.33) and (4.34). We have

$$\begin{aligned} p_{\tau_b^* + \tau_s^*}(t; r) &= \int_0^t p_{\tau_b^*}(t'; r) p_{\tau_s^*}(t - t'; r_b) dt' \\ &= \kappa^2 \int_0^t \left(\sum_{i=1}^\infty m_{b,i}(r, r_b) k_{b,i}(r_b) e^{\kappa k_{b,i}(r_b) t'} \sum_{j=1}^\infty m_{s,j}(r_b, r_s) k_{s,j}(r_s) e^{\kappa k_{s,j}(r_s) (t-t')} \right) dt' \\ &= \kappa^2 \sum_{i,j=1}^\infty e^{\kappa k_{s,j}(r_s) t} \int_0^t m_{b,i}(r, r_b) k_{b,i}(r_b) m_{s,j}(r_b, r_s) k_{s,j}(r_s) e^{\kappa (k_{b,i}(r_b) - k_{s,j}(r_s)) t'} dt' \\ &= \kappa^2 \sum_{i,j=1}^\infty m_{b,i}(r, r_b) k_{b,i}(r_b) m_{s,j}(r_b, r_s) k_{s,j}(r_s) \frac{e^{\kappa k_{b,i}(r_b) t} - e^{\kappa k_{s,j}(r_s) t}}{\kappa k_{b,i}(r_b) - \kappa k_{s,j}(r_s)}. \end{aligned} \quad (4.39)$$

The expectation of $\tau_b^* + \tau_s^*$ given by (4.39) is simply the sum of expectations of τ_b^* and τ_s^* , which are given in (4.37) and (4.38).

4.5.4 Numerical Example

Throughout this section we fix the following parameter values

$$\left. \begin{aligned} \kappa = 0.9, & \quad \theta = \frac{0.08}{0.9}, & \quad \sigma = \sqrt{0.033}, \\ \gamma = 0.4, & \quad \chi = 0.6, & \quad r = 0.08, \\ C = \$100,000, & \quad \rho = 0.01, & \quad T = 30 \text{ (years)}, \\ \delta_b = \delta_s = 0.06, & \quad K_b = K_s = \$5000. \end{aligned} \right\} \quad (4.40)$$

The parameters specific to the CIR model (κ, θ, σ) and initial risk-free rate of interest r were taken from [26, Example 10.3.2.2]. Note that the parameters (κ, θ, σ) defined in (4.40) satisfy the Feller condition $(2\kappa\theta \geq \sigma^2)$. The duration of the loan ($T = 30$ years) is standard for a fixed-rate mortgage in the United States. The fixed and proportional transaction costs are also typical for a US-based mortgage.

In Figure 5.16, we plot J_s and J_b using the expressions of the selling and buying value function (4.28), and (4.31). Note that $J_b(r)$ is an increasing function of r because the short term home price is inversely related to interest rate. Likewise, the function $J_s(r)$ is a decreasing function of r . Next, using (C.11) and (C.14), we obtain numerically the selling and buying threshold $r_s \approx 0.026$ and $r_b \approx 0.167$. We plot the probability density function of τ_b^* , the length of time the investor waits before buying, the probability density function of τ_s^* , the length of time the investor holds a home before selling, and the probability density function of $\tau_b^* + \tau_s^*$, the sum of both waiting times in Figure 5.19. Finally, in order to compute the expected length of time the investor waits before buying a home and the expected length of time the investor holds a home before selling it, assuming he follows the optimal strategies, we truncate the infinite sums in (4.37) and (4.38) at 100 terms and obtain

$$\mathbb{E}\left(\tau_b^* \mid R_0 = r < r_b\right) \approx 8.10, \mathbb{E}\left(\tau_s^* \mid R_0 = r_b\right) \approx 11.30, \mathbb{E}\left(\tau_b^* + \tau_s^* \mid R_0 = r\right) \approx 19.41. \quad (4.41)$$

These expectations are shown as vertical bars in their respective graphs in Figure 5.19.

4.6 Future Research

Currently, our modeling allows the investor to purchase and sell a single home. We can instead consider the possibility of the investor buying and selling a home multiple times. Specifically, suppose that the dynamics of home value is given in (4.3) and the investors buys the i -th home at time $\tau_{b,i}$ and sells it at time $\tau_{s,i}$, where $\tau_{b,1} < \tau_{s,1} < \tau_{b,2} < \tau_{s,2} < \dots$. Let $\bar{\tau} = (\tau_{b,1}, \tau_{s,1}, \tau_{b,2}, \tau_{s,2}, \dots)$. We formulate the *repeated optimal buying and selling function* \bar{J} using cost of home purchase (4.5) and revenue from home sale (4.6) and apply the discounting as follow

$$\begin{aligned} \bar{J}(r) = \sup_{\bar{\tau} \in \mathcal{T}} \mathbb{E} & \left[\sum_{k=1}^{\infty} \left(e^{-\chi \int_0^{\tau_{s,k}} R_s ds} (V_{\tau_{s,k}}(1 - \delta_s) - K_{s,\tau_{s,k}}) \right. \right. \\ & \left. \left. - e^{-\chi \int_0^{\tau_{b,k}} R_s ds} (V_{\tau_{b,k}}(1 + \delta_b) + K_{b,\tau_{b,k}}) \right) \middle| R_0 = r \right]. \end{aligned}$$

Similar repeated buying and selling problems have been addressed in [24] and [83].

4.7 Conclusion

In this paper, we have provided an expression for home prices as a function of risk-free rate of interest and its time integral, and the rate of wage growth. In this setting, we have considered an investor who wishes to maximize the discounted expected profit from buying a home and selling it at a later time. Using the expression of home prices, we have defined the optimal home buying and selling problems as a nested optimal stopping problem, for which its value function and optimal stopping rule can be characterized using a nonnegative concave majorant approach. When the risk-free rate of interest is modeled by a CIR process, we have provided an explicit characterization of the optimal buying and selling times. Additionally, in the case of CIR interest rates, we have analyzed the expected time the investor waits before buying as well as the expected time the investor waits before selling a home, assuming he follows the optimal buying and selling strategies. In future work, we plan to extend our results to include a scenario where the investor repeatedly buys and sells homes.

Chapter 5
FIGURES

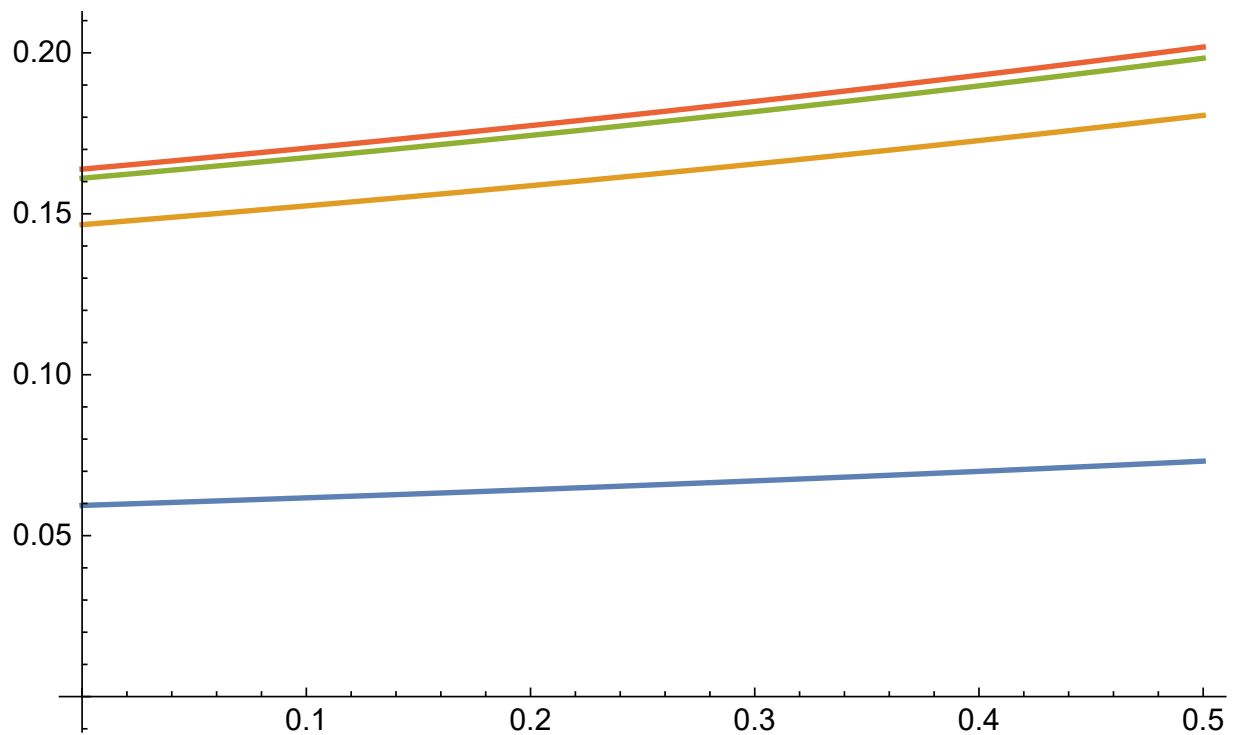


Figure 5.1: For the Vasicek short-rate model described in Section 3.4.1, we plot implied volatility Σ as a function of t with the maturity date of the options fixed at $T = 0.5$ and with the maturity date of the underlying bond taking the following values $\bar{T} = \{1, 3, 5, 10\}$, which correspond to the blue, orange, green, and red curves, respectively. The following model parameters remained fixed: $\kappa = 0.9$, $\delta = \sqrt{0.033}$, and $\theta = \frac{0.08}{0.9}$.

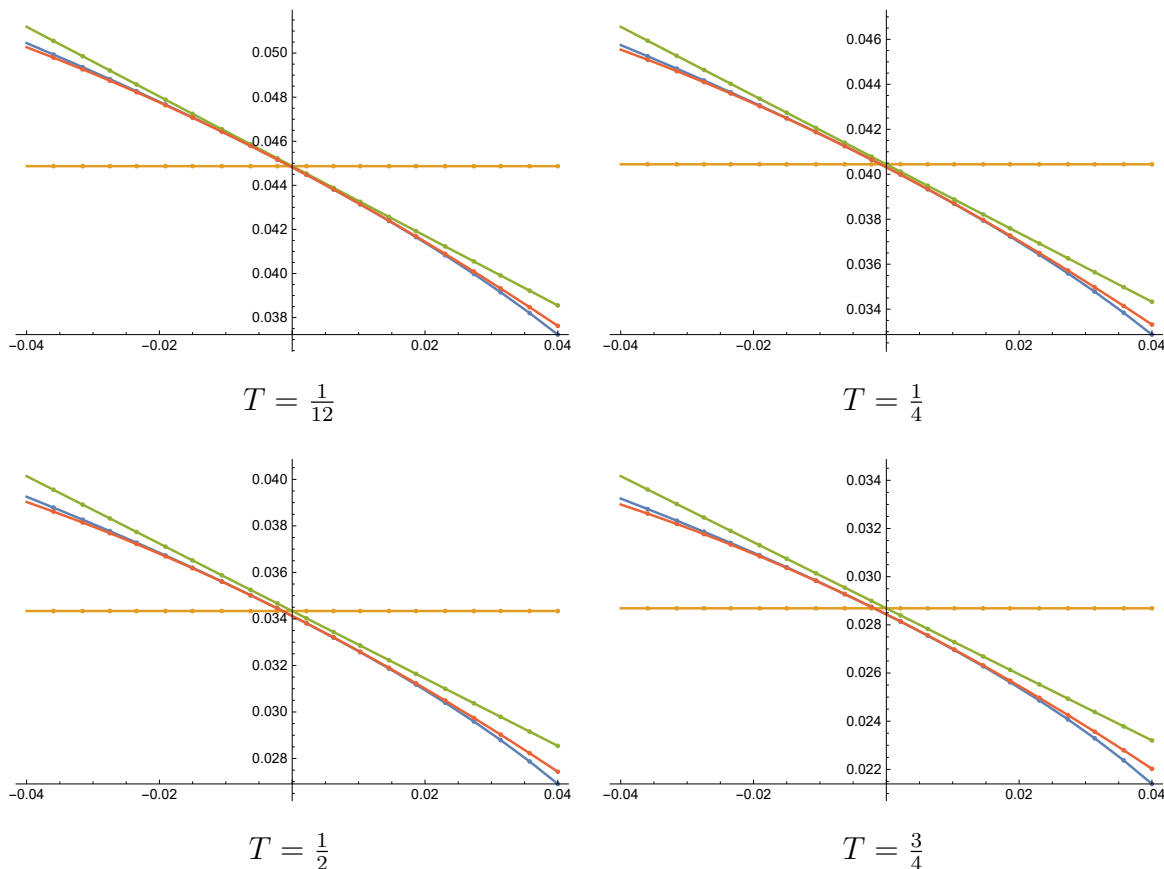


Figure 5.2: For the CIR short-rate model described in Section 3.4.2, we plot exact implied volatility Σ and approximate implied volatility $\bar{\Sigma}_n$ up to order $n = 2$ as a function of log-moneyness $k - x$ with the maturity date of the bond fixed at $\bar{T} = 2$ and with the maturity of the option taking the following values $T = \{\frac{1}{12}, \frac{1}{4}, \frac{1}{2}, \frac{3}{4}\}$. The zeroth, first, and second order approximate implied volatilities correspond to the orange, green and red curves, respectively, and the blue curve correspond to the exact implied volatility. The following parameters, which were taken from [26, Example 10.3.2.2], remained fixed $t = 0$, $\kappa = 0.9$, $\delta = \sqrt{0.033}$, $\theta = \frac{0.08}{0.9}$, $y = 0.08$.

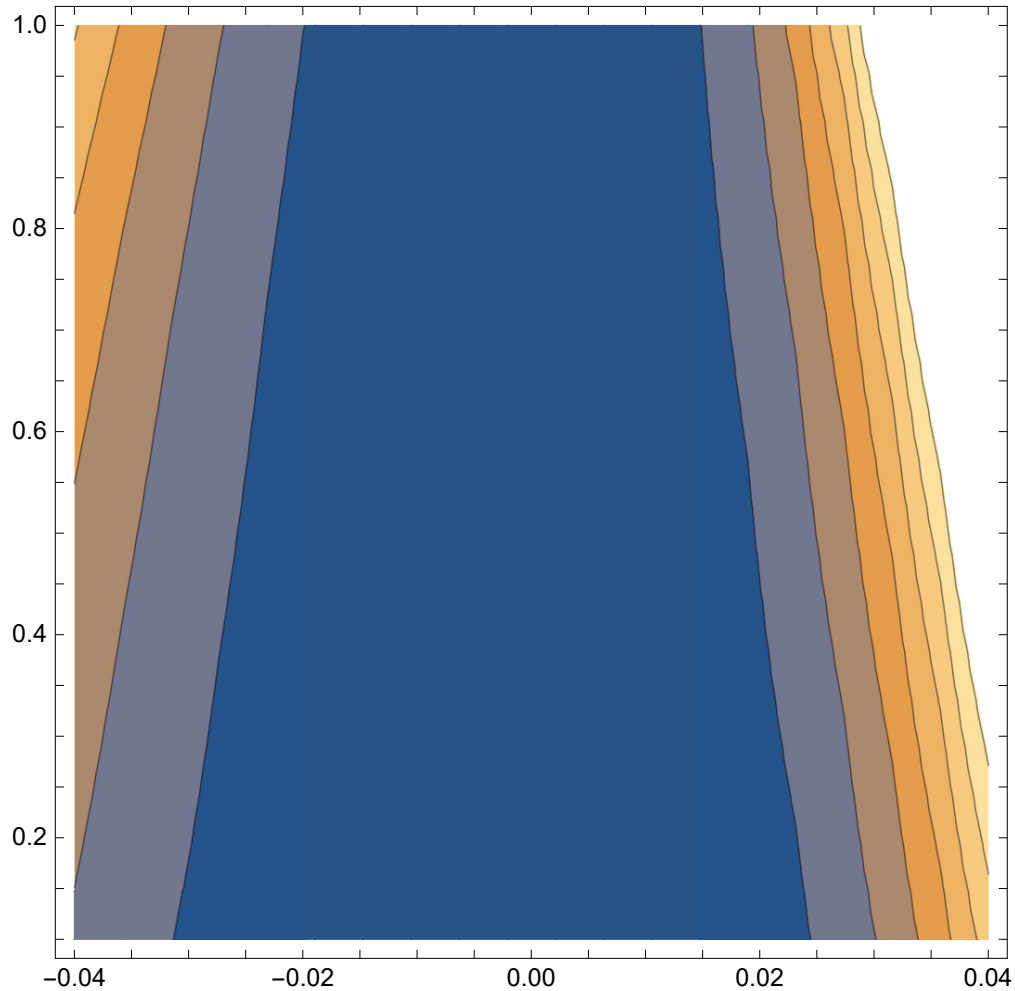


Figure 5.3: For the CIR short-rate model described in Section 3.4.2, we plot the absolute value of the relative error of our second order implied volatility approximation $|\bar{\Sigma}_2 - \Sigma|/\Sigma$ as a function of log-moneyness ($k - x$) and option maturity T . The horizontal axis represents log-moneyness ($k - x$) and the vertical axis represents option maturity T . Ranging from darkest to lightest, the regions above represent relative errors in increments of 0.2% from $< 0.2\%$ to $> 1.4\%$. The maturity date of the bond is fixed at $\bar{T} = 2$. The following parameters, which were taken from [26, Example 10.3.2.2], remained fixed $t = 0$, $\kappa = 0.9$, $\delta = \sqrt{0.033}$, $\theta = \frac{0.08}{0.9}$, $y = 0.08$.

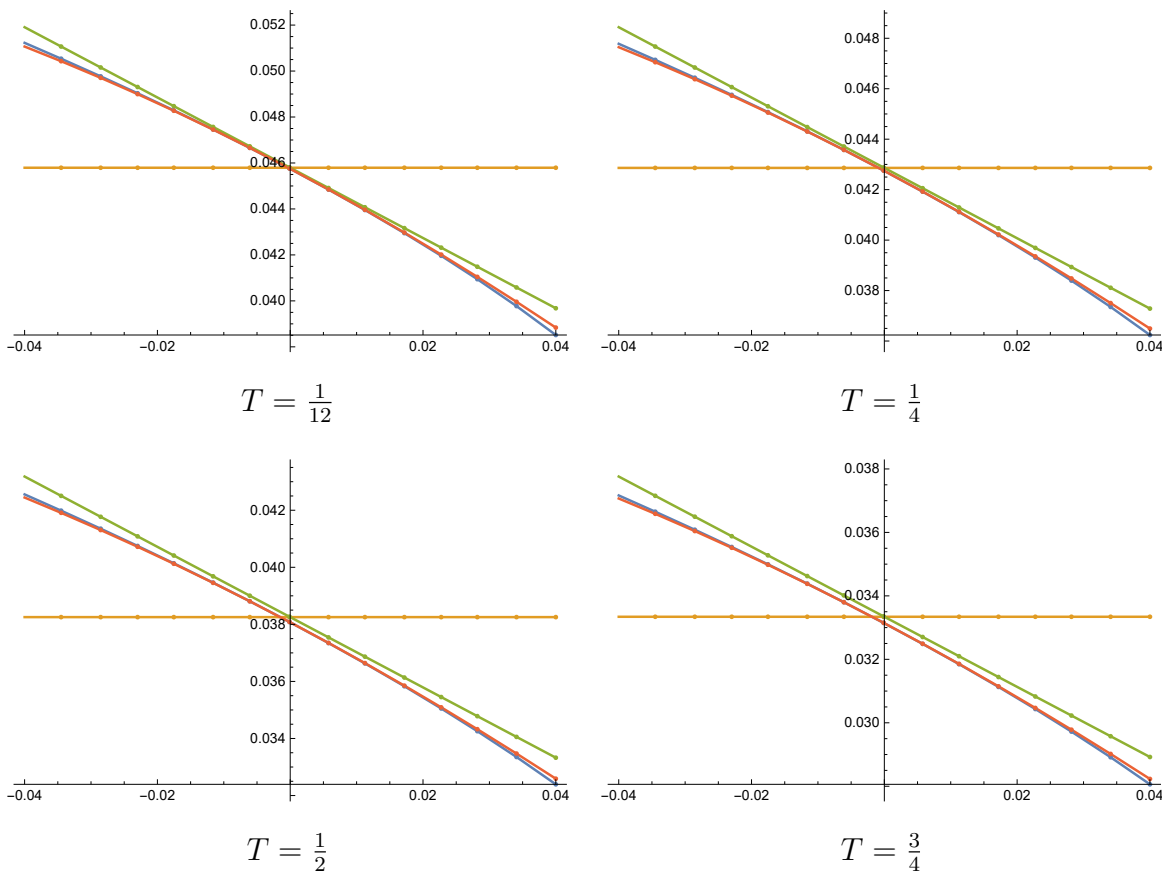


Figure 5.4: For the 2-D CIR short-rate model described in Section 3.4.3, we plot exact implied volatility Σ and approximate implied volatility $\bar{\Sigma}_n$ up to order $n = 2$ as a function of log-moneyness $k - x$ with the maturity date of the bond fixed at $\bar{T} = 2$ and with the maturity of the option taking the following values $T = \{\frac{1}{12}, \frac{1}{4}, \frac{1}{2}, \frac{3}{4}\}$. The zeroth, first, and second order approximate implied volatilities correspond to the orange, green and red curves, respectively, and the blue curve correspond to the exact implied volatility. The following parameters remained fixed $t = 0$, $\kappa_1 = \kappa_2 = 0.9$, $\delta_1 = \delta_2 = \sqrt{0.033}$, $\theta_1 = \theta_2 = \frac{0.08}{0.9}$, $y_1 = y_2 = 0.04$.

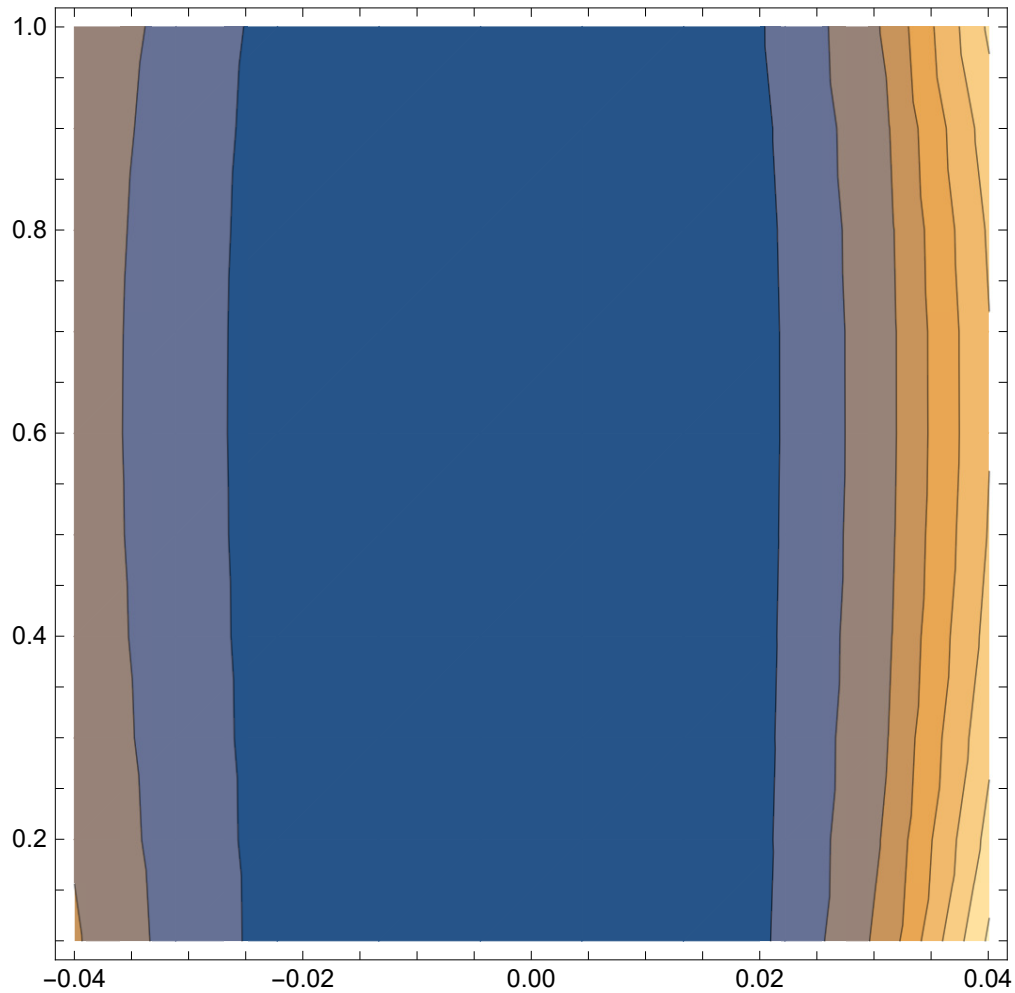


Figure 5.5: For the 2-D CIR short-rate model described in Section 3.4.3, we plot the absolute value of the relative error of our second order implied volatility approximation $|\bar{\Sigma}_2 - \Sigma|/\Sigma$ as a function of log-moneyness ($k - x$) and option maturity T . The horizontal axis represents log-moneyness ($k - x$) and the vertical axis represents option maturity T . Ranging from darkest to lightest, the regions above represent relative errors in increments of 0.1% from $< 0.1\%$ to $> 0.8\%$. The maturity date of the bond is fixed at $\bar{T} = 2$. The following parameters remained fixed $t = 0$, $\kappa_1 = \kappa_2 = 0.9$, $\delta_1 = \delta_2 = \sqrt{0.033}$, $\theta_1 = \theta_2 = \frac{0.08}{0.9}$, $y_1 = y_2 = 0.04$.

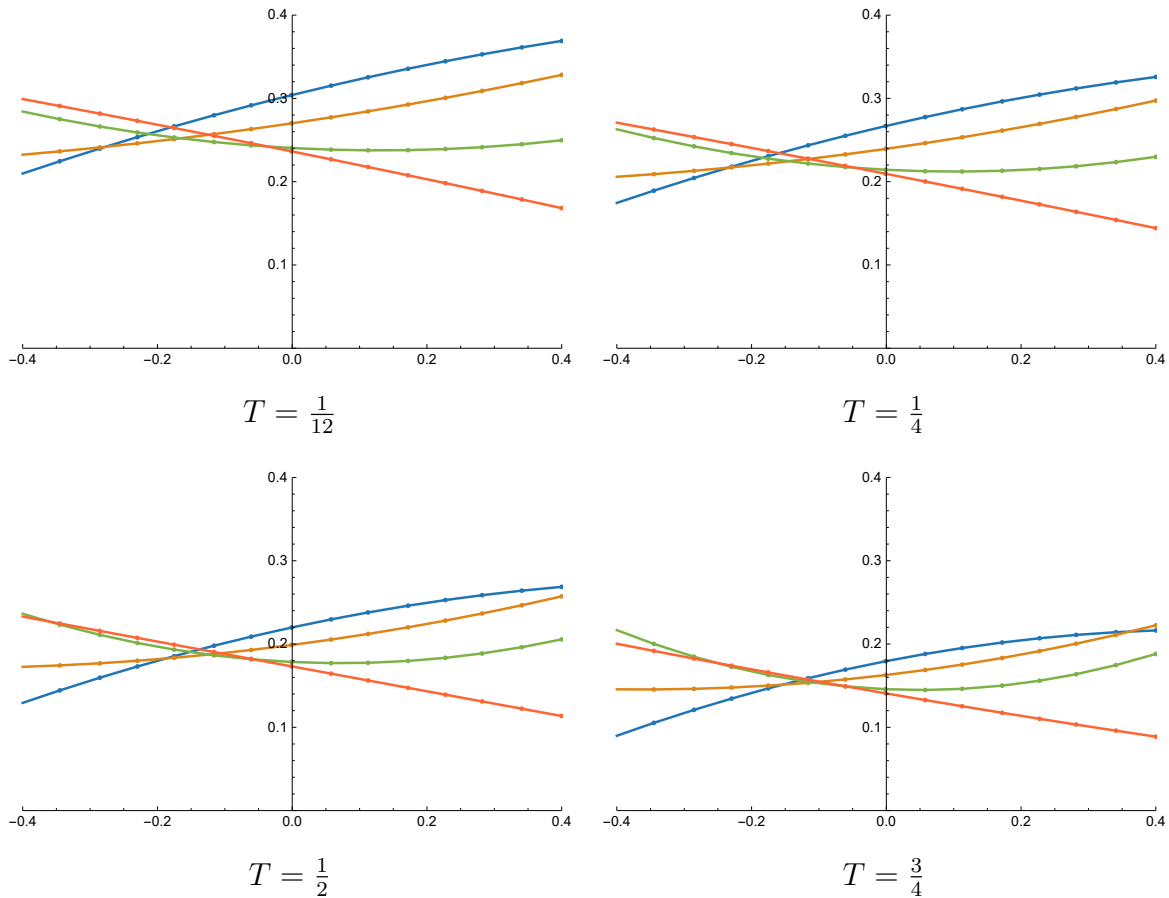


Figure 5.6: For the Fong-Vasicek short-rate model described in Section 3.4.4, we plot the approximate implied volatility $\bar{\Sigma}_2$ as a function of log-moneyness $k - x$ with the maturity date of the bond fixed at $\bar{T} = 2$, with the maturity of the option taking the following values $T = \{\frac{1}{12}, \frac{1}{4}, \frac{1}{2}, \frac{3}{4}\}$ and with the correlation parameter taking values $\rho = \{-0.7, -0.3, 0.3, 0.7\}$ corresponding to the blue, orange, green and red curves respectively. The following model parameters remained fixed in all four plots $t = 0$, $\kappa_1 = \kappa_2 = 0.9$, $\delta_2 = \sqrt{0.08}$, $\theta_1 = \theta_2 = 0.08$, $y_2 = 0.08$.

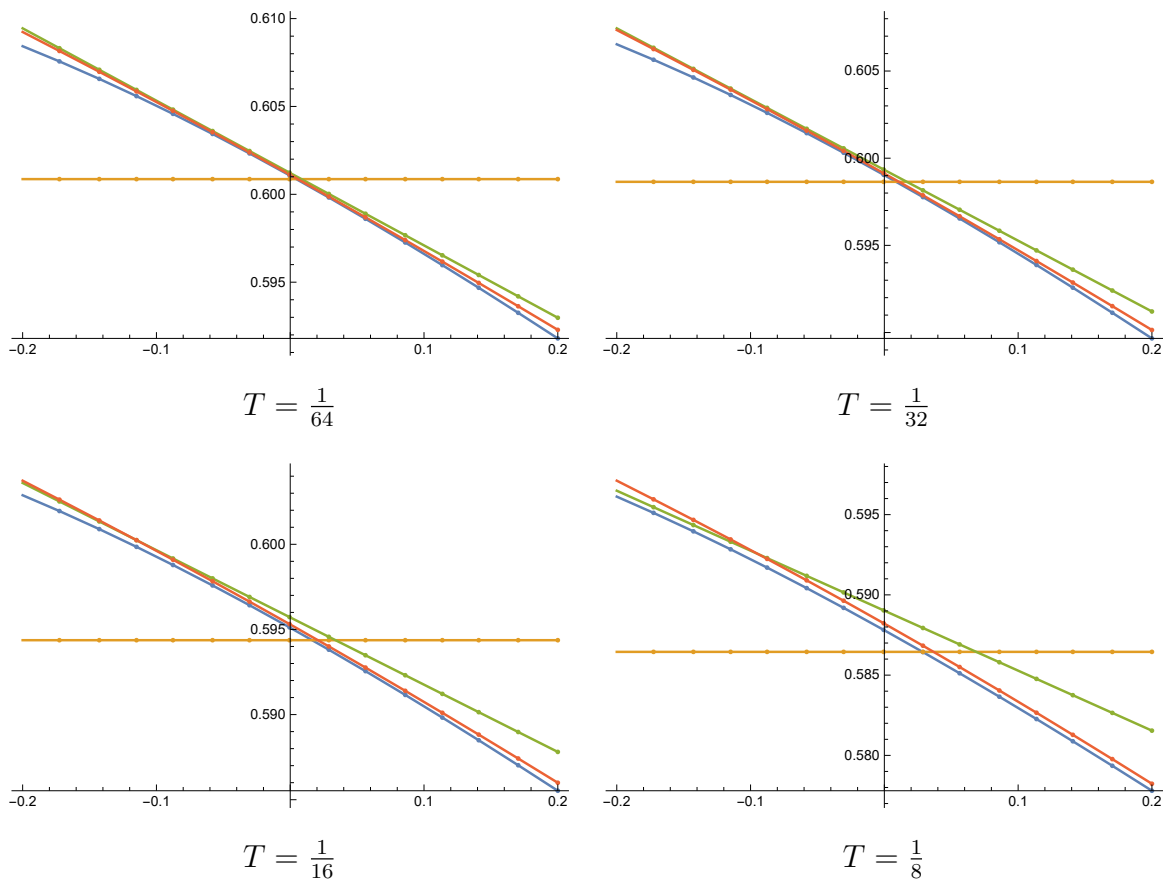


Figure 5.7: For the QOU model described in Section 3.5, we plot exact implied volatility Σ and approximate implied volatility $\bar{\sigma}_n$ up to order $n = 2$ as a function of log-moneyness $k - x$ with the initial date and settlement date of the caplet is fixed at $t = 0$ and $\bar{T} = 2$, respectively, and with the reset date of the caplet taking the following values $T = \{\frac{1}{64}, \frac{1}{32}, \frac{1}{16}, \frac{1}{8}\}$. The zeroth, first, and second order approximate implied volatilities correspond to the orange, green and red curves, respectively, and the blue curve corresponds to the exact implied volatility. The following parameters remained fixed: $q = 0$, $\kappa = 0.9$, $\theta = \frac{0.25}{0.9}$, $\delta = 0.2$

$$, y = \sqrt{0.08}.$$

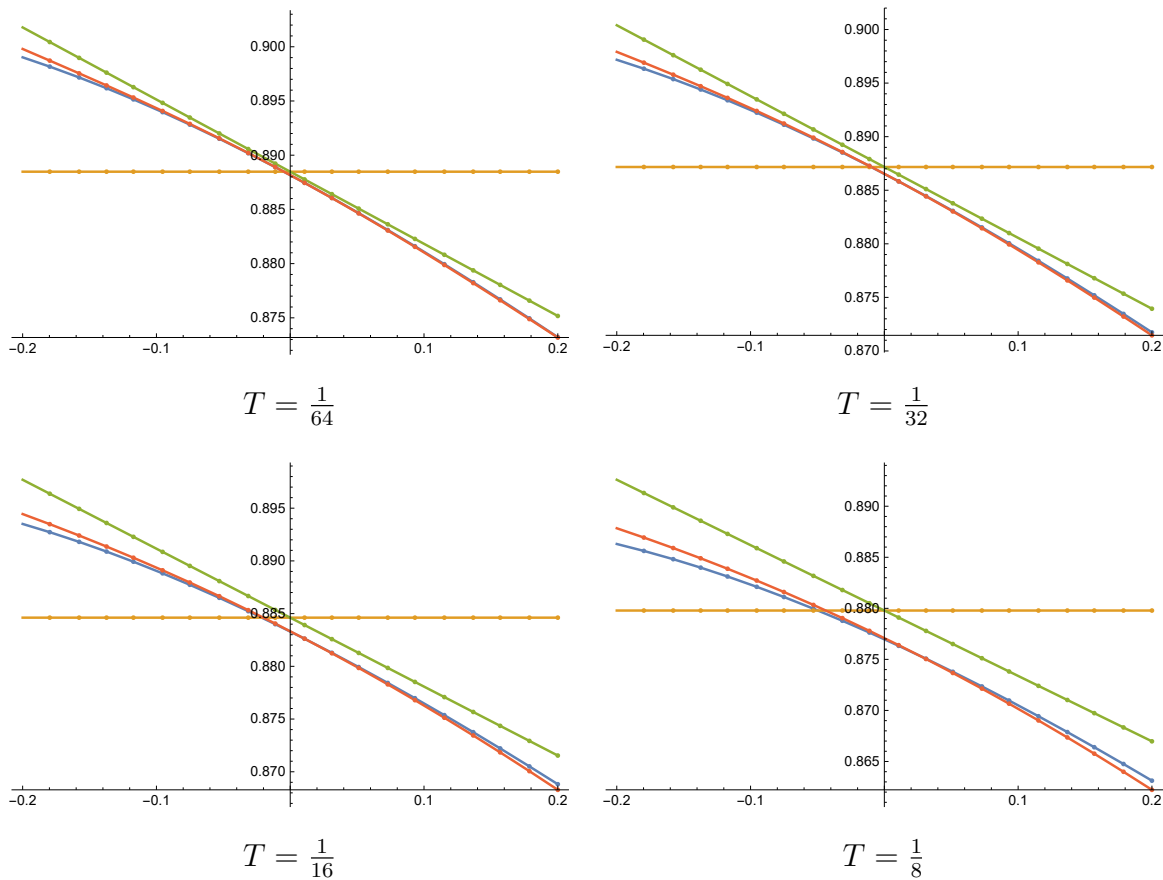


Figure 5.8: For the QOU model described in Section 3.5, we plot the exact implied volatility σ and approximate implied volatility $\bar{\sigma}_n$ up to order $n = 2$ as a function of log-moneyness $k - x$ with the initial date and settlement date of the caplet is fixed at $t = 0$ and $\bar{T} = 2$, respectively, and with the reset date of the caplet taking the following values $T = \{\frac{1}{64}, \frac{1}{32}, \frac{1}{16}, \frac{1}{8}\}$. The zeroth, first, and second order approximate implied volatilities correspond to the orange, green and red curves, respectively, and the blue curve corresponds to the exact implied volatility. The following parameters remained fixed: $\kappa = 0.045$, $\delta = \sqrt{0.035}$, $y = \sqrt{0.08}$, $\theta = q = 0$.

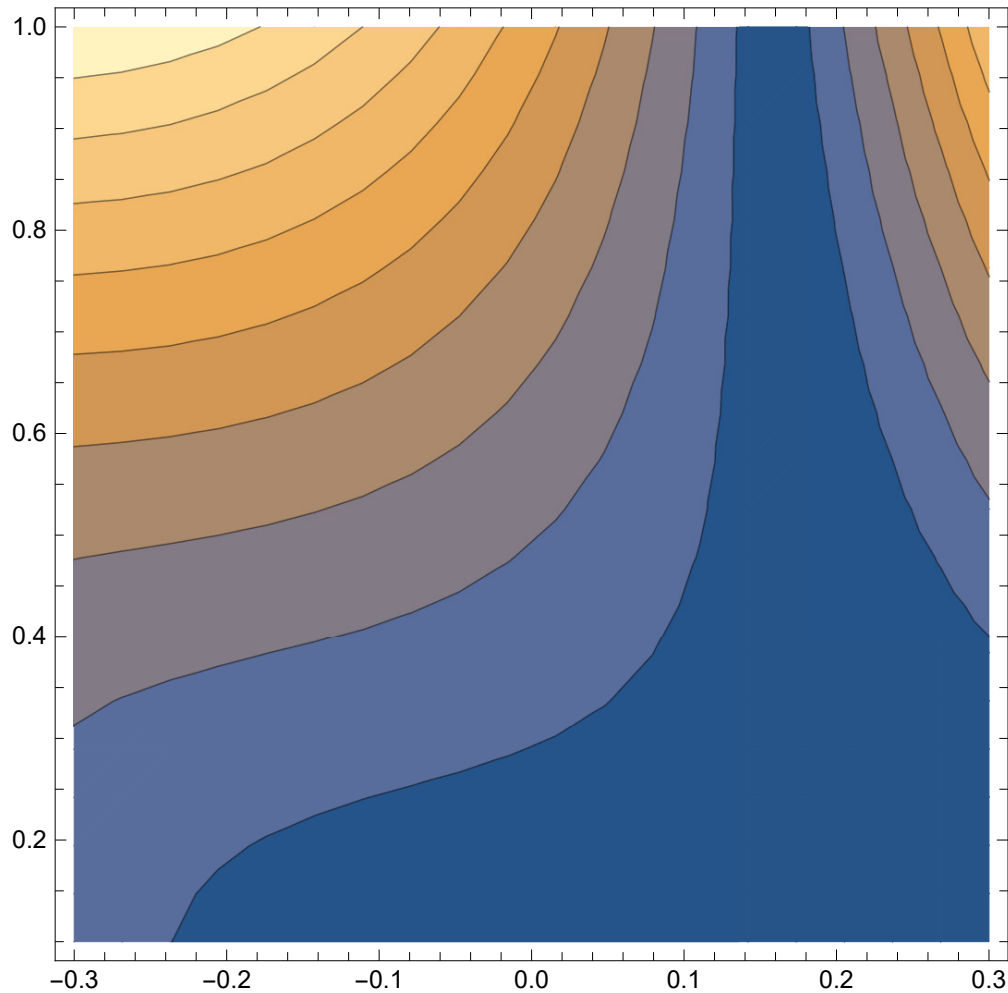


Figure 5.9: For the QOU model described in Section 3.5, we plot the absolute value of the relative error of our second order implied volatility approximation $|\bar{\sigma}_2 - \sigma|/\sigma$ as a function of log-moneyness $k - x$ and caplet reset date T . The horizontal axis represents log-moneyness $k - x$ and the vertical axis represents caplet reset date T . Ranging from darkest to lightest, the regions above represent relative errors in increments of 0.002 from < 0.002 to > 0.018 . The initial date and settlement date of the caplet is fixed at $t = 0$ and $\bar{T} = 2$, respectively. The following parameters remained fixed: $q = 0$, $\kappa = 0.9$, $\theta = \frac{0.25}{0.9}$, $\delta = 0.2$, $y = \sqrt{0.08}$.

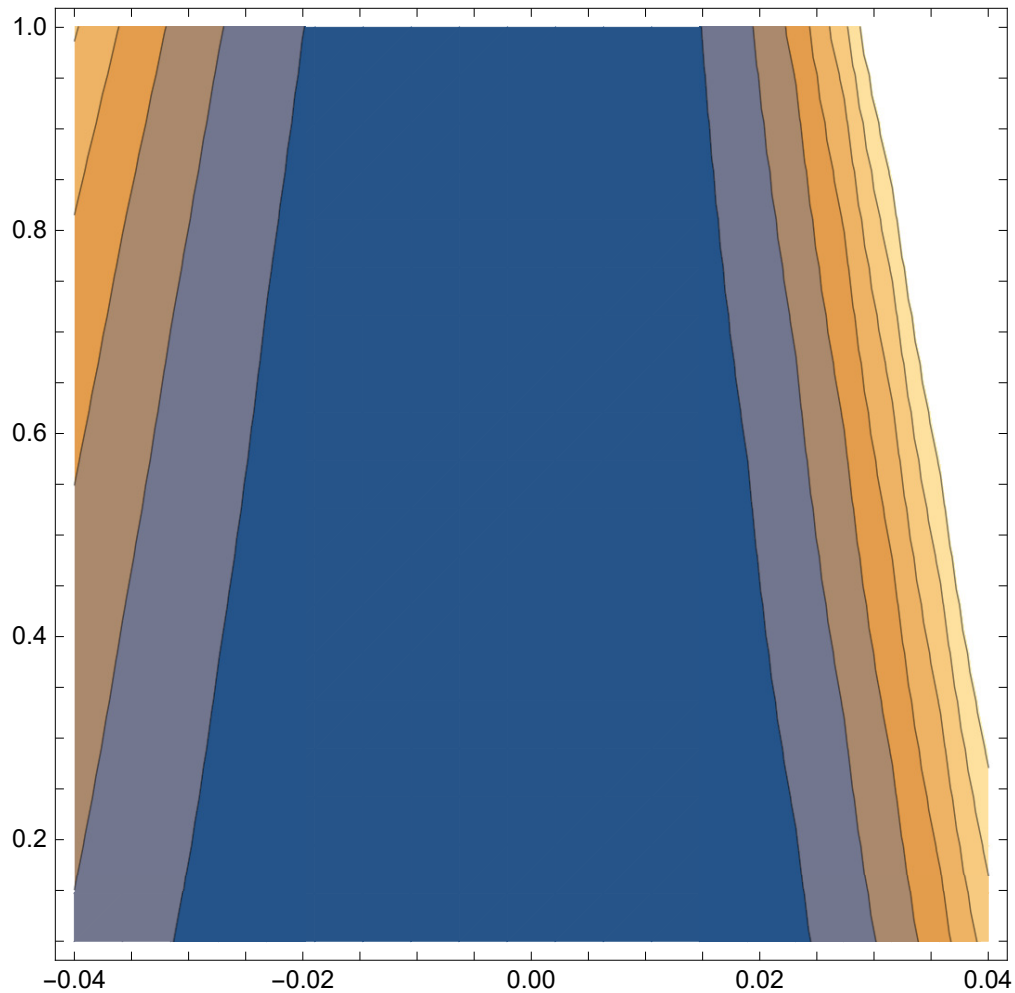


Figure 5.10: For the QOU model described in Section 3.5, we plot the absolute value of the relative error of our second order implied volatility approximation $|\bar{\sigma}_2 - \sigma|/\sigma$ as a function of log-moneyness $k - x$ and caplet reset date T . The horizontal axis represents log-moneyness $k - x$ and the vertical axis represents caplet reset date T . Ranging from darkest to lightest, the regions above represent relative errors in increments of 0.005 from < 0.005 to 0.03. The initial date and settlement date of the caplet is fixed at $t = 0$ and $\bar{T} = 2$, respectively. The following parameters remained fixed: $\kappa = 0.045$, $\delta = \sqrt{0.035}$, $y = \sqrt{0.08}$, $\theta = q = 0$.

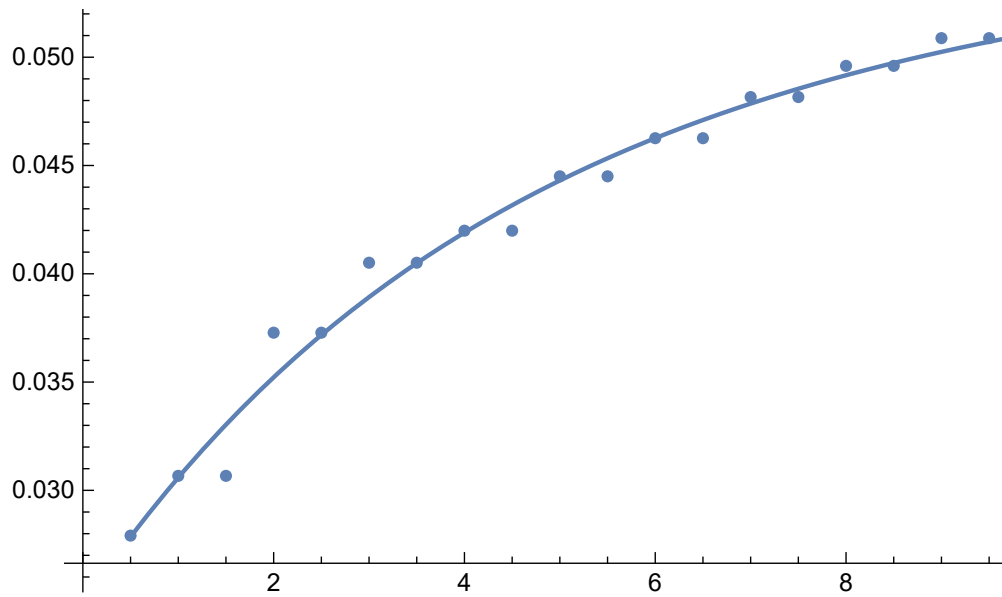


Figure 5.11: Using the parameters Φ^* given in (3.6), we plot the fitted simple forward rate curve $L_t^{T, T+\tau}(\Phi^*)$ along with L_i , the forward LIBOR curve data on the 18 November 2008 where $t = 0$ and $\tau = \frac{1}{2}$ are fixed. The horizontal axis represents T in years and the vertical axis represents the simple forward rate.

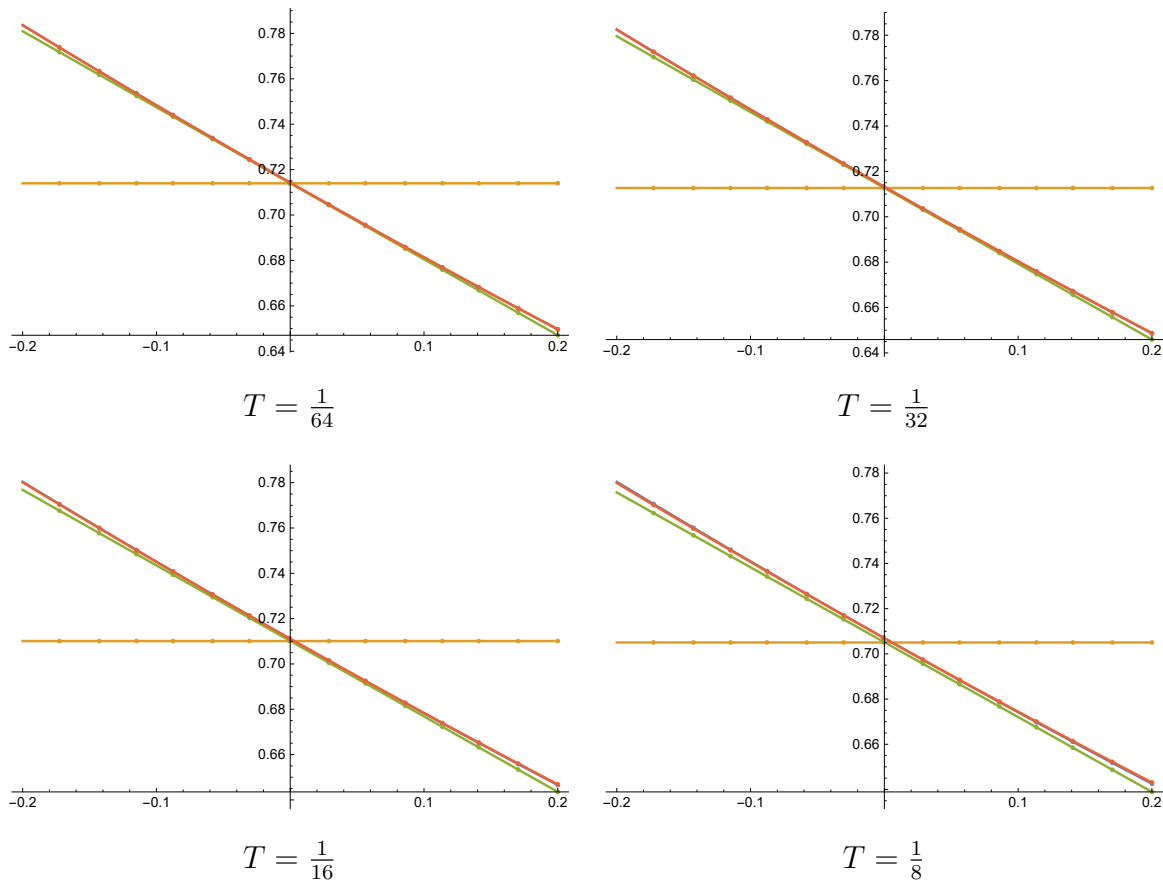


Figure 5.12: For the QOU model described in Section 3.5, we plot the exact implied volatility σ and approximate implied volatility $\bar{\sigma}_n$ up to order $n = 2$ as a function of log-moneyness $k - x$ with the initial date and settlement date of the caplet is fixed at $t = 0$ and $\bar{T} = 2$, respectively, and with the reset date of the caplet taking the following values $T = \{\frac{1}{64}, \frac{1}{32}, \frac{1}{16}, \frac{1}{8}\}$. The zeroth, first, and second order approximate implied volatilities correspond to the orange, green and red curves, respectively, and the blue curve corresponds to the exact implied volatility. The parameters $(\kappa, \theta, \delta, q, y) = (\kappa^*, \theta^*, \delta^*, q^*, y^*)$ are given by (3.6).

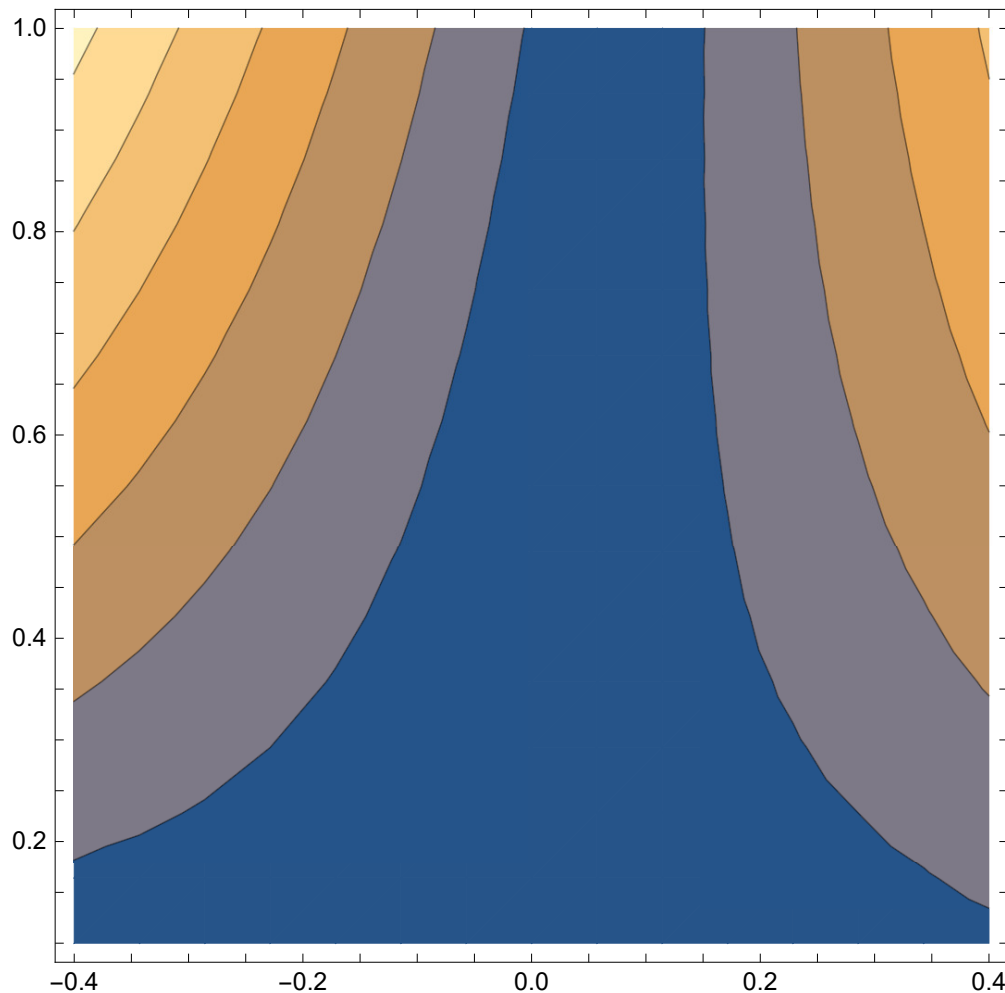


Figure 5.13: For the QOU model described in Section 3.5, we plot the absolute value of the relative error of our second order implied volatility approximation $|\bar{\sigma}_2 - \sigma|/\sigma$ as a function of log-moneyness $k - x$ and caplet reset date T . The horizontal axis represents log-moneyness $k - x$ and the vertical axis represents caplet reset date T . Ranging from darkest to lightest, the regions above represent relative errors in increments of 0.002 from < 0.002 to 0.012. The initial date and settlement date of the caplet is fixed at $t = 0$ and $\bar{T} = 2$, respectively. The parameters $(\kappa, \theta, \delta, q, y) = (\kappa^*, \theta^*, \delta^*, q^*, y^*)$ are given by (3.6).

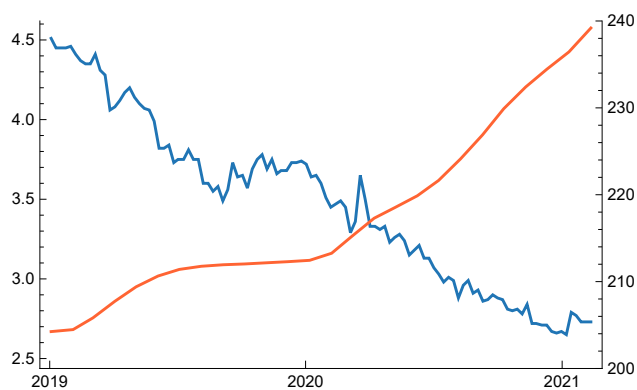


Figure 5.14: We plot, from January 2019 to January 2021, the Monthly S&P/Case-Shiller U.S. National Home Price Index [1] in orange with the scale on the right vertical axis, and Weekly 30-Year Fixed Rate Mortgage Average in the United States [2] in blue with the scale on the left vertical axis. Note that decreasing the federal mortgage rate has an effect of increasing the home price index during this short-term period.

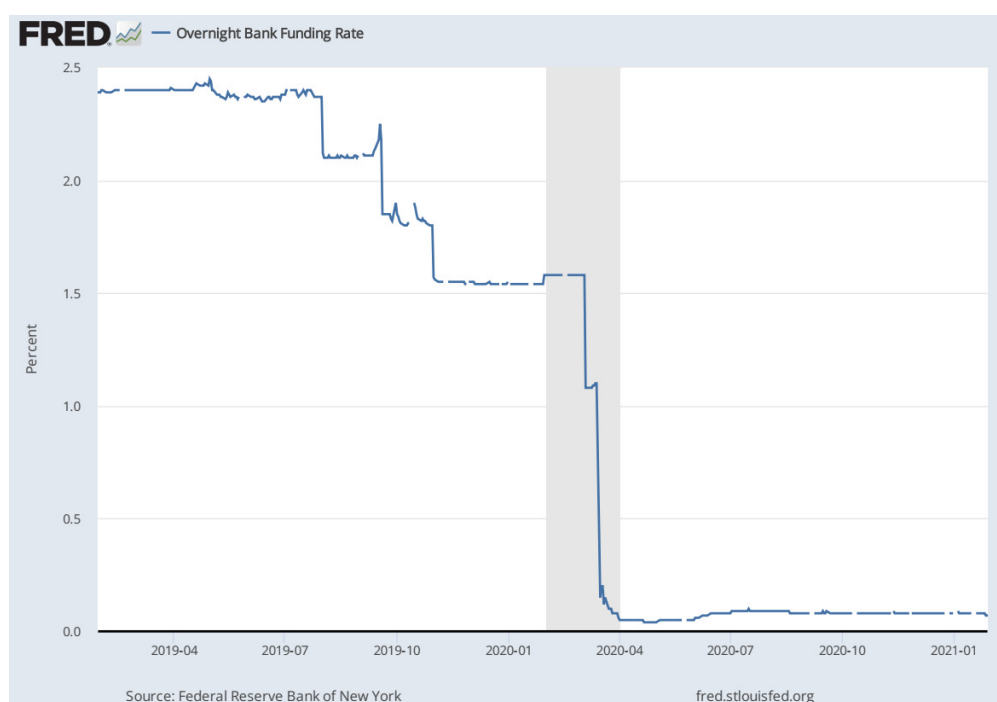


Figure 5.15: The graph shows, from January 2019 to January 2021, the Overnight Bank Funding Rate in percentage. Note the sharp drop in the funding rate in the shaded area.

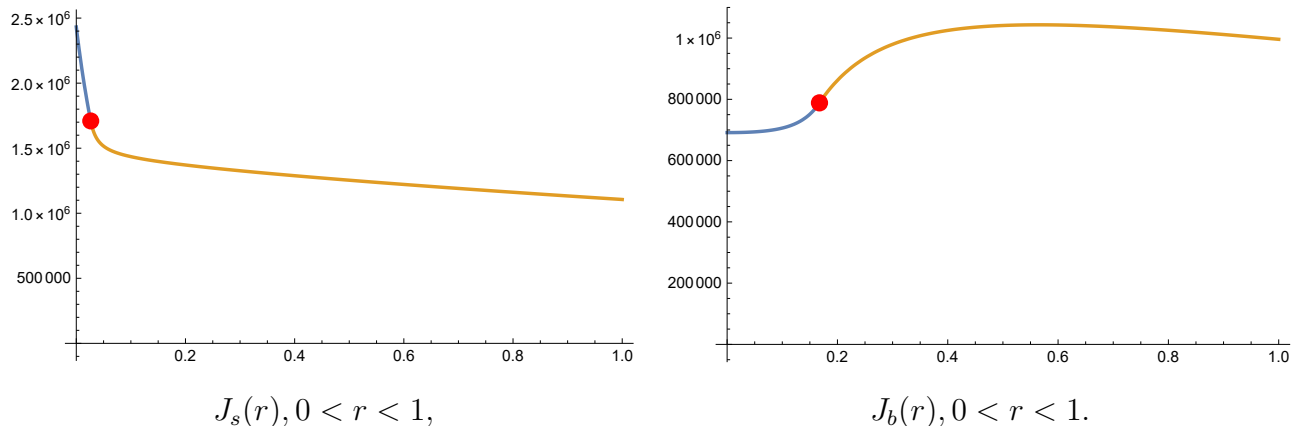


Figure 5.16: We plot the optimal selling and buying functions $J_s(r)$ and $J_b(r)$ when the interest rate is modeled by CIR process using (4.28) and (4.31) as a function of risk-free rate of interest r where $0 < r < 1$ using parameters defined in (4.40). We numerically solved for the selling and buying threshold using (C.11) and (C.14) to obtain $r_s \approx 0.026$ and $r_b \approx 0.167$ which is shown as red points in each respective graph.

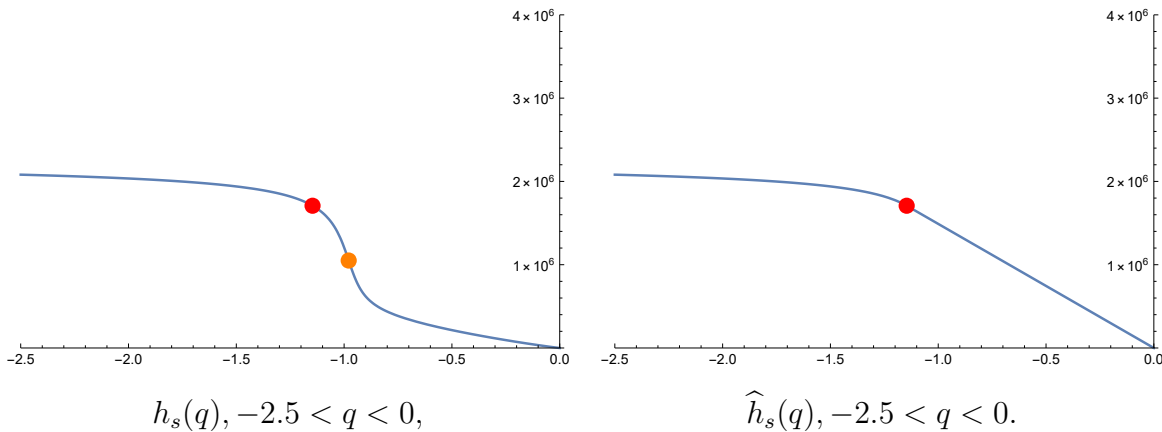


Figure 5.17: We plot the graphs of the functions $h_s(q)$ defined in (4.27) and its NCM $\widehat{h}_s(q)$ defined in (C.12) using parameter (4.40) for $-2.5 < q < 0$. The red point shows the point q_s which is numerically solved from (C.9), and the orange point shows the inflection point q_s^* of h_s which is numerically solved using the expression of h_s'' in (4.26).

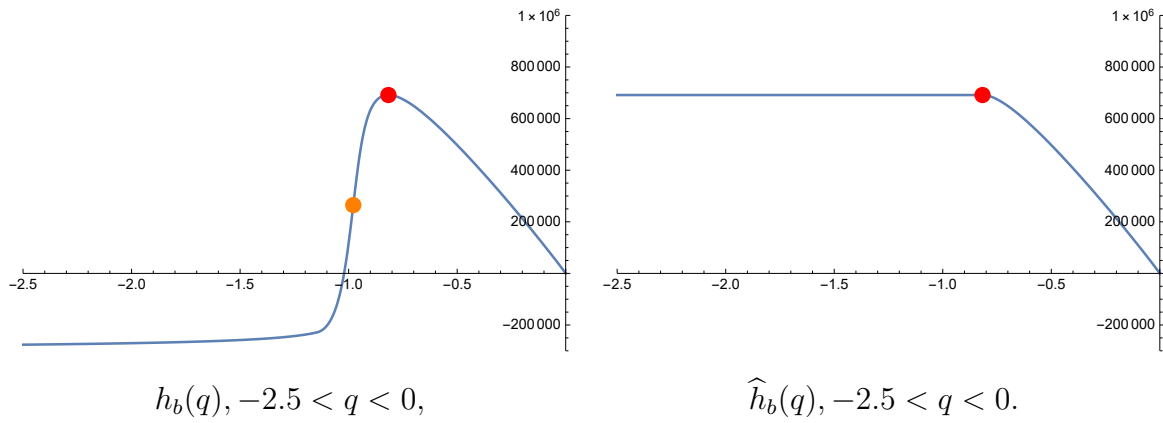


Figure 5.18: We plot the graphs of the functions $h_b(q)$ defined in (4.30) and its NCM $\hat{h}_b(q)$ defined in (C.13) using parameter (4.40) for $-2.5 < q < 0$. The red point shows the critical point q_b of h_b which is solved numerically using the expression h'_b in (4.25) and orange point shows the inflection point q_b^* of h_b which is numerically solved using the expression of h''_b in (4.26).

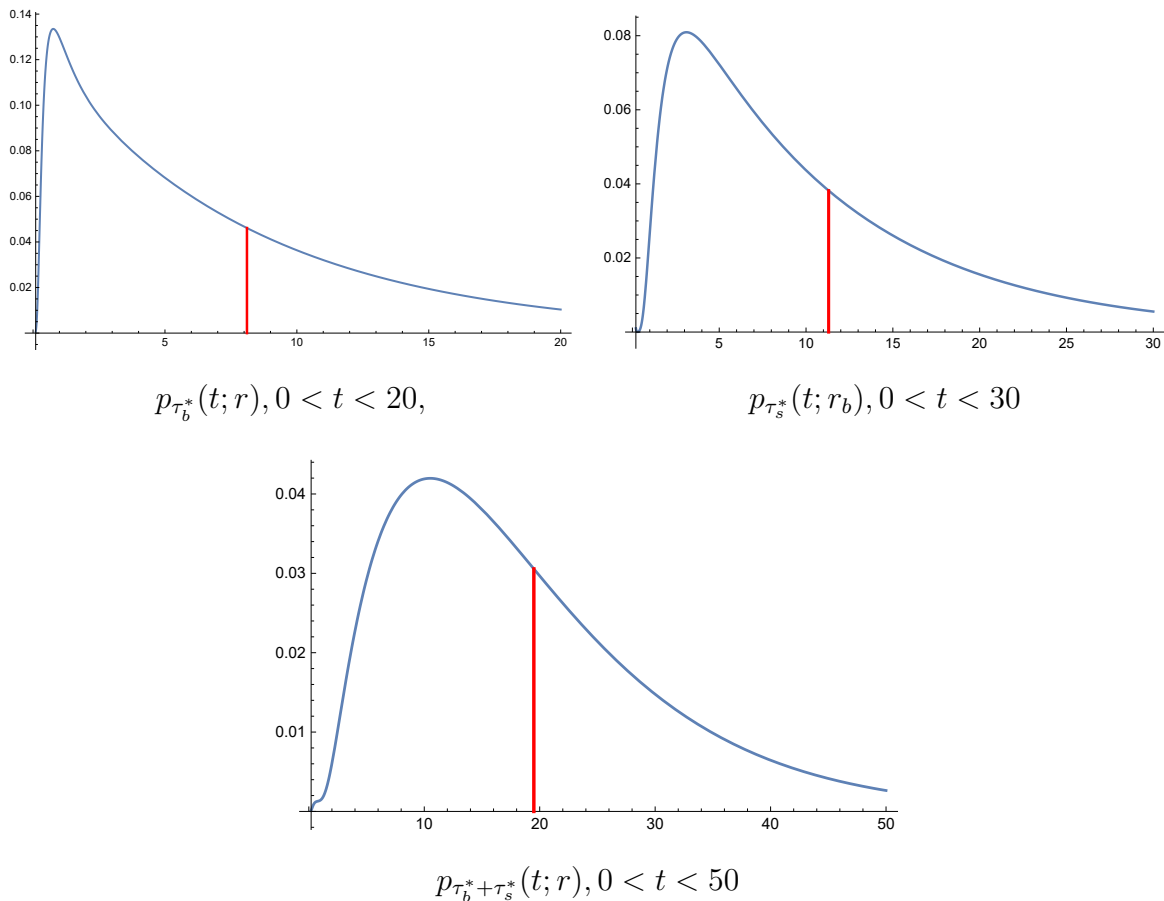


Figure 5.19: The following plots used $r = 0.08$ and other parameters from (4.40). The selling and buying threshold r_s and r_b are calculated numerically using (C.11) and (C.14) to obtain $r_s \approx 0.026$ and $r_b \approx 0.167$. We plot the density of the length of time the investor waits before buying $p_{\tau_b^*}(t; r)$ defined in (4.33) for $0 < t < 20$ using the first 100 terms of the truncated infinite sum. The density of the length of time the investor waits before selling $p_{\tau_s^*}(t; r_b)$ defined in (4.34) for $0 < t < 30$ is also plotted using the first 100 terms of the truncated infinite sum. Lastly, the density of the total time the investor waits to buy and sell a home $p_{\tau_b^* + \tau_s^*}(t; r)$ defined in (4.39) for $0 < t < 50$ is plotted using the first 100 indices in the truncated double infinite sum, giving a total of 10000 terms for the approximation. The expectations for each of the random variable calculated in (4.41) are shown as a vertical red bar in the respective graphs.

BIBLIOGRAPHY

- [1] Freddie Mac, 30-year fixed rate mortgage average in the United States [mortgage30us], Jan 2022.
- [2] S&P Dow Jones Indices LLC, S&P/Case-Shiller U.S. National Home Price Index [csushpinsa], Jan 2022.
- [3] Dong-Hyun Ahn, Robert F Dittmar, and A Ronald Gallant. Quadratic term structure models: Theory and evidence. *The Review of financial studies*, 15(1):243–288, 2002.
- [4] James Albrecht, Pieter A Gautier, and Susan Vroman. Directed search in the housing market. *Review of Economic Dynamics*, 19:218–231, 2016.
- [5] Flavio Angelini and Stefano Herzel. Notes and comments: An approximation of caplet implied volatilities in Gaussian models. *Decisions in Economics and Finance*, 28(2):113–127, 2006.
- [6] Paul M Anglin. How long does it take to buy one house and sell another? *Journal of Housing Economics*, 13(2):87–100, 2004.
- [7] John Armstrong, Martin Forde, Matthew Lorig, and Hongzhong Zhang. Small-time asymptotics under local-stochastic volatility with a jump-to-default: Curvature and the heat kernel expansion. *SIAM Journal on Financial Mathematics*, 8(1):82–113, 2017.
- [8] Andrea Barletta, Elisa Nicolato, and Stefano Pagliarani. The short-time behavior of vix-implied volatilities in a multifactor stochastic volatility framework. *Mathematical Finance*, 29(3):928–966, 2019.
- [9] Hatem Ben-Ameur, Michele Breton, Lotfi Karoui, and Pierre L’Ecuyer. A dynamic programming approach for pricing options embedded in bonds. *Journal of Economic Dynamics and Control*, 31(7):2212–2233, 2007.
- [10] Alain Bensoussan and J-L Lions. *Applications of variational inequalities in stochastic control*. Elsevier, 2011.
- [11] Louise Brown, Stanley McGreal, and Alastair Adair. The role of bidding in determining sales price for residential property. *Journal of Housing Research*, 22(1):39–57, 2013.

- [12] F Thomas Bruss and Thomas S Ferguson. Multiple buying or selling with vector offers. *Journal of Applied Probability*, 34(4):959–973, 1997.
- [13] Hans-Jürg Büttler and Jorg Waldvogel. Pricing callable bonds by means of green’s function 1. *Mathematical Finance*, 6(1):53–88, 1996.
- [14] Julio Carmona and Angel León. Investment option under CIR interest rates. *Finance Research Letters*, 4(4):242–253, 2007.
- [15] Christopher A Carolan. The least concave majorant of the empirical distribution function. *Canadian Journal of Statistics*, 30(2):317–328, 2002.
- [16] Peter Carr and Matthew Lorig. Robust hedging of barrier-style claims on price and volatility. *ArXiv preprint arXiv:1508.00632*, 2015.
- [17] Li Chen, Damir Filipović, and H Vincent Poor. Quadratic term structure models for risk-free and defaultable rates. *Mathematical Finance: An International Journal of Mathematics, Statistics and Financial Economics*, 14(4):515–536, 2004.
- [18] John C Cox, Jonathan E Ingersoll Jr, and Stephen A Ross. A theory of the term structure of interest rates. In *Theory of valuation*, pages 129–164. World Scientific, 2005.
- [19] Savas Dayanik. Optimal stopping of linear diffusions with random discounting. *Mathematics of Operations Research*, 33(3):645–661, 2008.
- [20] Savas Dayanik and Ioannis Karatzas. On the optimal stopping problem for one-dimensional diffusions. *Stochastic processes and their applications*, 107(2):173–212, 2003.
- [21] Jérôme Detemple Detemple, Matthew Lorig, Marcel Rindisbacher, Stephan Sturm, and Liangliang Zhang. Asymptotic expansion of non-linear FBSDE with pure diffusive Markov forward SDE and convergence. *Preprint*, 2015.
- [22] R. Durrett and K Burdzy. Brownian motion and martingales in analysis. *Metrika*, 32:413–414, 1985.
- [23] Martin Egozcue, Luis Fuentes García, and Ričardas Zitikis. An optimal strategy for maximizing the expected real-estate selling price: accept or reject an offer? *Journal of Statistical Theory and Practice*, 7(3):596–609, 2013.
- [24] Erik Ekström, Marcus Olofsson, and Martin Vannestål. A renewal theory approach to two-state switching problems with infinite values. *Journal of Applied Probability*, 57(1):1–18, 2020.

- [25] José E. Figueroa-López, Ruoting Gong, and Matthew Lorig. Short-time expansions for call options on leveraged ETFs under exponential lévy models with local volatility. *SIAM Journal on Financial Mathematics*, 9(1):347–380, 2018.
- [26] Damir Filipovic. *Term-Structure Models. A Graduate Course*. Springer, 2009.
- [27] H Gifford Fong and Oldrich A Vasicek. Fixed-income volatility management. *Journal of portfolio management*, 17(4):41, 1991.
- [28] Jean-Pierre Fouque, Sebastian Jaimungal, and Matthew Lorig. Spectral decomposition of option prices in fast mean-reverting stochastic volatility models. *SIAM Journal on Financial Mathematics*, 2(1), 2011.
- [29] Jean-Pierre Fouque and Matthew Lorig. A fast mean-reverting correction to Heston’s stochastic volatility model. *SIAM Journal on Financial Mathematics*, 2(1):221–254, 2011.
- [30] Jean-Pierre Fouque, Matthew Lorig, and Ronnie Sircar. Second order multiscale stochastic volatility asymptotics: stochastic terminal layer analysis and calibration. *Finance and Stochastics*, 20(3):543–588, 2016.
- [31] Martin Francu, Ron Kerman, and Gord Sinnamon. A new algorithm for approximating the least concave majorant. *arXiv preprint arXiv:1608.02581*, 2016.
- [32] Pavel V Gapeev and Hans Rudolf Lerche. Discounted optimal stopping for diffusions: free-boundary versus martingale approach. *London School of Economics and Political Science, Computational, Discrete and Applicable Mathematics LSE-CDAM-2009-03*, 2009.
- [33] Patrick S Hagan, Deep Kumar, Andrew S Lesniewski, and Diana E Woodward. Managing smile risk. *The Best of Wilmott*, 1:249–296, 2002.
- [34] Karl F Hofmann. Implied volatilities for options on backward-looking term rates. *Available at SSRN 3593284*, 2020.
- [35] John Hull and Alan White. Pricing interest-rate-derivative securities. *The review of financial studies*, 3(4):573–592, 1990.
- [36] Antoine Jacquier and Matthew Lorig. The smile of certain lévy-type models. *SIAM Journal on Financial Mathematics*, 4(1):804–830, 2013.

- [37] Antoine Jacquier and Matthew Lorig. From characteristic functions to implied volatility expansions. *Advances in Applied Probability*, 47(3):837–857, 09 2015.
- [38] Farshid Jamshidian. An exact bond option formula. *The journal of Finance*, 44(1):205–209, 1989.
- [39] Joerg Kienitz. Transforming volatility-multi curve cap and swaption volatilities. *Available at SSRN 2204702*, 2013.
- [40] Charles Ka Yui Leung and Chung-Yi Tse. Flipping in the housing market. *Journal of Economic Dynamics and Control*, 76:232–263, 2017.
- [41] Tim Leung and Xin Li. Optimal mean reversion trading with transaction costs and stop-loss exit. *International Journal of Theoretical and Applied Finance*, 18(03):1550020, 2015.
- [42] Tim Leung, Xin Li, and Zheng Wang. Optimal starting–stopping and switching of a CIR process with fixed costs. *Risk and Decision Analysis*, 5(2-3):149–161, 2014.
- [43] Tim Leung and Matthew Lorig. Optimal static quadratic hedging. *Quantitative Finance*, 16(9):1341–1355, 2016.
- [44] Tim Leung, Matthew Lorig, and Andrea Pascucci. Leveraged etf implied volatilities from etf dynamics. *Mathematical Finance*, 27(4):1035–1068, 2017.
- [45] Tim Leung, Matthew Lorig, and Andrea Pascucci. Leveraged ETF implied volatilities from etf dynamics. *Mathematical Finance*, 27(4):1035–1068, 2017.
- [46] Vadim Linetsky. Computing hitting time densities for CIR and ou diffusions: Applications to mean-reverting models. *Journal of Computational Finance*, 7:1–22, 2004.
- [47] Matthew Lorig. Time-changed fast mean-reverting stochastic volatility models. *International Journal of Theoretical and Applied Finance*, 14:1355 – 1383, 2011.
- [48] Matthew Lorig. The exact smile of certain local volatility models. *Quantitative Finance*, 13(6):897–905, 2013.
- [49] Matthew Lorig. Pricing derivatives on multiscale diffusions: An eigenfunction expansion approach. *Mathematical Finance*, 24(2):331–363, 2014.
- [50] Matthew Lorig. Indifference prices and implied volatilities. *Mathematical Finance*, 28(1):372–408, 2018.

- [51] Matthew Lorig and Oriol Lozano-Carbassé. Multiscale exponential Lévy models. *Quantitative Finance*, 15(1):91–100, 2015.
- [52] Matthew Lorig, Oriol Lozano-Carbassé, and Rafael Mendoza-Arriaga. Variance swaps on defaultable assets and market implied time-changes. *SIAM Journal on Financial Mathematics*, 7(1):273–307, 2016.
- [53] Matthew Lorig, Stefano Pagliarani, and Andrea Pascucci. A Taylor series approach to pricing and implied vol for LSV models. *Journal of Risk*, 17:1–17, 12 2014.
- [54] Matthew Lorig, Stefano Pagliarani, and Andrea Pascucci. A taylor series approach to pricing and implied volatility for local-stochastic volatility models. *Journal of Risk*, 17(2), 2014.
- [55] Matthew Lorig, Stefano Pagliarani, and Andrea Pascucci. Analytical expansions for parabolic equations. *SIAM Journal on Applied Mathematics*, 75:468–491, 2015.
- [56] Matthew Lorig, Stefano Pagliarani, and Andrea Pascucci. *Asymptotics for d-Dimensional Lévy-Type Processes*, pages 321–343. Springer International Publishing, Cham, 2015.
- [57] Matthew Lorig, Stefano Pagliarani, and Andrea Pascucci. A family of density expansions for Lévy-type processes with default. *Annals of Applied Probability*, 25(1):235–267, 2015.
- [58] Matthew Lorig, Stefano Pagliarani, and Andrea Pascucci. Pricing approximations and error estimates for local Lévy-type models with default. *Computers and Mathematics with Applications*, 69:1189–1219, May 2015.
- [59] Matthew Lorig, Stefano Pagliarani, and Andrea Pascucci. Explicit implied volatilities for multifactor local-stochastic volatility models. *Mathematical Finance*, 27(3):926–960, 2017.
- [60] Matthew Lorig, Stefano Pagliarani, and Andrea Pascucci. Explicit implied volatilities for multifactor local-stochastic volatility models. *Mathematical Finance*, 27(3):926–960, 2017.
- [61] Matthew Lorig and Ronnie Sircar. Portfolio optimization under local-stochastic volatility: Coefficient taylor series approximations and implied sharpe ratio. *SIAM Journal on Financial Mathematics*, 7(1):418–447, 2016.

- [62] Matthew Lorig and Ronnie Sircar. Stochastic volatility: Modeling and asymptotic approaches to option pricing & portfolio selection. In A. Akansu, S. Kulkarni, D. Malioutov, and I. Pollak, editors, *Financial Signal Processing and Machine Learning*, chapter 7, pages 135–161. Wiley, 2016.
- [63] Matthew Lorig and Natchanon Suaysom. Options on bonds: Implied volatilities from affine short-rate dynamics, 2021.
- [64] Matthew Lorig and Natchanon Suaysom. Optimal times to buy and sell a home. *arXiv preprint arXiv:2203.05545*, 2022.
- [65] Matthew Lorig and Natchanon Suaysom. Options on bonds: implied volatilities from affine short-rate dynamics. *Annals of Finance*, pages 1–34, 2022.
- [66] Matthew Lorig and Natchanon Suaysom. Explicit caplet implied volatilities for quadratic term-structure models. *International Journal of Financial Engineering*, 11(01):2350041, 2024.
- [67] Spiros H Martzoukos and Theodore M Barnhill Jr. The survival zone for a bond with both call and put options embedded. *Journal of Financial Research*, 21(4):419–430, 1998.
- [68] Stefano Pagliarani and Andrea Pascucci. Analytical approximation of the transition density in a local volatility model. *Cent. Eur. J. Math.*, 10(1):250–270, 2012.
- [69] Stefano Pagliarani and Andrea Pascucci. The exact taylor formula of the implied volatility. *Finance and Stochastics*, 21(3):661–718, 2017.
- [70] Goran Peskir and Albert Shiryaev. *Optimal stopping and free-boundary problems*. Springer, 2006.
- [71] Vladimir V Piterbarg. *Interest Rate Modeling. Volume 1-Foundations and Vanilla Models*. Atlantic Financial Press, 2010.
- [72] Ramon Rabinovitch. Pricing stock and bond options when the default-free rate is stochastic. *Journal of Financial and Quantitative Analysis*, pages 447–457, 1989.
- [73] Rainer Schöbel and Jianwei Zhu. Stochastic volatility with an Ornstein-Uhlenbeck process: an extension. *Review of Finance*, 3(1):23–46, 1999.
- [74] M Selby and Chris Strickland. Computing the Fong and Vasicek pure discount bond price formula. *Journal of Fixed Income*, September, 78084, 1995.

- [75] S.E. Shreve. *Stochastic calculus for finance II: Continuous-time models*. Springer Verlag, 2004.
- [76] SE Shreve, HM Soner, et al. Optimal investment and consumption with transaction costs. *The Annals of Applied Probability*, 4(3):609–692, 1994.
- [77] Steven E Shreve. *Stochastic calculus for finance II: Continuous-time models*, volume 11. Springer Science & Business Media, 2004.
- [78] Mike Staunton. Close encounters of the third order. *Wilmott*, 2014(70):52–53, 2014.
- [79] E.M. Stein and J.C. Stein. Stock price distributions with stochastic volatility: an analytic approach. *Review of financial Studies*, 4(4):727–752, 1991.
- [80] George E Uhlenbeck and Leonard S Ornstein. On the theory of the brownian motion. *Physical review*, 36(5):823, 1930.
- [81] Ramon Van Handel. Stochastic calculus, filtering, and stochastic control. *Course notes.*, URL <http://www.princeton.edu/rvan/acm217/ACM217.pdf>, 14, 2007.
- [82] Oldrich Vasicek. An equilibrium characterization of the term structure. *Journal of financial economics*, 5(2):177–188, 1977.
- [83] Zhengqin Zeng and Chi-Guhn Lee. Pairs trading: optimal thresholds and profitability. *Quantitative Finance*, 14(11):1881–1893, 2014.
- [84] Guo Dong Zhu. *Pricing Options on Trading Strategies*. PhD thesis, New York University, 2007.

Appendix A

EXPLICIT EXPRESSIONS FOR σ_0 , σ_1 AND σ_2

In this Appendix we give the expressions for the implied volatility approximation using (3.19) and (3.20) explicitly up to second order for $d = 1$ in terms of the coefficients c, f, g , and h of $\tilde{\mathcal{A}}$, given in (2.47) and (2.53), by performing Taylor's series expansion of the coefficients around $\bar{z}(t) = (x, y)$. To ease the notation, we define

$$\chi_{i,j}(t) \equiv \chi_{i,j}(t, x, y) = \frac{\partial_x^i \partial_y^j \chi(t, x, y)}{i!j!}, \quad \chi \in \{c, f, g, h\}.$$

The zeroth order term σ_0 is given by

$$\sigma_0 = \sqrt{\frac{2}{T-t} \int_t^T ds c_{0,0}(s)}.$$

Next, let us define

$$\mathcal{H}_n(\Theta) := \left(\frac{-1}{\sigma_0 \sqrt{2(T-t)}} \right)^n \mathbf{H}_n(\Theta), \quad \Theta := \frac{x - k - \frac{1}{2}\sigma_0^2(T-t)}{\sigma_0 \sqrt{2(T-t)}}.$$

where $\mathbf{H}_n(\Theta)$ is the n th-order *Hermite polynomial*. Then the first order term σ_1 is given by

$$\sigma_1 = \sigma_{1,0} + \sigma_{0,1},$$

where $\sigma_{1,0}$ and $\sigma_{0,1}$ are given by

$$\begin{aligned} \sigma_{1,0} &= \frac{1}{(T-t)\sigma_0} \int_t^T ds c_{1,0}(s) \int_t^s dq c_{0,0}(q) \left(2\mathcal{H}_1(\Theta) - 1 \right), \\ \sigma_{0,1} &= \frac{1}{(T-t)\sigma_0} \int_t^T ds c_{0,1}(s) \left(\int_t^s dq f_{0,0}(q) + \int_t^s dq h_{0,0}(q) \mathcal{H}_1(\Theta) \right). \end{aligned}$$

Lastly, the second order term σ_2 is given by

$$\sigma_2 = \sigma_{2,0} + \sigma_{1,1} + \sigma_{0,2},$$

where the terms $\sigma_{2,0}$, $\sigma_{0,2}$, $\sigma_{1,1}$ are given by

$$\begin{aligned}
\sigma_{2,0} = & \frac{1}{(T-t)\sigma_0} \left(\frac{1}{2} \int_t^T ds c_{2,0}(s) \left(\left(\int_t^s dq c_{0,0}(q) \right)^2 (4\mathcal{H}_2(\Theta) - 4\mathcal{H}_1(\Theta) + 1) \right. \right. \\
& + 2 \int_t^s dq c_{0,0}(q) \left. \right) + \int_t^T ds_1 \int_{s_1}^T ds_2 c_{1,0}(s_1) c_{1,0}(s_2) \left(\int_t^{s_1} dq_1 c_{0,0}(q_1) \int_t^{s_2} dq_2 c_{0,0}(q_2) \right. \\
& \times (4\mathcal{H}_4(\Theta) - 8\mathcal{H}_3(\Theta) + 5\mathcal{H}_2(\Theta) - \mathcal{H}_1(\Theta)) \\
& + \left. \left. \int_t^{s_1} dq_1 c_{0,0}(q_1) (6\mathcal{H}_2(\Theta) - 6\mathcal{H}_1(\Theta) + 1) \right) \right) \\
& - \frac{\sigma_{1,0}^2}{2} \left((T-t)\sigma_0(\mathcal{H}_2(\Theta) - \mathcal{H}_1(\Theta)) + \frac{1}{\sigma_0} \right),
\end{aligned}$$

$$\begin{aligned}
\sigma_{0,2} = & \frac{1}{(T-t)\sigma_0} \left(\frac{1}{2} \int_t^T ds c_{0,2}(s) \left(\left(\int_t^s dq h_{0,0}(q) \right)^2 \mathcal{H}_2(\Theta) \right. \right. \\
& + 2 \int_t^s dq_1 h_{0,0}(q_1) \int_t^s dq_2 f_{0,0}(q_2) \mathcal{H}_1(\Theta) + \left(\int_t^s dq f_{0,0}(q) \right)^2 + 2 \int_t^s dq g_{0,0}(q) \left. \right) \\
& + \int_t^T ds_1 \int_{s_1}^T ds_2 c_{0,1}(s_1) c_{0,1}(s_2) \left(\int_t^{s_1} dq_1 h_{0,0}(q_1) \int_t^{s_2} dq_2 h_{0,0}(q_2) \mathcal{H}_4(\Theta) \right. \\
& + \left(\int_t^{s_1} dq_1 f_{0,0}(q_1) \int_t^{s_2} dq_2 h_{0,0}(q_2) + \int_t^{s_1} dq_1 h_{0,0}(q_1) \int_t^{s_2} dq_2 f_{0,0}(q_2) \right. \\
& - \left. \left. \int_t^{s_1} dq_1 h_{0,0}(q_1) \int_t^{s_2} dq_2 h_{0,0}(q_2) \right) \mathcal{H}_3(\Theta) \right. \\
& + \left(2 \int_t^{s_1} dq g_{0,0}(q) + \int_t^{s_1} dq_1 f_{0,0}(q_1) \int_t^{s_2} dq_2 f_{0,0}(q_2) \right. \\
& - \left. \int_t^{s_1} dq_1 f_{0,0}(q_1) \int_t^{s_2} dq_2 h_{0,0}(q_2) - \int_t^{s_2} dq_1 f_{0,0}(q_1) \int_t^{s_1} dq_2 h_{0,0}(q_2) \right) \mathcal{H}_2(\Theta) \\
& - \left. \left. \left(2 \int_t^{s_1} dq g_{0,0}(q) + \int_t^{s_1} dq_1 f_{0,0}(q_1) \int_t^{s_2} dq_2 f_{0,0}(q_2) \right) \mathcal{H}_1(\Theta) \right) \right. \\
& + \int_t^T ds_1 \int_{s_1}^T ds_2 f_{0,1}(s_1) c_{0,1}(s_2) \left(\int_t^{s_1} dq h_{0,0}(q) \mathcal{H}_1(\Theta) + \int_t^{s_1} dq f_{0,0}(q) \right) \\
& + \int_t^T ds_1 \int_{s_1}^T ds_2 h_{0,1}(s_1) c_{0,1}(s_2) \left(\int_t^{s_1} dq h_{0,0}(q) \mathcal{H}_2(\Theta) + \int_t^{s_1} dq f_{0,0}(q) \mathcal{H}_1(\Theta) \right) \left. \right) \\
& - \frac{\sigma_{0,1}^2}{2} \left((T-t)\sigma_0(\mathcal{H}_2(\Theta) - \mathcal{H}_1(\Theta)) + \frac{1}{\sigma_0} \right).
\end{aligned}$$

$$\begin{aligned}
\sigma_{1,1} = & \frac{1}{(T-t)\sigma_0} \left(\frac{1}{2} \int_t^T ds c_{1,1}(s) \left(2 \int_t^s dq_1 c_{0,0}(q_1) \int_t^s dq_2 h_{0,0}(q_2) \mathcal{H}_2(\Theta) \right. \right. \\
& + \int_t^s dq_1 c_{0,0}(q_1) \left(2 \int_t^s dq_2 f_{0,0}(q_2) - \int_t^s dq_2 h_{0,0}(q_2) \right) \mathcal{H}_1(\Theta) \\
& \left. \left. - \int_t^s dq_1 c_{0,0}(q_1) \int_t^s dq_2 f_{0,0}(q_2) + \int_t^s dq_1 h_{0,0}(q_1) \right) \right) \\
& + \int_t^T ds_1 \int_{s_1}^T ds_2 c_{1,0}(s_1) c_{0,1}(s_2) \left(2 \int_t^{s_1} dq_1 c_{0,0}(q_1) \int_t^{s_2} dq_2 h_{0,0}(q_2) \mathcal{H}_4(\Theta) \right. \\
& + \int_t^{s_1} dq_1 c_{0,0}(q_1) \left(2 \int_t^{s_2} dq_2 f_{0,0}(q_2) - 3 \int_t^{s_2} dq_2 h_{0,0}(q_2) \right) \mathcal{H}_3(\Theta) \\
& + \left(\int_t^{s_1} dq c_{0,0}(q) \left(\int_t^{s_2} dq h_{0,0}(q) - 3 \int_t^{s_2} dq f_{0,0}(q) \right) + \int_t^{s_1} dq h_{0,0}(q) \right) \mathcal{H}_2(\Theta) \\
& + \left(\int_t^{s_1} dq_1 c_{0,0}(q_1) \int_t^{s_2} dq_2 f_{0,0}(q_2) - \int_t^{s_1} dq_1 h_{0,0}(q_1) \right) \mathcal{H}_1(\Theta) \left. \right) \\
& + \int_t^T ds_1 \int_{s_1}^T ds_2 c_{0,1}(s_1) c_{1,0}(s_2) \left(2 \int_t^{s_1} dq_1 h_{0,0}(q_1) \int_t^{s_2} dq_2 c_{0,0}(q_2) \mathcal{H}_4(\Theta) \right. \\
& + \left(2 \int_t^{s_1} dq_1 f_{0,0}(q_1) - 3 \int_t^{s_1} dq_1 h_{0,0}(q_1) \right) \int_t^{s_2} dq_2 c_{0,0}(q_2) \mathcal{H}_3(\Theta) \\
& + \left(\left(\int_t^{s_1} dq_1 h_{0,0}(q_1) - 3 \int_t^{s_1} dq_1 f_{0,0}(q_1) \right) \int_t^{s_2} dq_2 c_{0,0}(q_2) \right. \\
& \left. + 3 \int_t^{s_1} dq_1 h_{0,0}(q_1) \right) \mathcal{H}_2(\Theta) \\
& + \left(\int_t^{s_1} dq_1 f_{0,0}(q_1) \left(2 + \int_t^{s_2} dq_2 c_{0,0}(q_2) \right) - 2 \int_t^{s_1} dq_1 h_{0,0}(q_1) \right) \mathcal{H}_1(\Theta) \\
& \left. - \int_t^{s_1} dq_1 f_{0,0}(q_1) \right) \\
& + \int_t^T ds_1 \int_{s_1}^T ds_2 f_{1,0}(s_1) c_{0,1}(s_2) \int_t^{s_1} dq_1 c_{0,0}(q_1) \left(2\mathcal{H}_1(\Theta) - 1 \right) \\
& + 2 \int_t^T ds_1 \int_{s_1}^T ds_2 h_{1,0}(s_1) c_{0,1}(s_2) \int_t^{s_1} dq_1 c_{0,0}(q_1) \left(2\mathcal{H}_2(\Theta) - \mathcal{H}_1(\Theta) \right) \left. \right) \\
& - \sigma_{1,0} \sigma_{0,1} \left((T-t)\sigma_0 (\mathcal{H}_2(\Theta) - \mathcal{H}_1(\Theta)) + \frac{1}{\sigma_0} \right),
\end{aligned}$$

Note that, although $\mathcal{H}_3(\Theta)$ and $\mathcal{H}_4(\Theta)$ appear in the expressions for $\sigma_{2,0}$, $\sigma_{1,1}$ and $\sigma_{0,2}$, the 3rd and 4th order terms in $k-x$ cancel the 3rd and 4th order terms resulting from $\{\sigma_{1,0}^2 \mathcal{H}_2(\Theta), \sigma_{1,0}^2 \mathcal{H}_1(\Theta)\}$, $\{\sigma_{0,1} \sigma_{1,0} \mathcal{H}_2(\Theta), \sigma_{0,1} \sigma_{1,0} \mathcal{H}_1(\Theta)\}$, and $\{\sigma_{0,1}^2 \mathcal{H}_2(\Theta), \sigma_{0,1}^2 \mathcal{H}_1(\Theta)\}$,

respectively, resulting in a second order implied volatility expansion that is quadratic in $k - x$.

Appendix B

EXPRESSIONS FOR F , G_1 AND G_2 IN THE FONG-VASICEK SETTING

We can derive from (3.37) and (3.38) that

$$\begin{aligned}\mathfrak{F}(t; T) &= \kappa_1 \theta_1 \int_t^T ds \mathfrak{G}_1(s; T) + \kappa_2 \theta_2 \int_t^T ds \mathfrak{G}_2(s; T), \\ \mathfrak{G}_1(t; T) &= \frac{1 - e^{-\kappa_1(T-t)}}{\kappa_1},\end{aligned}$$

and from (3.39) that

$$\begin{aligned}\mathfrak{G}_2(t; T) &= \frac{e^{-\kappa_1(T-t)}}{\delta_2^2 \kappa_1^3} \left((\bar{\alpha}_1 + \bar{\alpha}_2 e^{\kappa_1(T-t)}) \right. \\ &\quad \left. + \frac{\bar{\beta} \bar{\lambda} U(\bar{\Phi} + 1, \bar{\Psi} + 1, e^{-\kappa_1(T-t)} \bar{\zeta}) + \bar{\gamma} M(\bar{\Phi} + 1, \bar{\Psi} + 1, e^{-\kappa_1(T-t)} \bar{\zeta})}{\bar{\lambda} U(\bar{\Phi}, \bar{\Psi}, e^{-\kappa_1(T-t)} \bar{\zeta}) + M(\bar{\Phi}, \bar{\Psi}, e^{-\kappa_1(T-t)} \bar{\zeta})} \right),\end{aligned}$$

where we have introduced constants

$$\begin{aligned}\bar{\alpha} &= \bar{\alpha}_1 + \bar{\alpha}_2, & \bar{\alpha}_1 &= \delta_2 \kappa_1^2 (\rho + i\bar{\rho}), \\ \bar{\alpha}_2 &= -\kappa_1^2 (\delta_2 \rho + \kappa_1 \kappa_2 + \bar{\beta}_2), & \bar{\beta} &= \delta_2 (\bar{\beta}_1 + i\bar{\rho}(\bar{\beta}_2 + \kappa_1^2)), \\ \bar{\beta}_1 &= \delta_2 \bar{\rho}^2 + \rho \kappa_1 (\kappa_1 - \kappa_2), & \bar{\beta}_2 &= \sqrt{(\delta_2 \rho + \kappa_1 \kappa_2)^2 - \delta_2^2}, \\ \bar{\Phi} &= \frac{\bar{\Psi}}{2} + \frac{\bar{\beta}_1}{2i\kappa_1^2 \bar{\rho}}, & \bar{\Psi} &= \frac{\bar{\beta}_2}{\kappa_1^2} + 1, \\ \bar{\zeta} &= \frac{i\delta_2 \bar{\rho}}{\kappa_1^2}, & \bar{\lambda} &= -\frac{\bar{\gamma} M(\bar{\Phi} + 1, \bar{\Psi} + 1, \bar{\zeta}) + \bar{\alpha} M(\bar{\Phi}, \bar{\Psi}, \bar{\zeta})}{\bar{\beta} U(\bar{\Phi} + 1, \bar{\Psi} + 1, \bar{\zeta}) + \bar{\alpha} U(\bar{\Phi}, \bar{\Psi}, \bar{\zeta})}, \\ \bar{\gamma} &= -\frac{2\bar{\Phi} \kappa_1^4 \bar{\zeta}}{\bar{\Psi}}.\end{aligned}$$

and where M and U are CHF of the first kind and second kind, respectively. Explicitly, we have

$$M(a, b, z) = \sum_{n=0}^{\infty} \frac{a(a+1)\dots(a+n)}{b(b+1)\dots(b+n)} \frac{z^n}{n!},$$

$$U(a, b, z) = \frac{\Gamma_e(1-b)}{\Gamma_e(a+1-b)} M(a, b, z) + \frac{\Gamma_e(b-1)}{\Gamma_e(a)} z^{1-b} M(a+1-b, 2-b, z),$$

where Γ_e is the *Euler Gamma function*.

Appendix C

RELEVANT EXPRESSIONS FOR U_+, U_-, \widehat{H}_S AND \widehat{H}_B

C.1 Expressions for u_+ and u_-

We solve (4.21) following [14]. Consider the substitution $u(r) := e^{-\nu r} v(r)$ where

$$\nu := \frac{\xi - \kappa}{\sigma^2}, \quad \xi := \sqrt{\kappa^2 + 2\sigma^2(\chi - \gamma)},$$

then (4.21) simplifies to

$$rv''(r) + \left(\frac{2\kappa\theta}{\sigma^2} - \frac{2\xi}{\sigma^2} r \right) v'(r) + 2 \frac{\kappa\theta\nu}{\sigma^2} v(r) = 0. \quad (\text{C.1})$$

Performing the change of variable $v(r) := w(\zeta r)$ where $\zeta := \frac{2\xi}{\sigma^2}$ in (C.1) we obtain that $w(r)$ satisfies

$$rw''(r) + \left(\frac{2\kappa\theta}{\sigma^2} - r \right) w'(r) - \frac{\kappa\theta}{\sigma^2} \left(1 - \frac{\kappa}{\xi} \right) w(r) = 0,$$

which, with the shorthand $\alpha := \frac{\kappa}{\theta} \sigma^2 \left(1 - \frac{\kappa}{\xi} \right)$, $\beta := \frac{2\kappa\theta}{\sigma^2}$, can be written as

$$rw''(r) + (\beta - r)w'(r) - \alpha w(r) = 0. \quad (\text{C.2})$$

Equation (C.2) is commonly known as *Kummer's Equation* which has two independent solutions $w = (w_+, w_-)$ where

$$\begin{aligned} w_+(r) &= M(\alpha, \beta, r) = M\left(\frac{\kappa\theta}{\sigma^2} \left(1 - \frac{\kappa}{\xi}\right), \frac{2\kappa\theta}{\sigma^2}, r\right), \\ w_-(r) &= U(\alpha, \beta, r) = U\left(\frac{\kappa\theta}{\sigma^2} \left(1 - \frac{\kappa}{\xi}\right), \frac{2\kappa\theta}{\sigma^2}, r\right), \end{aligned}$$

and where M and U are *Confluent Hypergeometric Function* (CHF) of the first kind and second kind, defined by

$$\begin{aligned} M(\alpha, \beta, r) &= \sum_{n=0}^{\infty} \frac{\alpha(\alpha+1)\dots(\alpha+n)r^n}{\beta(\beta+1)\dots(\beta+n)n!}, \\ U(\alpha, \beta, r) &= \frac{\Gamma(1-\beta)}{\Gamma(\alpha+1-\beta)}M(\alpha, \beta, r) + \frac{\Gamma(\beta-1)}{\Gamma(\alpha)}r^{1-\beta}M(\alpha+1-\beta, 2-\beta, r), \\ &= \frac{1}{\Gamma(\alpha)} \int_0^{\infty} dt e^{-rt} t^{\alpha-1} (1+t)^{\beta-\alpha-1}, \end{aligned} \quad (\text{C.3})$$

and Γ is the *Euler gamma function*. Note that since $\chi > \gamma$, then the parameters α, β, ν, ξ are all positive. Substitute back w, v into u we obtain $u = (u_+(r), u_-(r)) = (e^{-\nu r} w_+(\zeta r), e^{-\nu r} w_-(\zeta r))$ which is the form of (4.22). It is clear that since each parameter in the argument of CHF is positive, u_+ and u_- are positive. Next we will show that u_+ and u_- are strictly increasing and decreasing, respectively. First we establish some basic properties of CHFs, which are well known.

Lemma C.1.1. *We have that the derivatives of CHF of the first and second kind are*

$$\begin{aligned} \frac{d}{dr} M(\alpha, \beta, \zeta r) &= \frac{\alpha\zeta}{\beta} M(\alpha+1, \beta+1, \zeta r), \\ \frac{d}{dr} U(\alpha, \beta, \zeta r) &= -\alpha\zeta U(\alpha+1, \beta+1, \zeta r). \end{aligned} \quad (\text{C.4})$$

Proof. We can show (C.4) by noting that

$$\begin{aligned} \frac{d}{dr} M(\alpha, \beta, \zeta r) &= \sum_{n=0}^{\infty} \frac{d}{dr} \frac{\alpha(\alpha+1)\dots(\alpha+n)\zeta^n r^n}{\beta(\beta+1)\dots(\beta+n)n!} \\ &= \sum_{n=1}^{\infty} \frac{\alpha(\alpha+1)\dots(\alpha+n)\zeta^n r^{n-1}}{\beta(\beta+1)\dots(\beta+n)(n-1)!} \\ &= \frac{\alpha\zeta}{\beta} \sum_{n=0}^{\infty} \frac{(\alpha+1)\dots(\alpha+1+n)\zeta^n r^n}{(\beta+1)\dots(\beta+1+n)n!} = \frac{\alpha\zeta}{\beta} M(\alpha+1, \beta+1, r). \end{aligned}$$

Using the relationship between M and U in (C.3) and the derivative formula of M , we perform similar calculation to obtain the derivative formula for U . \square

Lemma C.1.2. *The function u_+ is increasing and the function u_- is decreasing.*

Proof. Note that using (C.4) we obtain

$$\begin{aligned}
\frac{du_+(r)}{dr} &= \frac{d}{dr} \left(e^{-\nu r} M(\alpha, \beta, \zeta r) \right) = e^{-\nu r} \left(-\nu M(\alpha, \beta, \zeta r) + \frac{\alpha \zeta}{\beta} M(\alpha + 1, \beta + 1, \zeta r) \right) \\
&= -\nu e^{-\nu r} \left(M(\alpha, \beta, \zeta r) - M(\alpha + 1, \beta + 1, \zeta r) \right) \\
&= -\nu e^{-\nu r} \sum_{n=0}^{\infty} \left(\frac{\alpha(\alpha + 1) \dots (\alpha + n)}{\beta(\beta + 1) \dots (\beta + n)} - \frac{(\alpha + 1) \dots (\alpha + 1 + n)}{(\beta + 1) \dots (\beta + 1 + n)} \right) \frac{(\zeta r)^n}{n!} \\
&= -\nu e^{-\nu r} (\alpha - \beta) \sum_{n=0}^{\infty} \frac{(\alpha + 1) \dots (\alpha + n)}{(\beta + 1) \dots (\beta + n)} \left(\frac{1 + n}{\beta(\beta + 1 + n)} \right) \frac{(\zeta r)^n}{n!} \\
&= e^{-\nu r} \frac{\alpha \zeta}{\beta} \frac{\kappa \theta}{\sigma^2} \left(1 + \frac{\kappa}{\xi} \right) \sum_{n=0}^{\infty} \frac{(\alpha + 1) \dots (\alpha + n)}{(\beta + 1) \dots (\beta + n)} \left(\frac{1 + n}{\beta(\beta + 1 + n)} \right) \frac{(\zeta r)^n}{n!} > 0. \quad (\text{C.5})
\end{aligned}$$

This means that u_+ is increasing. Note that using (C.4) we obtain

$$\begin{aligned}
\frac{du_-(r)}{dr} &= \frac{d}{dr} \left(e^{-\nu r} U(\alpha, \beta, \zeta r) \right) \\
&= e^{-\nu r} \left(-\nu U(\alpha, \beta, \zeta r) - \alpha \zeta U(\alpha + 1, \beta + 1, \zeta r) \right) < 0. \quad (\text{C.6})
\end{aligned}$$

Since $\nu, \alpha, \zeta > 0$, $U(\alpha, \beta, \zeta r) > 0$ and $U(\alpha + 1, \beta + 1, \zeta r) > 0$ which is clear from the integral representation of U in (C.3), u_- is decreasing. \square

C.2 Expressions for \hat{h}_s and \hat{h}_b

From (4.25) and (4.26), since g is strictly increasing, we know that $g'(r) > 0$ and we automatically have $\sigma^2 r u_+(r) (g'(r))^2 > 0$. It remains to check the sign of (with the shorthand $r := g^{-1}(q)$)

$$h^*(r) := u_+(r) f'(r) - f(r) u'_+(r), \quad h^{**}(r) := \left(\mathcal{A} - (\chi - \gamma) r \right) f(r), \quad (\text{C.7})$$

to identify the sign of slope and convexity of h , respectively.

C.2.1 Expressions for \hat{h}_s

We first started by determining the slope of h_s . From (C.7) and (4.27) we need to consider the sign of

$$h_s^*(r) := u_+(r) f'_s(r) - f_s(r) u'_+(r).$$

Note that from Lemma C.1.2, $u_+(r), u'_+(r) > 0$ and it is clear that $f_s(r) > 0$ and $f'_s(r) < 0$ since $f_s(r)$ is a linear function of $v(r)$ which we have proven in (4.4) that it is decreasing in r , $f_s(r)$ must also be a decreasing function of r as well. Thus $h_s^*(r) = u_+(r)f'_s(r) - u'_+(r)f_s(r) < 0$ and this means that the function h_s is strictly decreasing.

To determine the convexity of h_s we consider the sign of h_s^{**} given by

$$\begin{aligned} h_s^{**}(r) &:= \left(\kappa(\theta - r)\partial_r + \frac{1}{2}\sigma^2 r \partial_r^2 - (\chi - \gamma)r \right) f_s(r) \\ &= \frac{1}{2(\rho + r)^3} \left(C(1 - \delta_s)r\sigma^2 (2 - e^{-T(\rho+r)} (\rho^2 T^2 + 2\rho T(rT + 1) + r^2 T^2 + 2rT + 2)) \right. \\ &\quad + 2r(\rho + r)^2 (\chi - \gamma) (K_s(\rho + r) - C(\delta_s - 1) (e^{-T(\rho+r)} - 1)) \\ &\quad \left. + 2C(\delta_s - 1)\kappa(\rho + r)(r - \theta)e^{-T(\rho+r)} (-e^{T(\rho+r)} + \rho T + rT + 1) \right). \end{aligned} \quad (\text{C.8})$$

To determine the inflection point r_s^* , we solve for $h_s^{**}(r_s^*) = 0$. Due to the complexity of this function, we numerically solved (C.8) using parameters in (4.40) which gives us that the polynomial has only one real root $r_s^* \in (0, \infty)$. This means that the function h_s changes its convexity at exactly one point $q_s^* := g(r_s^*)$. Thus the function h_s is concave on $(-\infty, q_s^*)$ and convex on $(q_s^*, 0)$.

With all this information on the slope and convexity of h_s , along with the inflection point q_s^* , we can now accurately plot h_s using parameters in (4.40) in Figure 5.17. Suppose that the tangent line of h_s passing through 0 intersects h_s at a point $(q_s, h_s(q_s))$. We can solve for q_s from (C.9)

$$\frac{h_s(q_s)}{q_s} = h'_s(q_s). \quad (\text{C.9})$$

Substituting $q_s = g(r_s)$ and using (4.25) we obtain

$$\frac{h_s(q_s)}{q_s} = -\frac{f_s(r_s)}{u_-(r_s)}, \quad h'_s(q_s) = \frac{f'_s(r_s)u_+(r_s) - f_s(r_s)u'_+(r_s)}{u'_+(r_s)u_-(r_s) - u_+(r_s)u'_-(r_s)}. \quad (\text{C.10})$$

Using (C.10) we can rewrite (C.9) in terms of r_s by

$$\frac{u'_-(r_s)}{u_-(r_s)} = \frac{f'_s(r_s)}{f_s(r_s)}. \quad (\text{C.11})$$

Equation (C.11) can be solved numerically to obtain the selling threshold r_s . From Figure 5.17 we can see that since $q_s < q_s^*$, the NCM of h_s is the h_s itself on $(-\infty, q_s)$ and on $(q_s, 0)$ it is the tangent line to h_s passing through 0. With all the information we can explicitly write \widehat{h}_s as

$$\widehat{h}_s(q) = \begin{cases} h_s(q) & q \leq q_s \\ q \frac{h_s(q_s)}{q_s} & q > q_s \end{cases}. \quad (\text{C.12})$$

C.2.2 Expressions for \widehat{h}_b

We first started by determining the slope of h_b . From (C.7) and (4.30) we need to consider the sign of

$$h_b^*(r) := u_+(r)f_b'(r) - f_b(r)u_+'(r),$$

which is given by a piecewise function

$$h_b^*(r) = \begin{cases} h_{11}^*(r) & r \leq r_s \\ h_{12}^*(r) & r > r_s \end{cases},$$

where

$$\begin{aligned}
h_{11}^*(r) &:= e^{-\nu r} M(\alpha, \beta, \zeta r) (f_s(r) - (v(r)(1 + \delta_b) + K_b))' \\
&\quad - (f_s(r) - (v(r)(1 + \delta_b) + K_b)) (e^{-\nu r} M(\alpha, \beta, \zeta r))' \\
&= \frac{C e^{-T(\rho+r)} (-e^{T(\rho+r)} + T(\rho+r) + 1) (K_b(\delta_s - 1) - K_s(\delta_b + 1))}{(\rho+r)^2}, \\
h_{12}^*(r) &:= e^{-\nu r} M(\alpha, \beta, \zeta r) (f_s(r_s) \frac{u_-(r)}{u_-(r_s)} - (v(r)(1 + \delta_b) + K_b))' \\
&\quad - (f_s(r_s) \frac{u_-(r)}{u_-(r_s)} - (v(r)(1 + \delta_b) + K_b)) (e^{-\nu r} M(\alpha, \beta, \zeta r))' \\
&= \frac{1}{(\rho+r)^2 (\rho+r_s) U(\alpha, \beta, r_s \zeta)} \\
&\quad \left(e^{\nu(r-r_s)-T(\rho+r)} \left(-C(\delta_s - 1) e^{-T(\rho+r_s)} \left(e^{T(\rho+r_s)} - 1 \right) - K_s(\rho+r_s) \right) \right. \\
&\quad \left(U(\alpha, \beta, r \zeta) \left(-C(\delta_b + 1) \left((\rho\nu + \nu r + 1) e^{T(\rho+r)} - \rho(\nu + T) - \nu r - rT - 1 \right) \right. \right. \\
&\quad \left. \left. - K_b \nu (\rho+r)^2 e^{T(\rho+r)} \right) + \alpha \zeta (\rho+r) U(\alpha+1, \beta+1, r \zeta) \left(C(\delta_b + 1) \left(e^{T(\rho+r)} - 1 \right) \right. \right. \\
&\quad \left. \left. + K_b (\rho+r) e^{T(\rho+r)} \right) \right).
\end{aligned}$$

We numerically identify the critical point r_b where $h_b^*(r_b) = 0$ using parameter (4.40). Since h_{11}^* is strictly negative we know that $r_b > r_s$. Next, for the convexity of h_b , we consider the signs of

$$h_b^{**}(r) := \left(\kappa(\theta - r) \partial_r + \frac{1}{2} \sigma^2 r \partial_r^2 - (\chi - \gamma)r \right) f_b(r).$$

We can write

$$h_b^{**}(r) = \begin{cases} h_{11}^{**}(r) & r \leq r_s \\ h_{12}^{**}(r) & r \geq r_s \end{cases},$$

where

$$\begin{aligned}
h_{11}^{**}(r) &= (\kappa(\theta - r)\partial_r + \frac{1}{2}\sigma^2 r\partial_r^2 - (\chi - \gamma)r)(f_s(r) - (v(r)(1 + \delta_b) + K_b)) \\
&= \frac{1}{2(\rho + r)^3} \left(Cr\sigma^2(\delta_s + \delta_b)e^{-T(\rho+r)}(\rho^2 T^2 + 2\rho T(rT + 1)) \right. \\
&\quad \left. - 2e^{T(\rho+r)} + r^2 T^2 + 2rT + 2 \right) \\
&\quad + 2r(\rho + r)^2(\chi - \gamma)(-C\delta_s e^{-T(\rho+r)} - C\delta_b e^{-T(\rho+r)} + \rho(K_b + K_s) \\
&\quad + C\delta_s + C\delta_b + K_b r + K_s r) \\
&\quad + 2C\kappa(\rho + r)(\delta_s + \delta_b)(r - \theta)e^{-T(\rho+r)}(-e^{T(\rho+r)} + \rho T + rT + 1) \Big) \\
h_{12}^{**}(r) &= (\kappa(\theta - r)\partial_r + \frac{1}{2}\sigma^2 r\partial_r^2 - (\chi - \gamma)r)\left(f_s(r_s)\frac{u_-(r)}{u_-(r_s)} - (v(r)(1 + \delta_b) + K_b)\right) \\
&= -r(\chi - \gamma)\left(\frac{e^{\nu(r-r_s)}U(\alpha, \beta, r\zeta)\left(\frac{C(\delta_s-1)(e^{-T(\rho+r_s)}-1)}{\rho+r_s} - K_s\right)}{U(\alpha, \beta, r_s\zeta)}\right. \\
&\quad \left. + \frac{C(\delta_b + 1)(e^{-T(\rho+r)} - 1)}{\rho + r} - K_b\right) \\
&\quad + \frac{1}{2}r\sigma^2\left(\frac{\alpha(\alpha + 1)\zeta^2 e^{\nu(r-r_s)}U(\alpha + 2, \beta + 2, r\zeta)\left(\frac{C(\delta_s-1)(e^{-T(\rho+r_s)}-1)}{\rho+r_s} - K_s\right)}{U(\alpha, \beta, r_s\zeta)}\right. \\
&\quad \left. + \frac{\nu^2 e^{\nu(r-r_s)}U(\alpha, \beta, r\zeta)\left(\frac{C(\delta_s-1)(e^{-T(\rho+r_s)}-1)}{\rho+r_s} - K_s\right)}{U(\alpha, \beta, r_s\zeta)}\right. \\
&\quad \left. + \frac{2\alpha\zeta\nu e^{\nu(r-r_s)}U(\alpha + 1, \beta + 1, r\zeta)(C(\delta_s - 1)e^{-T(\rho+r_s)}(e^{T(\rho+r_s)} - 1) + K_s(\rho + r_s))}{(\rho + r_s)U(\alpha, \beta, r_s\zeta)}\right. \\
&\quad \left. + \frac{CT^2(\delta_b + 1)e^{-T(\rho+r)}}{\rho + r} + \frac{2CT(\delta_b + 1)e^{-T(\rho+r)}}{(\rho + r)^2} + \frac{2C(\delta_b + 1)(e^{-T(\rho+r)} - 1)}{(\rho + r)^3}\right) \\
&\quad + \kappa(\theta - r)\left(\frac{\alpha\zeta e^{\nu(r-r_s)}U(\alpha + 1, \beta + 1, r\zeta)}{(\rho + r_s)U(\alpha, \beta, r_s\zeta)}\right. \\
&\quad \times (C(\delta_s - 1)e^{-T(\rho+r_s)}(e^{T(\rho+r_s)} - 1) + K_s(\rho + r_s)) \\
&\quad \left. + \frac{\nu e^{\nu(r-r_s)}U(\alpha, \beta, r\zeta)\left(\frac{C(\delta_s-1)(e^{-T(\rho+r_s)}-1)}{\rho+r_s} - K_s\right)}{U(\alpha, \beta, r_s\zeta)}\right. \\
&\quad \left. - \frac{CT(\delta_b + 1)e^{-T(\rho+r)}}{\rho + r} - \frac{C(\delta_b + 1)(e^{-T(\rho+r)} - 1)}{(\rho + r)^2}\right).
\end{aligned}$$

Due to the complexity of the above functions, we numerically solve for the inflection point $q_b^* := g(r_b^*)$ of h_b by solving for $h_b^{**}(r_b^*) = 0$.

With all the information above, we can now accurately plot h_b using the parameters in (4.40) in Figure 5.18, we can see that the NCM of h_b is the horizontal line (note that the NCM of an increasing function is the horizontal line of the maximum of that function) with value q_b on $(-\infty, q_b)$. Since $q_b^* < q_b$, on $(q_b, 0)$ the graph of h_b is decreasing, nonnegative and concave, so clearly the NCM of this part of the function is h_b itself. With all the information we can write \widehat{h}_b as

$$\widehat{h}_b(q) = \begin{cases} h_b(q_b) & q \leq q_b \\ h_b(q) & q > q_b \end{cases}, \quad (\text{C.13})$$

where q_b can be solved by setting (4.25) to zero which is equivalent to

$$\frac{u'_+(r_b)}{u_+(r_b)} = \frac{f'_b(r_b)}{f_b(r_b)}. \quad (\text{C.14})$$

We solve for the buying threshold r_b using (C.14) and set $q_b = g(r_b)$ to obtain q_b .

C.3 Constant discount rate

Suppose that, for a payment P_t received at time t the investor assigns a present value of $\mathbb{E}(e^{-\chi t} P_t)$ instead of $\mathbb{E}(e^{-\chi \int_0^t R_s ds} P_t)$ as in Section 4.3. Revising the processes in Section 4.3 to obtain the optimal buying and selling problems, we can see that all steps applied in Section 4.3 can also be applied in this setting, except that the process Λ is changed to a modified process reflecting the change in integral discounting rate to constant discounting rate. The modified process $\widetilde{\Lambda} = (\widetilde{\Lambda}_t)_{t \geq 0}$ is defined by

$$\widetilde{\Lambda}_t := \chi t - \gamma \int_0^t R_s ds. \quad (\text{C.15})$$

Having the form of the modified process, we can define a *modified buying value function and selling function*, \widetilde{J}_b and \widetilde{J}_s as

$$\widetilde{J}_b(r) := \sup_{\tau_b \in \mathcal{T}} \mathbb{E} \left[e^{-\widetilde{\Lambda}_{\tau_b}} f_b(R_{\tau_b}) \middle| R_0 = r \right], \quad \widetilde{J}_s(r) := \sup_{\tau_s \in \mathcal{T}} \mathbb{E} \left[e^{-\widetilde{\Lambda}_{\tau_s}} f_s(R_{\tau_s}) \middle| R_0 = r \right],$$

and *modified optimal selling and buying strategies* $\tilde{\tau}_s^*$ and $\tilde{\tau}_b^*$ are defined in the same way as (4.29) and (4.32). The functions f_s and f_b remain unchanged and are given by (4.8) and (4.10), respectively. In this setting, the ODE (4.15) becomes

$$\left(\mathcal{A} - \chi + \gamma r\right)\tilde{u}(r) = 0. \quad (\text{C.16})$$

Note that for a given generator \mathcal{A} and constant γ , positive strictly increasing and positive strictly decreasing solutions of (C.16) will only exist if χ is larger than some threshold value.

Remark C.3.1. Still another possible form of discounting would be for the investor to assign a present value of $\mathbb{E}(e^{-\chi t - \int_0^t R_s ds} P_t)$ for a payment P_t received at time t . This simply results in the change $\gamma \rightarrow \gamma - 1$ in (C.15).

C.3.1 CIR Interest Rate

We now focus on the case in which the interest rate R is modeled by CIR process. In this setting, (C.16) is given by

$$\left(\kappa(\theta - r)\partial_r + \frac{1}{2}\sigma^2 r\partial_r^2 - \chi + \gamma r\right)\tilde{u}(r) = 0.$$

The solution $\tilde{u} = (\tilde{u}_+, \tilde{u}_-)$, where \tilde{u}_+ is positive strictly increasing and \tilde{u}_- is positive strictly decreasing are of the form (C.17)

$$\tilde{u}_+(r) = e^{-\nu r} M(\alpha, \beta, \zeta r), \quad \tilde{u}_-(r) = e^{-\nu r} U(\alpha, \beta, \zeta r), \quad (\text{C.17})$$

where the parameters $(\alpha, \beta, \xi, \zeta, \nu)$ are defined as

$$\begin{aligned} \alpha &:= \frac{\kappa\theta}{\sigma^2} \left(1 - \frac{\kappa - \sigma^2\chi/\kappa\theta}{\xi}\right), & \beta &:= \frac{2\kappa\theta}{\sigma^2}, & \xi &:= \sqrt{\kappa^2 - 2\gamma\sigma^2}, \\ \zeta &:= \frac{2\xi}{\sigma^2}, & \nu &= \frac{\xi - \kappa}{\sigma^2}. \end{aligned}$$

Note that while the form of the functions (C.17) is the same as (4.22), the value of the constants has been modified, reflecting the change from stochastic to constant discounting.

We would like to find a sufficient condition for positive strictly increasing solutions \tilde{u}_+ and

positive strictly decreasing solutions \tilde{u}_- to exist. To this end, we note that the derivative of \tilde{u}_+ can be written using (C.5) as

$$\frac{du_+(r)}{dr} = -\nu e^{-\nu r} (\alpha - \beta) \sum_{n=0}^{\infty} \frac{(\alpha + 1) \dots (\alpha + n)}{(\beta + 1) \dots (\beta + n)} \left(\frac{1 + n}{\beta(\beta + 1 + n)} \right) \frac{(\zeta r)^n}{n!}.$$

As $\nu < 0, \zeta > 0$, the derivative is guaranteed to be positive if $\alpha > \beta > 0$, which is equivalent to

$$\chi > \frac{\beta}{2} \left(\kappa - \sqrt{\kappa^2 - 2\gamma\sigma^2} \right).$$

Thus, if χ is large enough, \tilde{u}_+ will be strictly increasing. Performing similar analysis using the derivative of u_- in (C.6), we can see that this condition is also sufficient to guarantee \tilde{u}_- is decreasing.